GER 13260

HIGH-ALTITUDE TETHERED BALLOON SYSTEMS STUDY

James A. Menke

Goodyear Aerospace Corporation
Akron, Ohio

Contract F 19628-67-C-0145

Task Report No. 1
Schedule Sub-Line Item 1AA

10 May 1967

AFCRL Project Monitors: Mr. Lewis Grass
Edward Young, Captain, USAF

Sponsored by

ADVANCED RESEARCH PROJECTS AGENCY
DEPARTMENT OF DEFENSE

Monitored by

AIR FORCE CAMBRIDGE RESEARCH LABORATORIES
UNITED STATES AIR FORCE
BEDFORD, MASSACHUSETTS

FOREWORD

This research was supported by the Advanced Research Projects Agency, and was monitored by the Air Force Cambridge Research Laboratories under Contract No. F 19628-67-C-0145.

The project is being carried out under the direction of Mr. Lewis Grass and Captain Edward Young as Contract Monitors for the Air Force Cambridge Research Laboratories. Mr. James Menke is the Goodyear Aerospace Project Engineer. Technical assistance was provided by Mr. Louis Girard, Mr. William Conley, Mr. Lewis Handler, and Mr. John Bezbatchenko. The contractor's report number is GER 13260.

BLANK PAGE

TABLE OF CONTENTS

LIST OF ILLUSTRATIONS

LIST OF TABLES

SYMBOLS

b	difference in weight densities of air and inflation gas ($=0.862\ \rho_{alt}\ g$), lb/ft^3
C_D	aerodynamic drag coefficient
C_L	aerodynamic lift coefficient
D	aerodynamic drag, lb
D_A	aerodynamic drag of balloon, lb
D_N	net drag, horizontal component of tension at the top end of the cable (for the lower segment in a tandem balloon system, this includes the aerodynamic drag of the middle balloon and the horizontal component of tension at the lower end of the top cable), lb
d	blowdown distance or distance from top end of cable to bottom end measured parallel to earth plane, ft
f	fineness ratio or ratios of length to diameter
h	float altitude above mean sea level, ft
h_1	altitude above mean sea level at which cable is parallel to earth plane, ft
L	aerodynamic lift, lb
L_N	net lift of balloon or vertical component of tension at the top end of the cable, lb
q	dynamic pressure ($=1/2\ \rho_{alt}V^2$), lb/ft^2
t	time at float altitude, hr
$\forall$	balloon hull volume, ft^3
v	wind velocity relative to balloon, knots
W_B	total balloon weight, lb
W_c	total weight of cable segment, lb
w	unit weight of balloon fabric, lb/ft^2
α	angle of attack, deg
θ_B	angle between the cable and the vertical at the bottom end of the cable segment, deg
ρ_{alt}	density of air at float altitude, $slugs/ft^3$
ρ_0	density of air at mean sea level, $slugs/ft^3$

Note: Pounds in the above list are pounds-force.

SECTION I

SUMMARY

An investigation of the problems related to high-altitude tethered balloon systems is in progress. This report covers the work accomplished during the first quarter of the program.

Various tethered balloon systems were investigated to determine what combination of balloons and cables has the greatest potential for high-altitude tethering. Aerodynamic characteristics, stress, weight, and other design factors were evaluated for five different balloon shapes. Cable profile parameters were evaluated considering weight, cross section area, and breaking strength of the three cable types. Data is presented in graphic form which relates balloon quantities to cable profile quantities for operation in winter and summer at two different geographic locations and float altitudes of 50,000 and 100,000 feet.

System concepts were evaluated under ARPA Contracts SD-198 through SD-201 (References 1 through 4). Since different wind profiles were assumed for each of these concepts, modifications to balloon weight and cable size were made in an effort to compare each system on an equitable basis. As a result, it was found that the systems proposed by Vitro Corporation of America and Minneapolis-Honeywell Regulator Company provided solutions. However, it should be emphasized that with other modifications, the systems proposed by Goodyear Aerospace Corporation (GAC) and General Mills Inc (GMI) may also provide solutions. To summarize, the comparisons are not too meaningful, because each contractor proposed a system for operation in different wind conditions.

Results show that balloons can be tethered at altitudes above 50,000 feet, but that no one system is best for all wind and altitude conditions. Round or natural shape balloons provide better performance in light winds at high altitudes, whereas aerodynamically shaped balloons provide better performance in high winds at intermediate altitudes. Cables made of glass fibers and epoxy resin provide better overall performance for all wind and altitude conditions investigated than either nylon or steel. In a few cases where net lift at the top of the cable is very small, steel wire appears to be better.

SECTION II

INTRODUCTION

Various tethered balloon concepts including systems described in References 1 through 4 were investigated. During the course of the investigation, it became apparent that aerodynamic effects on the balloon and cable are the most important and that operating problems, telemetry, control requirements, and ground equipment needs are similar for each system and of secondary importance relative to system feasibility.

Therefore, the major portion of the investigation thus far was that of determining aerostatic and aerodynamic lift, drag, and weight for several balloon shapes as a function of wind velocity, altitude, and other factors. A second major effort was that of determining cable size, weight, blowdown distance, and angle at the ground for various loading conditions at the top end of the cable. Variables considered were float altitude, wind profile, and cable materials.

Performance parameters for the balloons and cables are presented independent of each other. For some wind conditions, a single balloon system cannot be tethered at altitudes above 50,000 feet, but tandem balloon systems could provide a solution.

The concepts proposed in References 1 through 4 were investigated and compared. It was difficult to make comparisons, because each system was designed for a different wind profile. A decision was made to assume a Summer I and Winter I wind profile for the design of each system and to calculate performance based on volume, float altitude, and balloon type proposed in References 1 through 4. This decision necessitated calculations of new balloon and cable weights to satisfy the wind loads on the system.

When it became apparent that the frequency of occurrence of winds and expected flight durations at the intended operating locations were vital to the investigation, AFCRL initiated a study whereby design wind profiles were generated based on probability calculations.

The AFCRL study provided wind design criteria to be used in the sense of a "first approximation" evaluation of several different tethered balloon systems. The data represents best-fit estimates of integrated winds, which take into consideration the interrelations between winds at one level in the atmosphere and all levels above and below that level from the surface to 100,000 feet. Development of the data was made by matching cumulative frequency distributions with integrated wind distributions. The 75 percentile frequency distributions showed the best correlations with the 90 percentile integrated wind profiles, and these are the data given. These data should only be used in static evaluations; i.e., the tethered system is fully deployed. A much larger, statistically representative, sample of wind profiles will be needed to evaluate the operational efficiency of ascent of the systems to designed floating altitude.

All balloon and cable parameters are based on wind profiles resulting from the AFCRL study. These wind profiles are given in Table I. Winds for summer and winter at location I were selected for design calculations. The Summer I profile represents a moderate wind and Winter I the most severe wind. Velocity and dynamic pressure profiles are presented in graphic form in Figures 1 and 2. The 1962 U.S. Standard Atmosphere was used as the source for all other atmospheric data.

All design factors such as balloon and cable weight, stresses, balloon superpressure, and volume are based on a system where all balloons are at their design float altitude; i.e., loads on the system during launch and retrieval have not been considered.

Because of the large number of computations required and in some cases due to the type of solution available, digital computer and plotter facilities were used for almost all of the calculations.

Table I. Seventy-Five Percentile Winds for Summer and Winter at Three Geographic Locations

Height (ft)	Wind Velocity (knots)					
	Winter Location			Summer Location		
	I	II	III	I	II	III
Surface	15.0	10.0	10.0	10.0	10.0	7.0
5,000	27.9	20.3	20.0	22.3	20.0	12.0
10,000	44.9	35.6	15.1	26.5	18.6	16.5
15,000	62.6	58.2	18.0	31.9	18.7	19.0
20,000	80.5	78.9	21.4	38.0	19.1	20.7
25,000	99.0	92.2	25.5	47.1	20.2	19.2
30,000	115.9	105.4	29.7	56.3	21.3	17.6
35,000	125.1	111.6	35.9	64.7	25.8	18.3
40,000	125.4	115.8	43.2	72.8	32.2	20.2
45,000	113.9	110.7	38.2	62.8	36.2	20.8
50,000	102.5	105.5	31.4	50.4	39.8	21.3
55,000	91.4	97.3	25.0	37.9	43.1	22.9
60,000	79.6	75.5	23.0	26.0	42.9	30.0
65,000	67.2	47.7	24.4	25.1	43.8	34.7
70,000	60.1	33.2	27.8	25.0	45.3	40.0
75,000	55.7	29.9	33.2	27.3	48.2	46.1
80,000	48.8	28.5	37.8	29.8	51.0	51.5
85,000	39.2	29.7	41.4	34.8	54.1	55.3
90,000	35.5	30.9	40.4	36.8	56.5	61.3
95,000	34.7	31.9	39.9	35.7	58.2	68.1
100,000	35.0	32.7	42.3	43.9	59.4	72.6

Note: Data was provided by AFCRL.

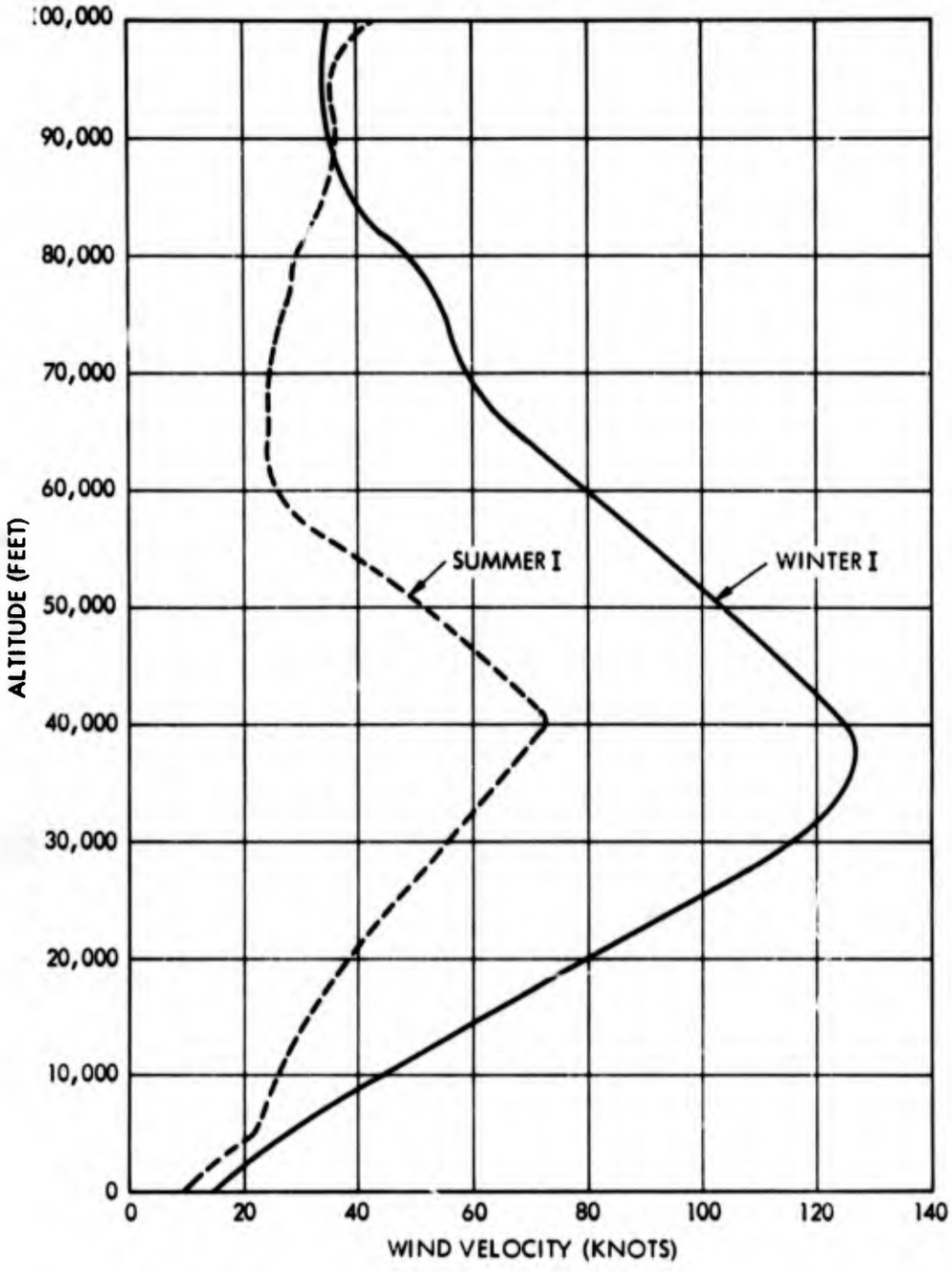

Figure 1. Variation of Wind Velocity with Altitude at Geographic Location I

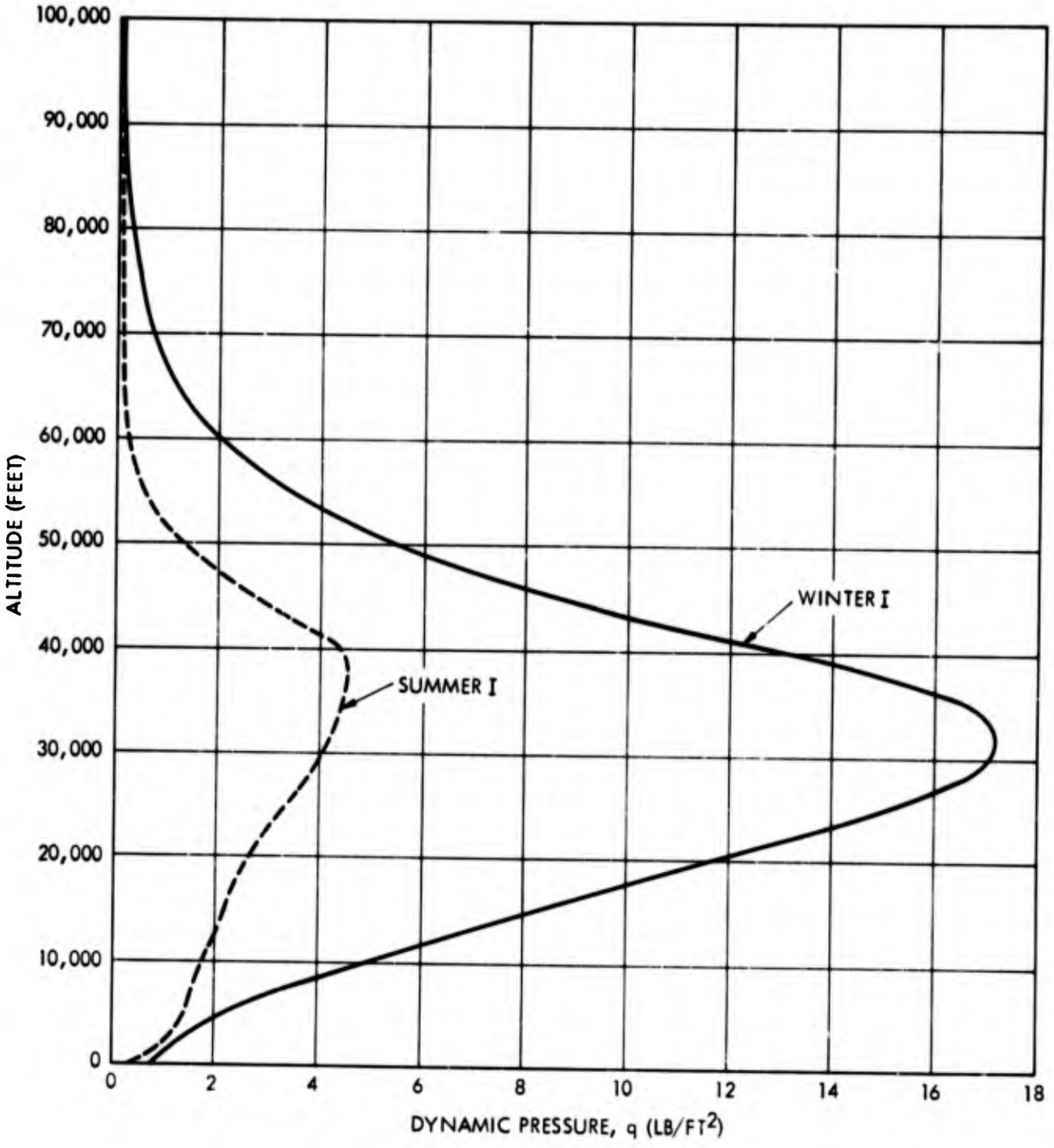

Figure 2. Variation of Dynamic Pressure with Altitude at Geographic Location I

SECTION III

TETHER CABLE TYPES AND PROPERTIES

Braided nylon rope, missile wire, and Glastran were selected as potential materials for tether cables. Physical properties data obtained from three vendors are given in Figures 3 and 4. The data are representative of the three materials used in cable construction. Glastran, a stranded E glass fiber construction manufactured by Packard Electric Division of General Motors, has the highest strength per weight of any of the three types, and it provides better overall design features than the other two types for the wind conditions assumed in this study. Missile wire, a stranded steel cable manufactured by American Chain and Cable Co, is used for aircraft tow targets. For equivalent breaking strengths, missile wire has the smallest cross section, and therefore aerodynamic forces would be expected to be less. Braided nylon rope made by Samson Cordage Works was selected as being representative of ropes made of nylon.

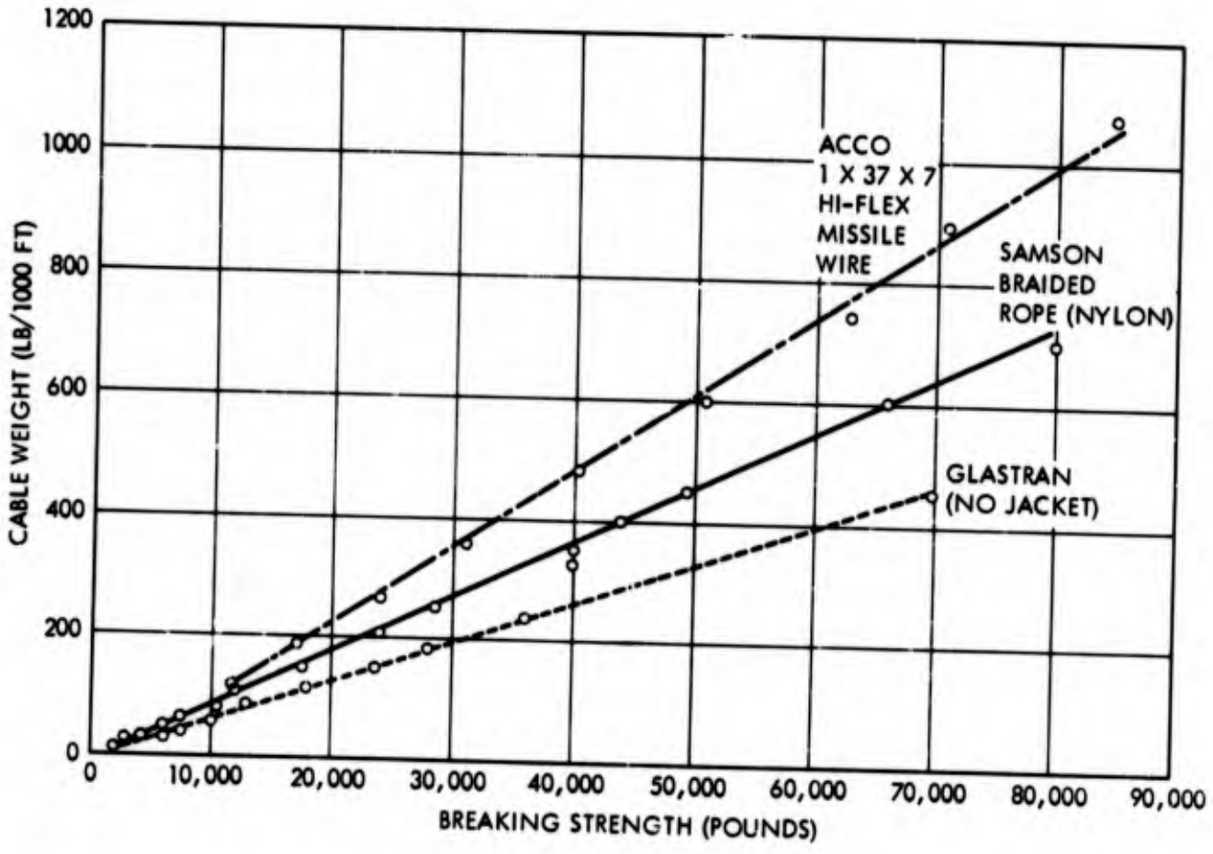

Figure 3. Cable Weight versus Breaking Strength for Various Tether Cable Materials

Although nylon rope has a higher strength per weight than steel, it is heavier than Glastran and also larger in cross section and therefore would not be expected to provide better design features. Design data was therefore prepared for only missile wire and Glastran, since it is obvious that results for Glastron would be better than for nylon in all wind conditions. It should also be noted that strength per weight is constant for strength greater than about 9000 pounds and that strength per weight is higher for strength values below 9000 pounds.

It should also be emphasized that the performance results obtained thus far in this study are based only on breaking strength, weight, cross section area, and specific wind conditions. Other factors such as cost, handling problems, fatigue, abrasion resistance, weatherability, splicing efficiency, and availability of tapered construction need to be investigated.

Low-drag cables having airfoil shaped sections were not considered, because sufficient design data is not available at this time.

Single-strand glass composite cables are expected to provide somewhat better performance than the stranded type; however, bend radii will be larger for the larger cables.

Another possible improvement is the use of S glass fibers instead of E glass. The filament strength of S glass is about 665,000 lb/in.^{2}, whereas E glass is 500,000 lb/in.^{2}.

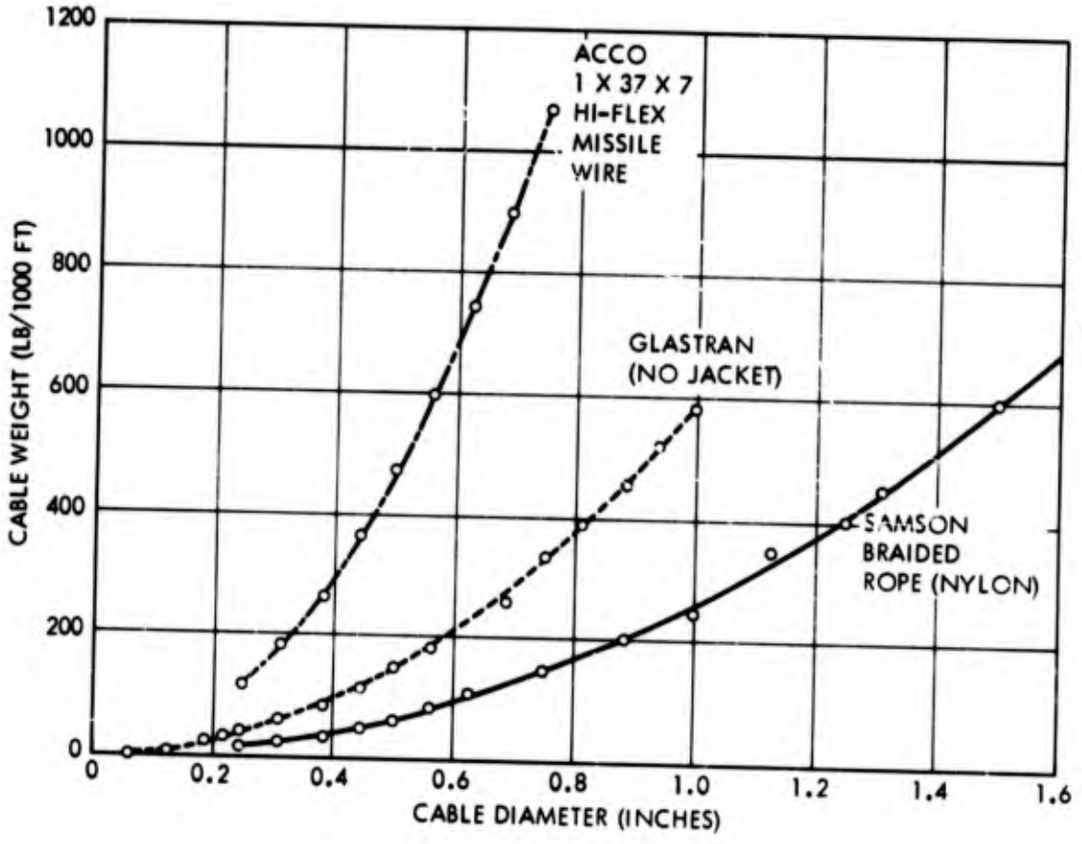

Figure 4. Cable Weight versus Cable Diameter for Various Tether Cable Materials

SECTION IV

TETHER CABLE PROFILE PARAMETERS

The profile parameters chosen for representation are angle between the cable and the vertical at the bottom end of the cable (θ_B), top end excursion or blowdown distance relative to the bottom end (d), and total weight of the cable segment (W_c). A supplemental factor is presented in conjunction with θ_B to define the altitude at which θ_B occurs (h_1). These parameters are shown in Figure 5.

Occasions arise where the cable segment tends to become horizontal at points above mean sea level, in which case the factor h_1 could be used to define altitude at which a second balloon should be added.

Parameters relating cable profile quantities to loading forces are presented in Figures 6 through 19. Abscissas and ordinates for the curves are respectively net lift or vertical component of tension at the top end of the cable (L_N) and net lift-to-drag ratio or tangent of the angle of application of the tension force at the top end of the cable (L_N/D_N).

Selection of the parameters shown in the graphs was based on the following information. Float altitudes were selected as the extremes of the region of interest, namely 50,000 and

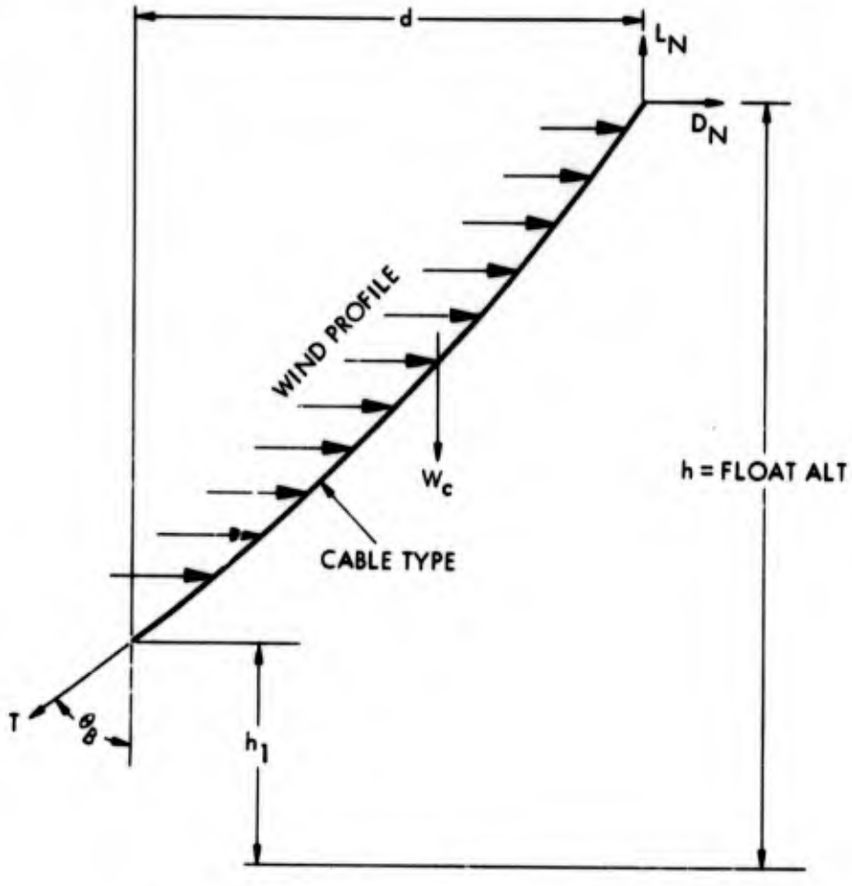

Figure 5. Tether Cable Profile Parameters

100,000 feet. Wind profiles Winter I and Summer I were selected from Table I as representing a moderate and the most severe winds existing at the three locations. Cable types chosen were based on the information presented in Figures 3 and 4, which relate cable properties.

Flexibility of the cable design solution is made possible by use of the equations given in Reference 1. GAC's IBM S/360, Model 40 digital computer was used for solutions of these equations. The computer program is flexible in that specific values of cable weight and diameter can be assumed, or cable weight, diameter, and breaking strength can be assumed to be a function of cable tension. Any float altitude, wind profile, and cable strength-weight-diameter relation may be specified. Design curves are then obtained by specifying particular values of L_N and L_N/D_N. Note that each point on the curves represents a unique cable design for the specified condition. That is, an iteration for a new tapered cable solution, based on a constant stress design using a factor of safety as selected, is obtained for each L_N/D_N. This procedure results in a cable tapering from a maximum diameter at the top to some lesser value below. It should be noted that a tapered cable may not be obtainable in all materials due to lack of manufacturing methods and equipment. Nevertheless, results of these profile calculations show comparative performance, and the data approximates a spliced configuration containing various sizes. Derivation of the difference equations and equations defining cable properties is given in Appendix I.

Glastran cable was selected because its strength-to-weight ratio is greater than nylon or missile wire cables, as shown in Figure 3, and thus will result in lighter cables for a given stress. As wind forces increase, however, the diameter of the cable becomes important; for this reason, missile wire was also chosen, since its diameter-to-weight ratio is less than the other two.

A summary of the graphs plotted is given in Table II. Each of the graphs is obtained by fairing the desired parametric curve through the many L_N versus L_N/D_N points plotted from individual computer runs. The process involved here is much the same as utilized for drawing contour maps. For this reason "eyeball" judgment of the curves was used in some areas where data points were far apart. These families of curves, however, provide sufficient accuracy for an initial estimate of profile parameters, as is the purpose here.

A method of using Figures 6 through 19 and preliminary conclusions based on data given in the figures are presented. It should be noted, however, that at the primary purpose of the curves is to establish a method of making comparisons and provide a method for careful scrutiny.

Table II. Summary of Tether Cable Profile Parameters Plotted

Float Altitude (ft)	Wind Profile	Cable Type	Parameters Plotted		
			θ_B and h_1	d	W_c
50,000	Summer I	Glastran	Fig. 6	Fig. 7	Fig. 8
50,000	Summer I	Missile wire	Fig. 9	Fig. 10	Fig. 11
50,000	Winter I	Glastran	Fig. 12	Fig. 13	Fig. 14
50,000	Winter I	Missile wire	Fig. 15	Fig. 16	Fig. 17
100,000	Summer I	Glastran	Fig. 18	None	None
100,000	Summer I	Missle wire	Fig. 19	None	None

It is not intended that final conclusions be drawn from the curves, but rather that selections of different values of the parameters be made for further study. The different values are obtained from analyses of other factors, such as realistic safe cable loads resulting from fatigue tests, analysis of gust loads on the balloon, etc. It would be presumptuous to assume that a problem with as many variables as exist here could be solved with the limited number of curves presented. Examples of the great number of significant variables to be considered are float altitude, wind profile, cable type, number of balloons, type of balloon, volume of balloon, and angle of attack.

To use the curves, proceed as follows:

(1) Select the proper group of graphs where float altitude, wind profile, and cable type are common to each.

(2) Choose the value of θ_B and h_1, d, or W_c to be satisfied by interpolating between curves for the proper L_N and L_N/D_N values. By choosing one of these parameters, a line is defined on the respective curve that shows a continuous range of L_N and L_N/D_N that will satisfy the chosen parameter. If one of the other parameters is also chosen, a second range of L_N versus L_N/D_N values is defined. If the chosen values are compatible, the lines will intersect and the point of intersection gives the only values of L_N and L_N/D_N that will satisfy both conditions.

(3) Example

(a) Given: h = 50,000 ft
wind = Winter I
cable type = missile wire

(b) Required: $\theta_B = 90^o$ at h_1 = 15,000 ft
d = 35,000 ft

(c) From Figure 15, the line defining ranges of L_N and L_N/D_N for $\theta_B = 90^o$ at h_1 = 15,000 feet is found, and from Figure 16, the range of L_N and L_N/D_N for d = 35,000 feet is found. It can be seen that these lines intersect at L_N = 54,000 pounds and L_N/D_N = 11.5. Cable weight (W_c) is now also defined and is given in Figure 17. Cable weight for L_N = 54,000 pounds and L_N/D_N = 11.5 is about 40,000 pounds. This is the total cable weight from float altitude to 15,000 feet above mean sea level, the point where it becomes horizontal.

(d) The next step is to determine what balloon size and type, if any, will have a net lift of 54,000 pounds and a net lift-to-drag ratio of 12. An example of this is given in a later section.

Other variations for use of these curves can be made by specifying other cable parameters or balloon parameters, as discussed in a later section.

Initial conclusions inferred from a study of the graphs are as follows:

(1) For Summer I winds and cables extending downward from 50,000 feet above mean sea level.

(a) Single-increment cable solutions are possible for both glass cable and missile wire, provided that adequate values of L_N and L_N/D_N are applied at the cable top end. The definition of single increment as used here is a length of cable having loads applied at each end and only aerodynamic forces and weight applied over its entire length.

(b) Glass cable provides solutions with more favorable bottom end cable conditions (θ_B and h_1) than does missile wire for all cases except for very small L_N values (less than 5000 pounds).

(2) For Winter I winds and cables extending downward from 50,000 feet above mean sea level.

(a) No realistic single-increment solutions are available for either glass cable or missile wire. Reasonable solutions are available, however, if another balloon is utilized at an intermediate altitude (e.g., at altitudes from 10,000 to 30,000 feet). Since a single-increment solution is not possible, no combination of balloons where all balloons are at altitudes above 50,000 feet will provide a solution.

(b) Glass cable provides solutions with more favorable bottom end cable conditions than does missile wire for all cases except for small L_N values (less than 5000 pounds).

(3) For Summer I winds and cables extending downward from 100,000 feet above mean sea level.

(a) No reasonable single-increment solutions are available for missile wire. Reasonable solutions are available, however, if another balloon is utilized at an intermediate altitude (e.g., at altitudes from 10,000 to 40,000 feet).

(b) Glass cable provides single-increment solutions if adequate L_N and L_N/D_N values are applied.

(4) Glastran cable (Figure 18) exhibits an unusual series of dips near a value of L_N = 5000 pounds. Missile wire (Figure 19) does not exhibit this dip. It is believed that this dip can be explained by the equation that was used to describe the strength-weight relation of Glastran cable (See Appendix I for equations used to define cable properties.) A discontinuity exists at a breaking strength of 9000 pounds.

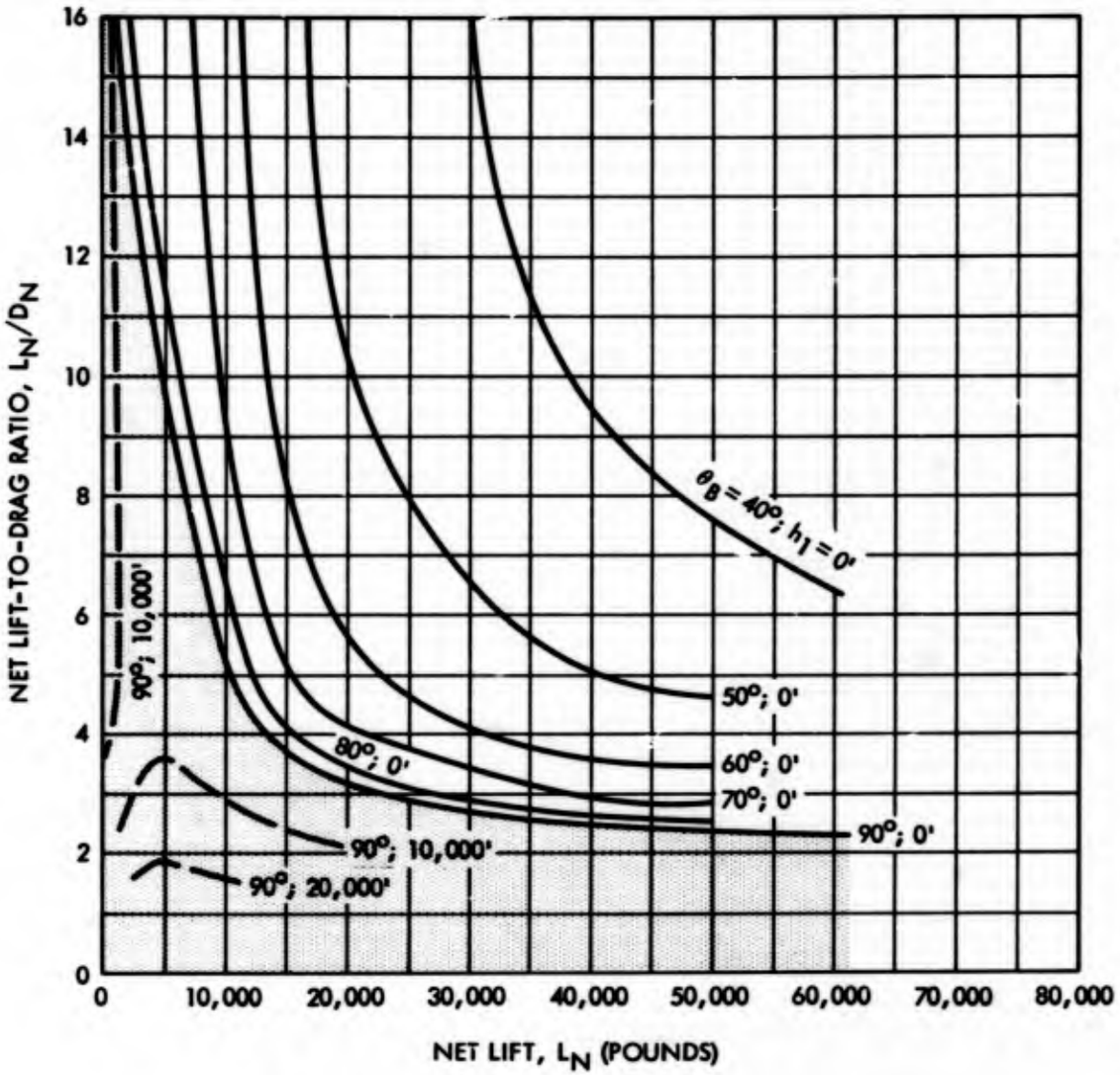

NOTES:

1. EACH POINT ON THE CURVES REPRESENTS A UNIQUE CABLE FOR THE VALUES OF L_N AND D_N AT THE TOP END OF THE CABLE.
2. EACH UNIQUE CABLE IS TAPERED SUCH THAT BREAKING STRENGTH IS EQUAL TO TWICE THE TENSION AT ANY POINT ON THE CABLE.
3. SHADED AREA REPRESENTS L_N AND D_N VALUES FOR CASES WHERE CABLE BECOMES HORIZONTAL TO GROUND PLANE AT ELEVATIONS ABOVE MSL.

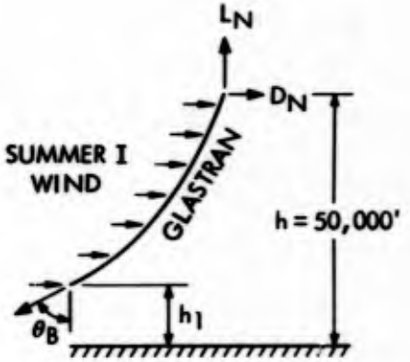

Figure 6. Angle at Bottom End of Cable for Glastran at 50,000 Feet in Summer I Wind

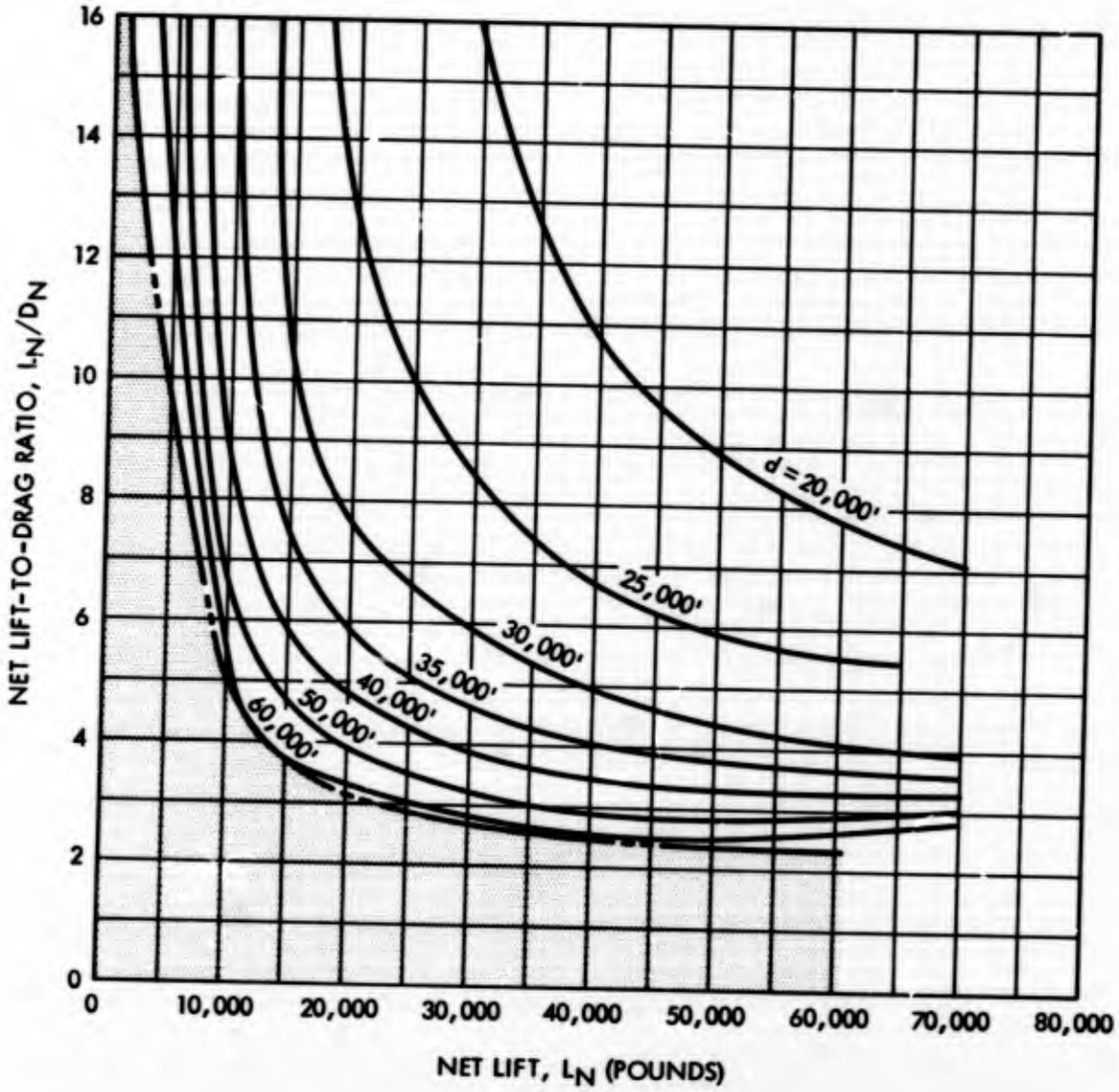

NOTES:

1. EACH POINT ON THE CURVES REPRESENTS A UNIQUE CABLE FOR THE VALUES OF L_N AND D_N AT THE TOP END OF THE CABLE.
2. EACH UNIQUE CABLE IS TAPERED SUCH THAT BREAKING STRENGTH IS EQUAL TO TWICE THE TENSION AT ANY POINT ON THE CABLE.
3. SHADED AREA REPRESENTS L_N AND D_N VALUES FOR CASES WHERE CABLE BECOMES HORIZONTAL TO GROUND PLANE AT ELEVATIONS ABOVE MSL.

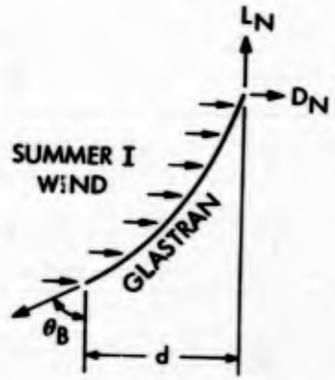

Figure 7. Blowdown Distance for Glastran at 50,000 Feet in Summer I Wind

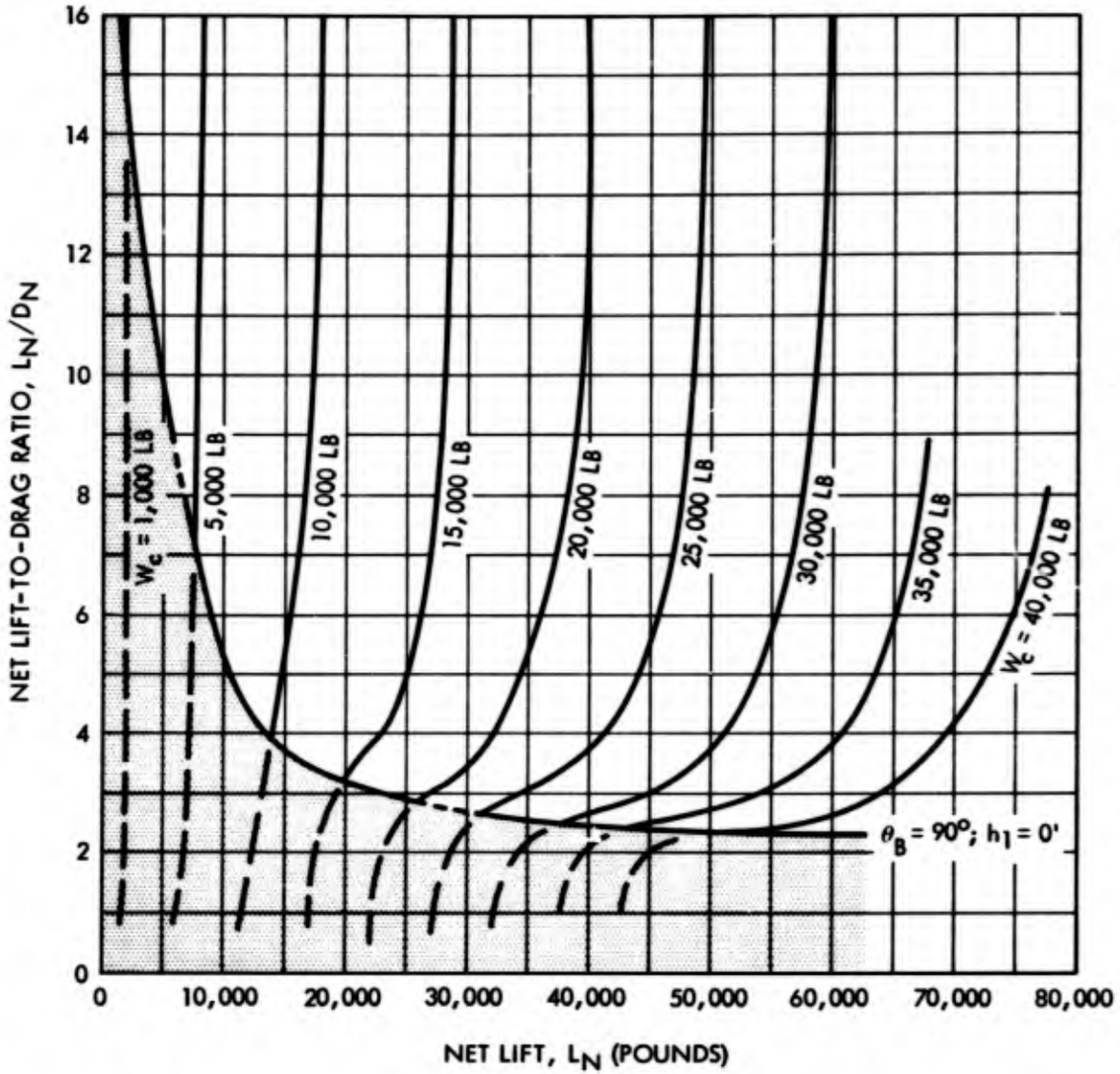

NOTES:

1. EACH POINT ON THE CURVES REPRESENTS A UNIQUE CABLE FOR THE VALUES OF L_N AND D_N AT THE TOP END OF THE CABLE.
2. EACH UNIQUE CABLE IS TAPERED SUCH THAT BREAKING STRENGTH IS EQUAL TO TWICE THE TENSION AT ANY POINT ON THE CABLE.
3. SHADED AREA REPRESENTS L_N AND D_N VALUES FOR CASES WHERE CABLE BECOMES HORIZONTAL TO GROUND PLANE AT ELEVATIONS ABOVE MSL.

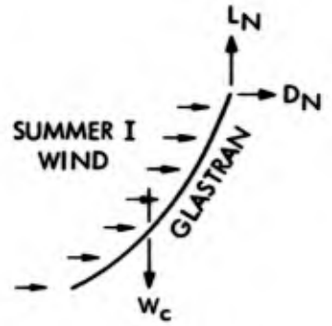

Figure 8. Cable Weight for Glastran at 50,000 Feet in Summer I Wind

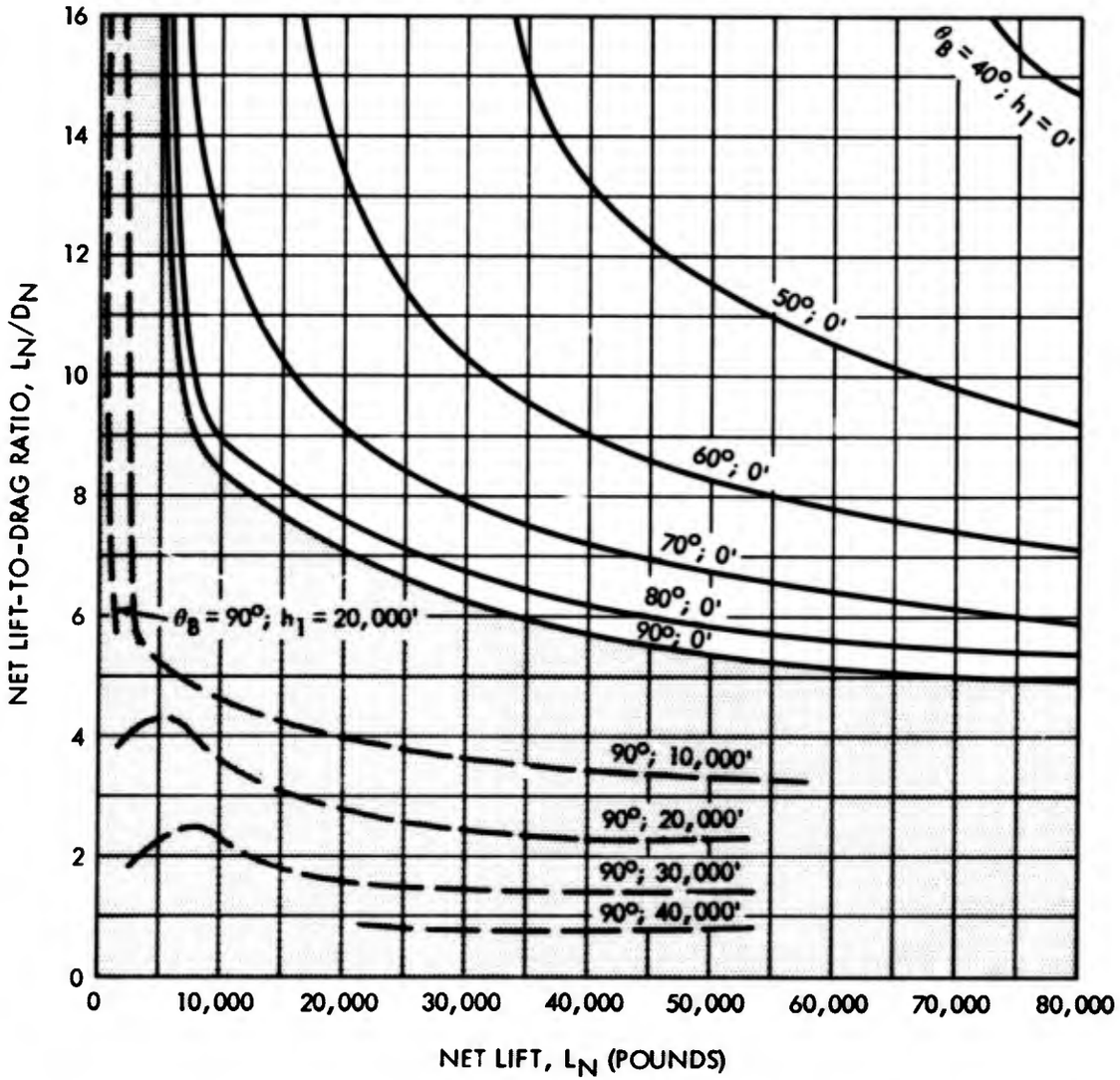

NOTES:

1. EACH POINT ON THE CURVES REPRESENTS A UNIQUE CABLE FOR THE VALUES OF L_N AND D_N AT THE TOP END OF THE CABLE.
2. EACH UNIQUE CABLE IS TAPERED SUCH THAT BREAKING STRENGTH IS EQUAL TO TWICE THE TENSION AT ANY POINT ON THE CABLE.
3. SHADED AREA REPRESENTS L_N AND D_N VALUES FOR CASES WHERE CABLE BECOMES HORIZONTAL TO GROUND PLANE AT ELEVATIONS ABOVE MSL.

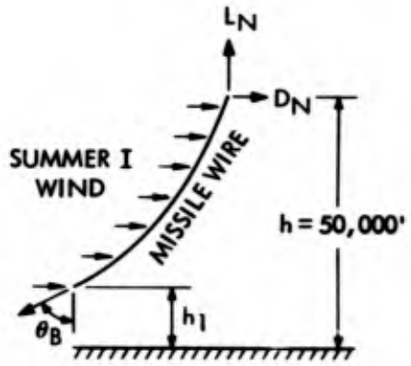

Figure 9. Angle at Bottom End of Cable for Missile Wire at 50,000 Feet in Summer I Wind

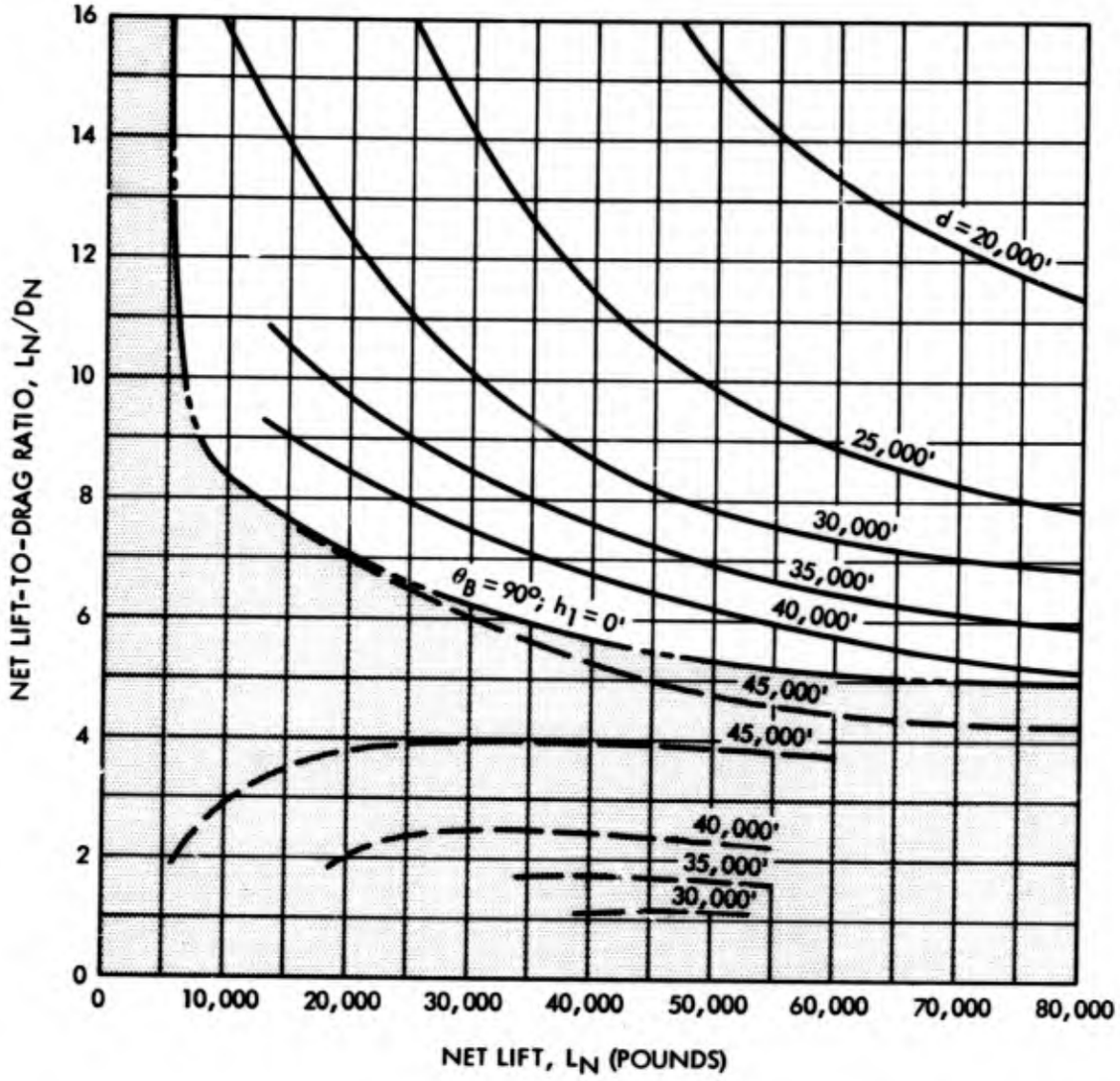

NOTES:

1. EACH POINT ON THE CURVES REPRESENTS A UNIQUE CABLE FOR THE VALUES OF L_N AND D_N AT THE TOP END OF THE CABLE.
2. EACH UNIQUE CABLE IS TAPERED SUCH THAT BREAKING STRENGTH IS EQUAL TO TWICE THE TENSION AT ANY POINT ON THE CABLE.
3. SHADED AREA REPRESENTS L_N AND D_N VALUES FOR CASES WHERE CABLE BECOMES HORIZONTAL TO GROUND PLANE AT ELEVATIONS ABOVE MSL.

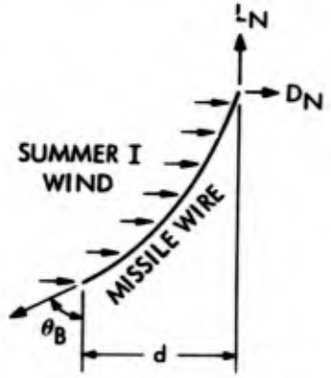

Figure 10. Blowdown Distance for Missile Wire at 50,000 Feet in Summer I Wind

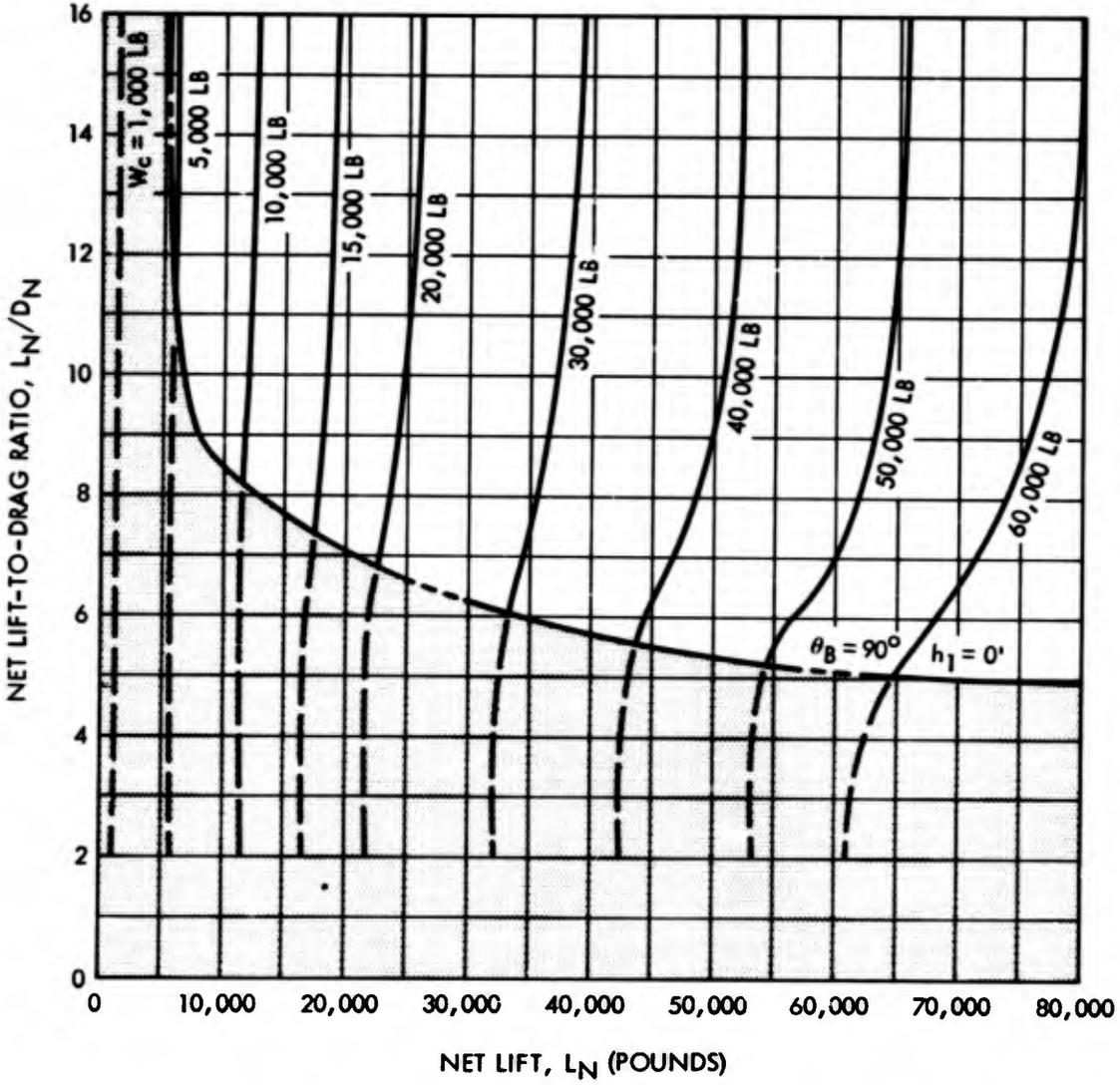

NOTES:

1. EACH POINT ON THE CURVES REPRESENTS A UNIQUE CABLE FOR THE VALUES OF L_N AND D_N AT THE TOP END OF THE CABLE.
2. EACH UNIQUE CABLE IS TAPERED SUCH THAT BREAKING STRENGTH IS EQUAL TO TWICE THE TENSION AT ANY POINT ON THE CABLE.
3. SHADED AREA REPRESENTS L_N AND D_N VALUES FOR CASES WHERE CABLE BECOMES HORIZONTAL TO GROUND PLANE AT ELEVATIONS ABOVE MSL.

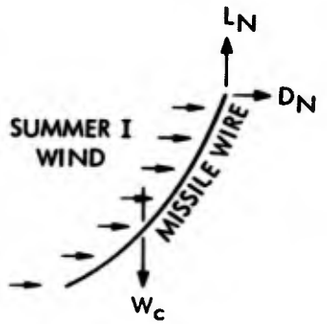

Figure 11. Cable Weight for Missile Wire at 50,000 Feet in Summer I Wind

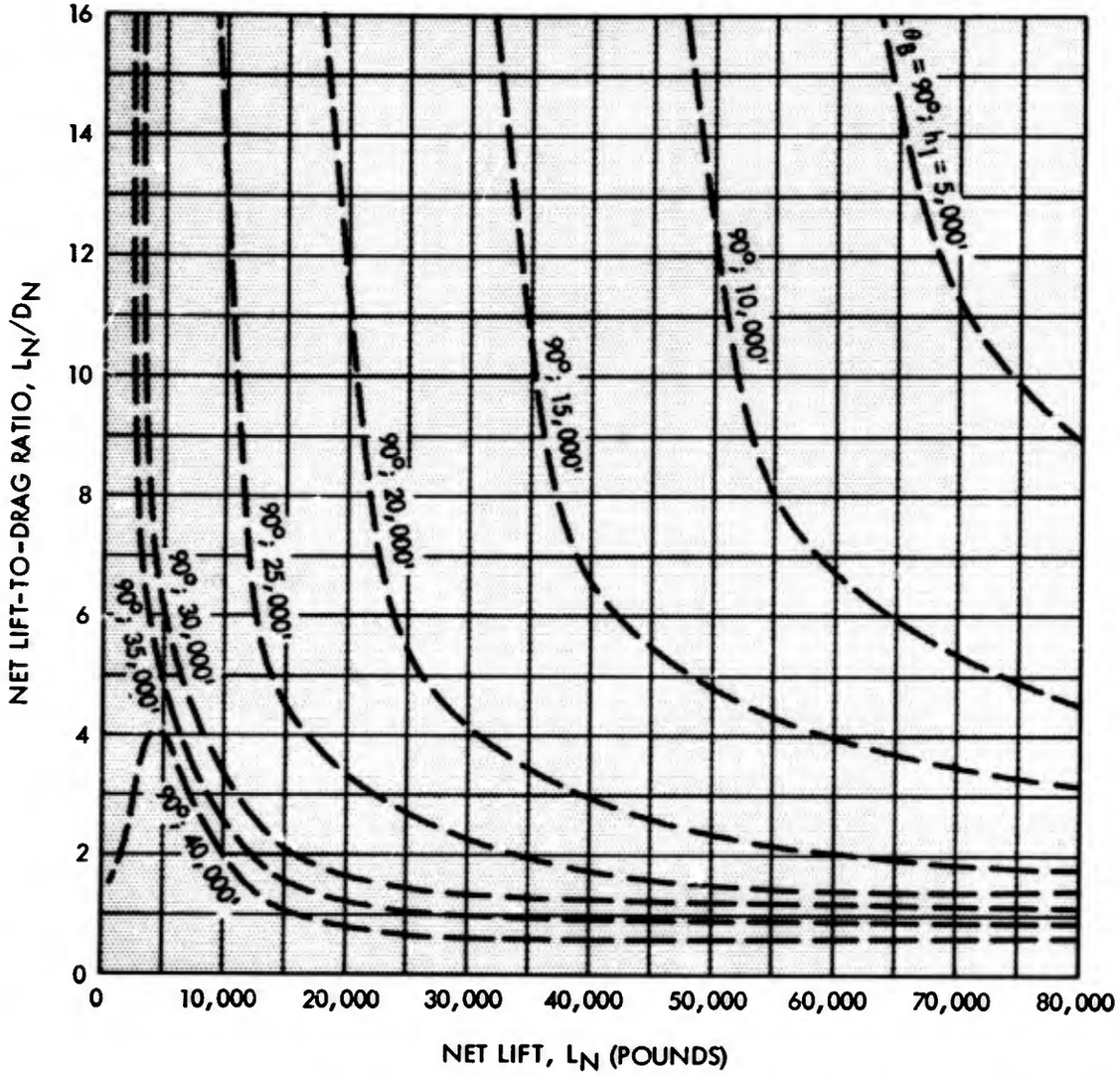

NOTES:

1. EACH POINT ON THE CURVES REPRESENTS A UNIQUE CABLE FOR THE VALUES OF L_N AND D_N AT THE TOP END OF THE CABLE.
2. EACH UNIQUE CABLE IS TAPERED SUCH THAT BREAKING STRENGTH IS EQUAL TO TWICE THE TENSION AT ANY POINT ON THE CABLE.
3. SHADED AREA REPRESENTS L_N AND D_N VALUES FOR CASES WHERE CABLE BECOMES HORIZONTAL TO GROUND PLANE AT ELEVATIONS ABOVE MSL.

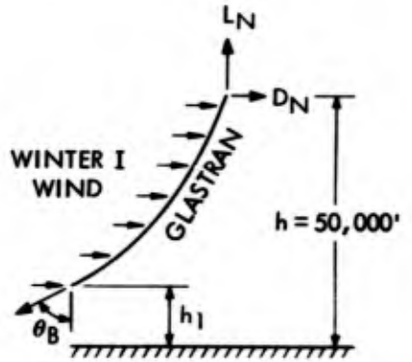

Figure 12. Angle at Bottom End of Cable for Glastran at 50,000 Feet in Winter I Wind

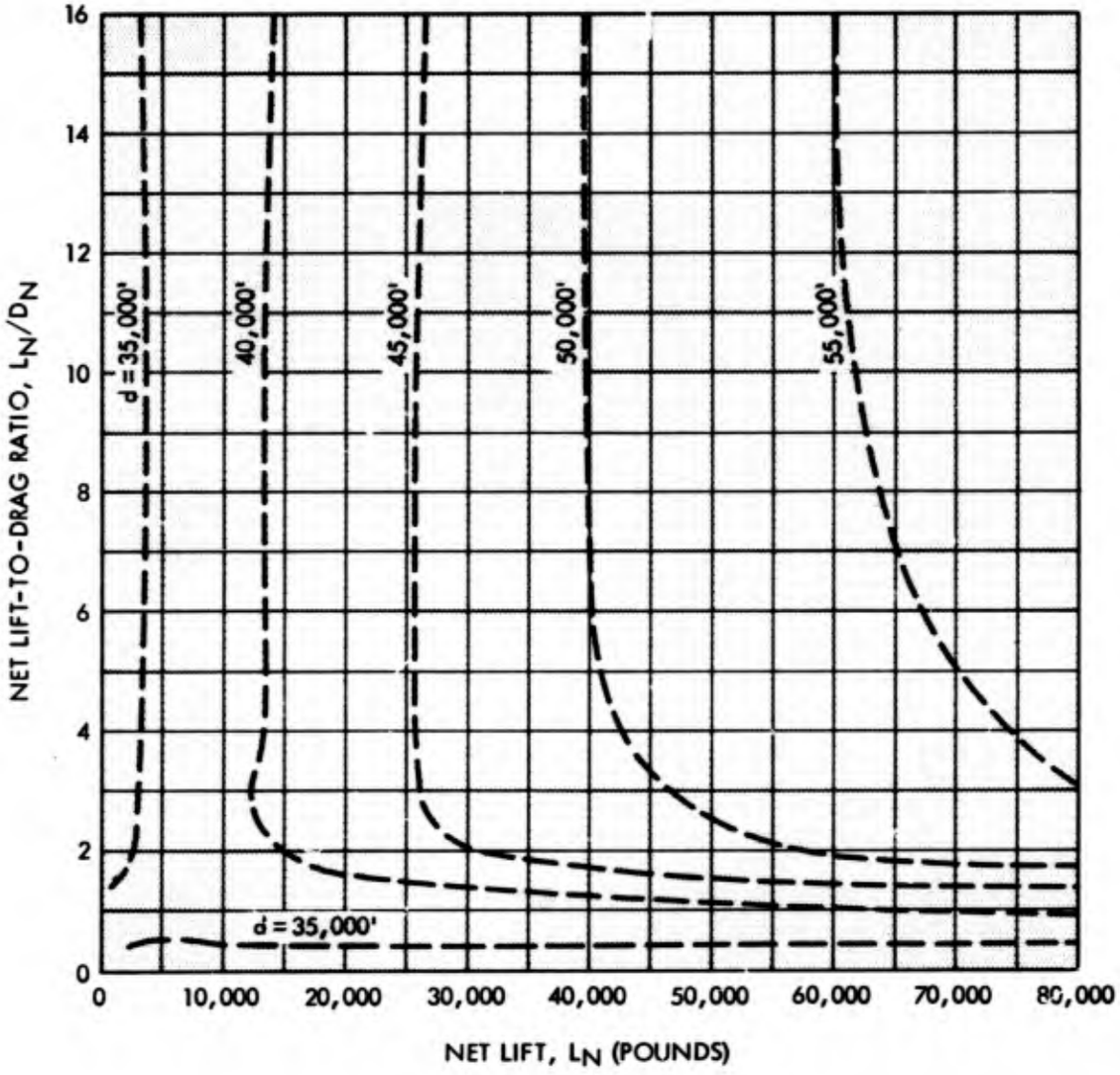

NOTES:

1. EACH POINT ON THE CURVES REPRESENTS A UNIQUE CABLE FOR THE VALUES OF L_N AND D_N AT THE TOP END OF THE CABLE.
2. EACH UNIQUE CABLE IS TAPERED SUCH THAT BREAKING STRENGTH IS EQUAL TO TWICE THE TENSION AT ANY POINT ON THE CABLE.
3. SHADED AREA REPRESENTS L_N AND D_N VALUES FOR CASES WHERE CABLE BECOMES HORIZONTAL TO GROUND PLANE AT ELEVATIONS ABOVE MSL.

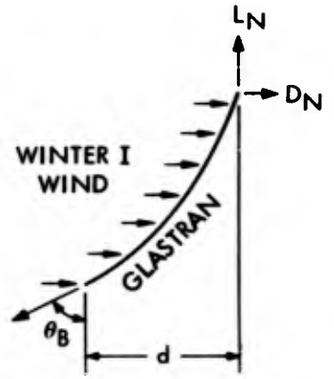

Figure 13. Blowdown Distance for Glastran at 50,000 Feet in Winter I Wind

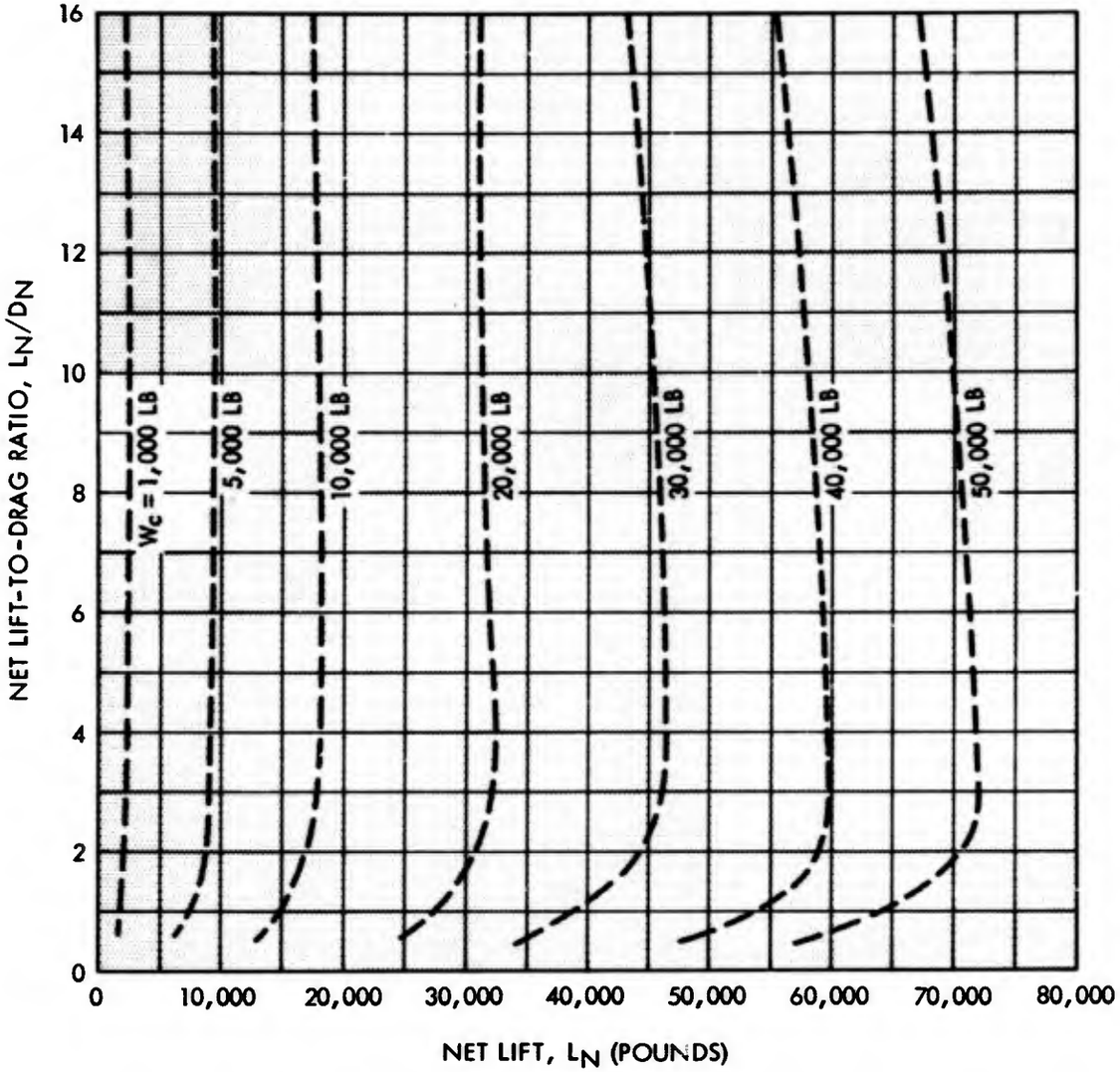

NOTES:

1. EACH POINT ON THE CURVES REPRESENTS A UNIQUE CABLE FOR THE VALUES OF L_N AND D_N AT THE TOP END OF THE CABLE.
2. EACH UNIQUE CABLE IS TAPERED SUCH THAT BREAKING STRENGTH IS EQUAL TO TWICE THE TENSION AT ANY POINT ON THE CABLE.
3. SHADED AREA REPRESENTS L_N AND D_N VALUES FOR CASES WHERE CABLE BECOMES HORIZONTAL TO GROUND PLANE AT ELEVATIONS ABOVE MSL.

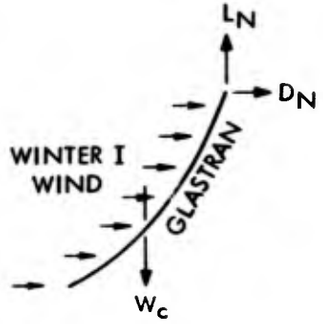

Figure 14. Cable Weight for Glastran at 50,000 Feet in Winter I Wind

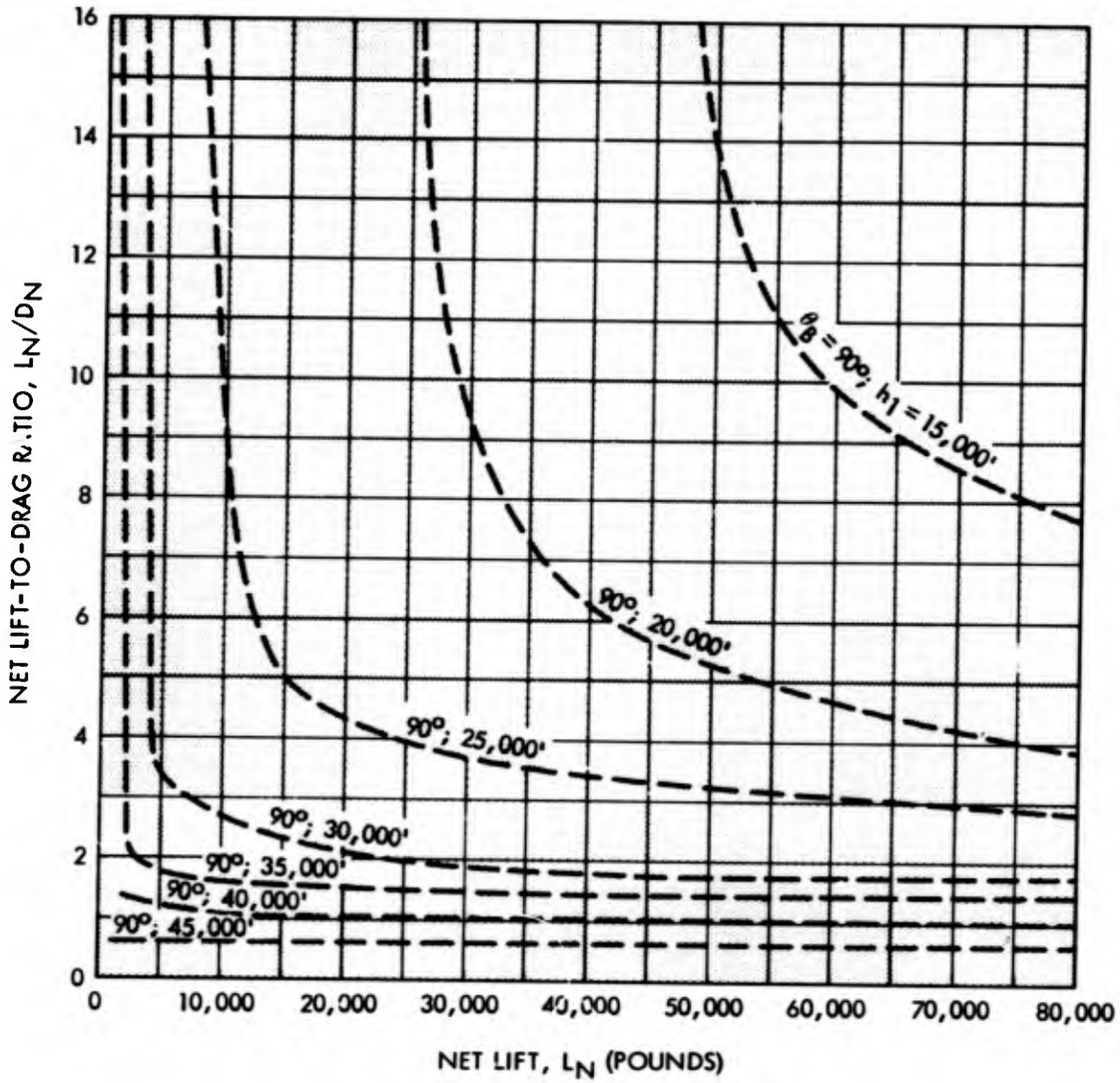

NOTES:

1. EACH POINT ON THE CURVES REPRESENTS A UNIQUE CABLE FOR THE VALUES OF L_N AND D_N AT THE TOP END OF THE CABLE.
2. EACH UNIQUE CABLE IS TAPERED SUCH THAT BREAKING STRENGTH IS EQUAL TO TWICE THE TENSION AT ANY POINT ON THE CABLE.
3. SHADED AREA REPRESENTS L_N AND D_N VALUES FOR CASES WHERE CABLE BECOMES HORIZONTAL TO GROUND PLANE AT ELEVATIONS ABOVE MSL.

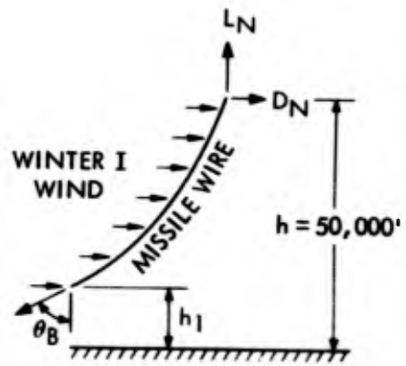

Figure 15. Angle at Bottom End of Cable for Missile Wire at 50,000 Feet in Winter I Wind

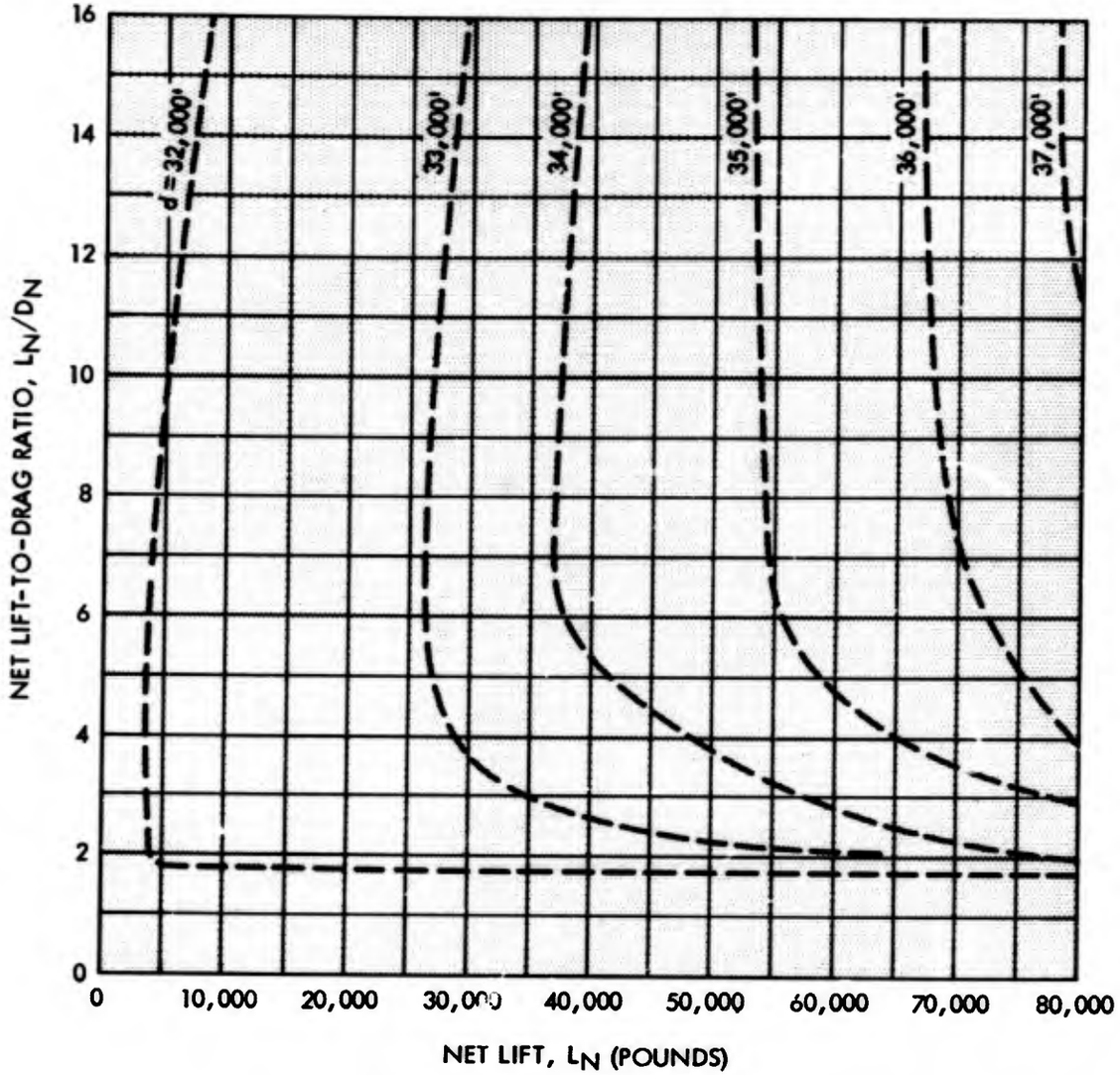

NOTES:

1. EACH POINT ON THE CURVES REPRESENTS A UNIQUE CABLE FOR THE VALUES OF L_N AND D_N AT THE TOP END OF THE CABLE.
2. EACH UNIQUE CABLE IS TAPERED SUCH THAT BREAKING STRENGTH IS EQUAL TO TWICE THE TENSION AT ANY POINT ON THE CABLE.
3. SHADED AREA REPRESENTS L_N AND D_N VALUES FOR CASES WHERE CABLE BECOMES HORIZONTAL TO GROUND PLANE AT ELEVATIONS ABOVE MSL.

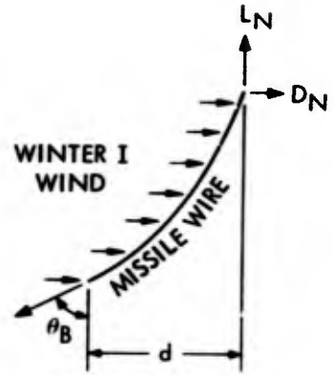

Figure 16. Blowdown Distance for Missile Wire at 50,000 Feet in Winter I Wind

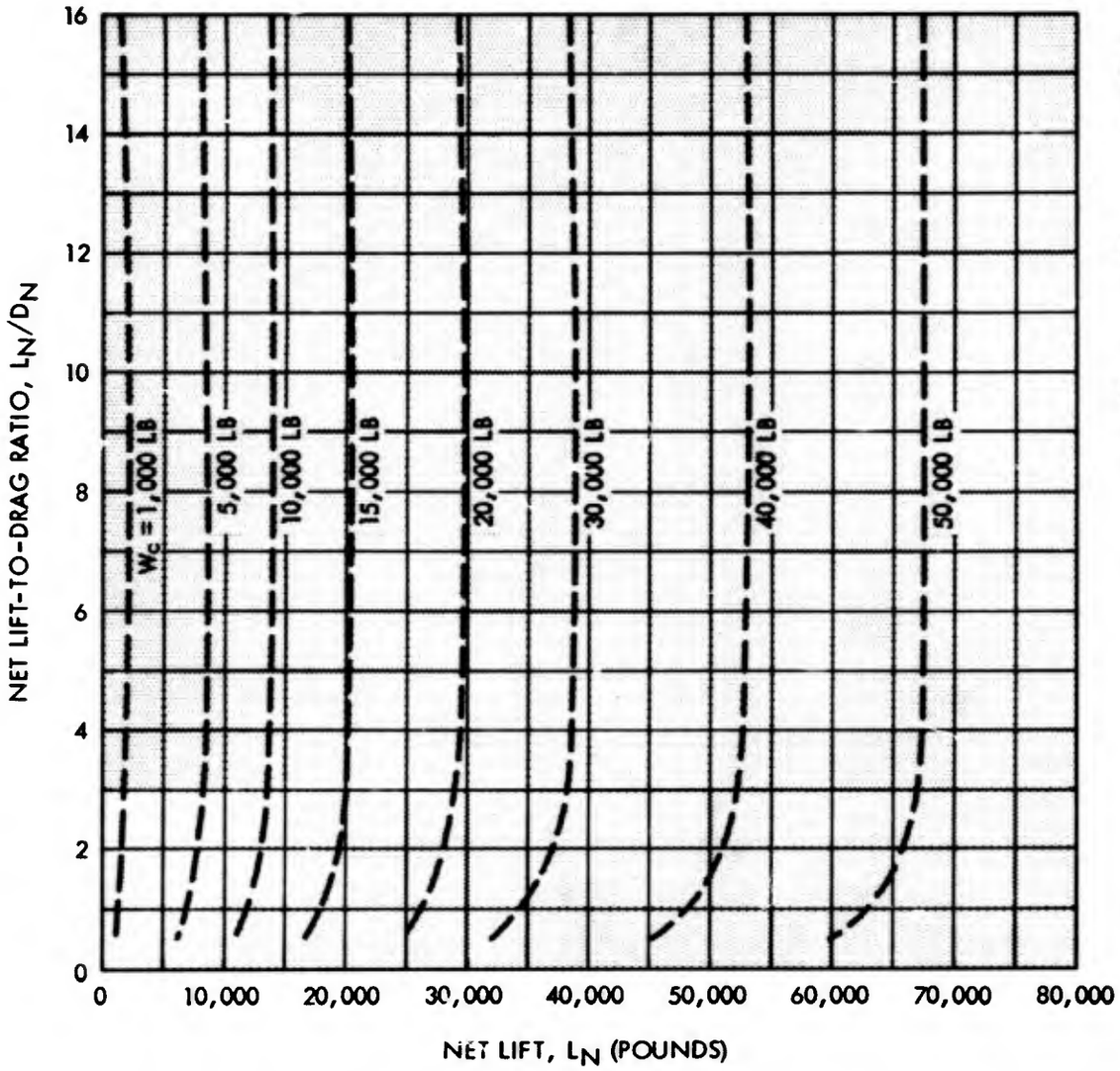

NOTES:

1. EACH POINT ON THE CURVES REPRESENTS A UNIQUE CABLE FOR THE VALUES OF L_N AND D_N AT THE TOP END OF THE CABLE.
2. EACH UNIQUE CABLE IS TAPERED SUCH THAT BREAKING STRENGTH IS EQUAL TO TWICE THE TENSION AT ANY POINT ON THE CABLE.
3. SHADED AREA REPRESENTS L_N AND D_N VALUES FOR CASES WHERE CABLE BECOMES HORIZONTAL TO GROUND PLANE AT ELEVATIONS ABOVE MSL.

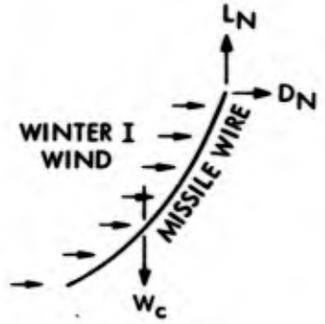

Figure 17. Cable Weight for Missile Wire at 50,000 Feet in Winter I Wind

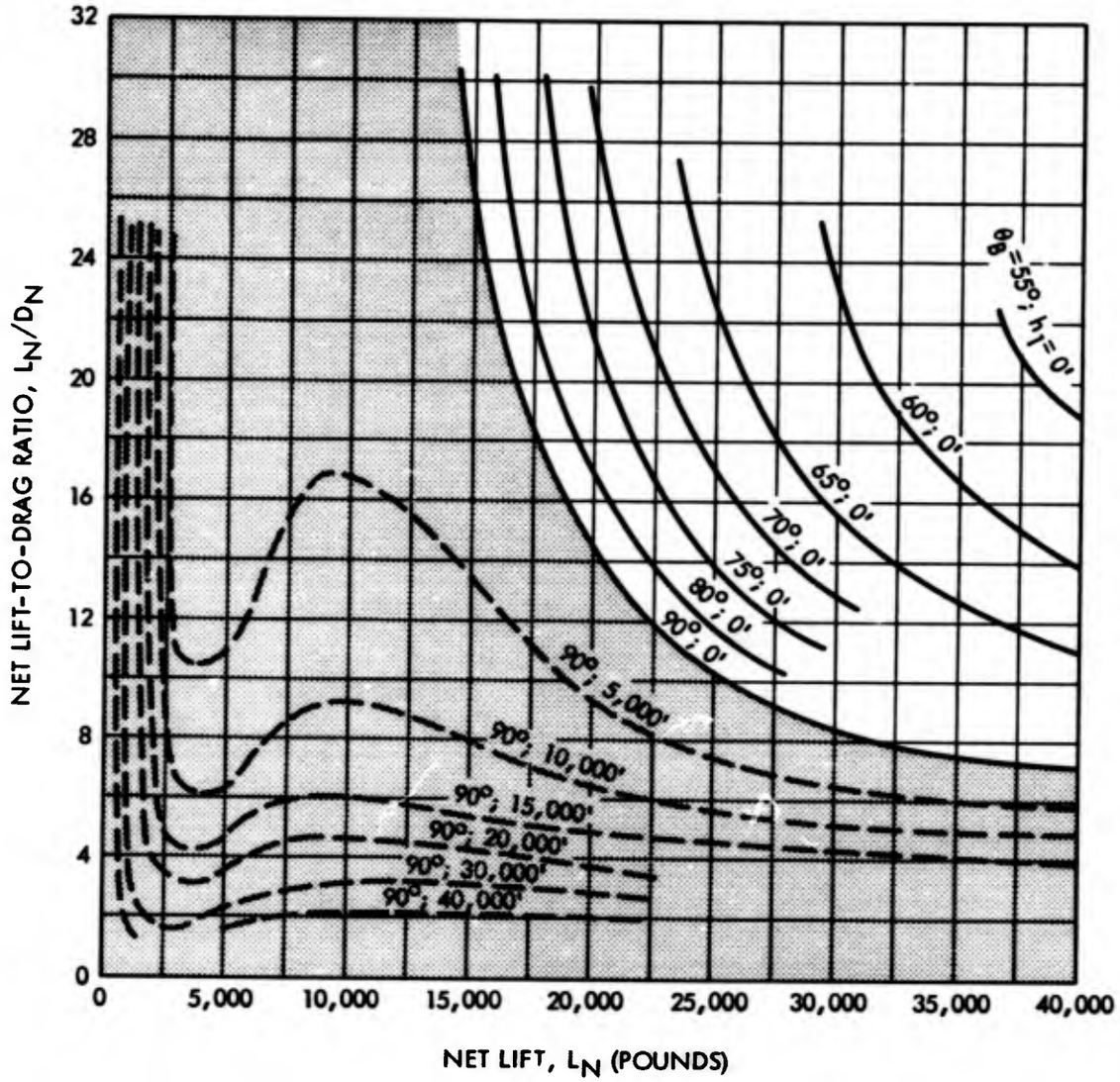

NOTES:

1. EACH POINT ON THE CURVES REPRESENTS A UNIQUE CABLE FOR THE VALUES OF L_N AND D_N AT THE TOP END OF THE CABLE.
2. EACH UNIQUE CABLE IS TAPERED SUCH THAT BREAKING STRENGTH IS EQUAL TO TWICE THE TENSION AT ANY POINT ON THE CABLE.
3. SHADED AREA REPRESENTS L_N AND D_N VALUES FOR CASES WHERE CABLE BECOMES HORIZONTAL TO GROUND PLANE AT ELEVATIONS ABOVE MSL.

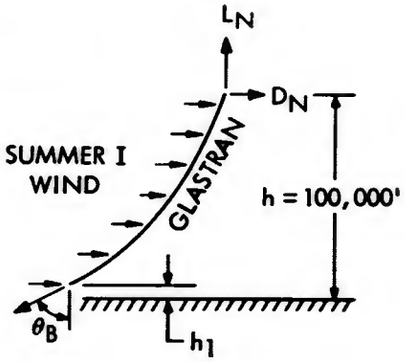

Figure 18. Angle at Bottom End of Cable for Glastran at 100,000 Feet in Summer I Wind

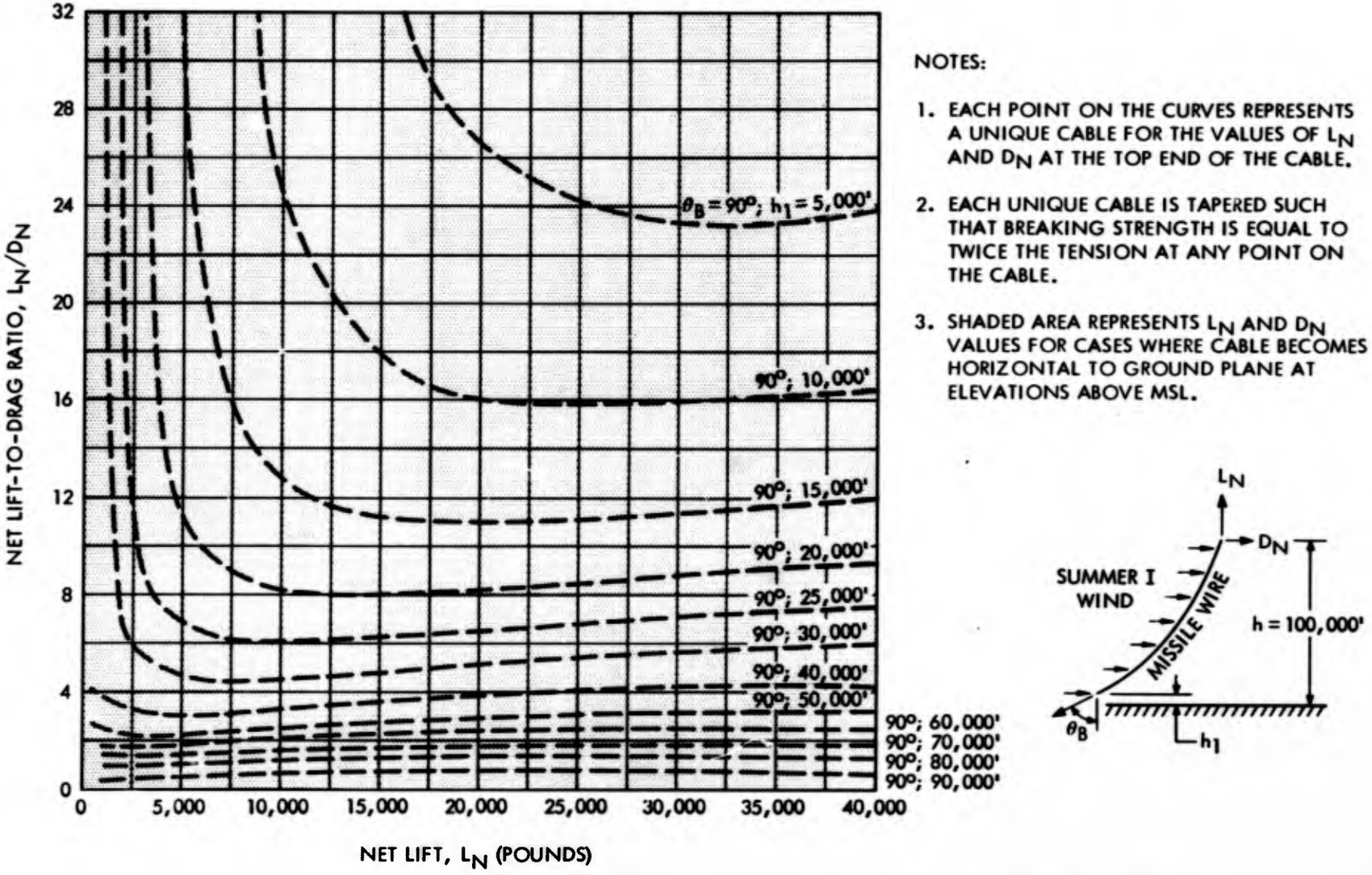

Figure 19. Angle at Bottom End of Cable for Missile Wire at 100,000 Feet in Summer I Wind

SECTION V

BALLOON TYPES AND CHARACTERISTICS

A. BALLOONS SELECTED FOR STUDY

To evaluate the merits of various balloon shapes, four aerodynamically shaped balloons and a superpressure, natural shape balloon were investigated. The aerodynamically shaped balloons investigated were Navy Class C, Vee-Balloon[1], modified Mark II, and ram air C. These shapes were selected for investigation because a wide range of physical and functional characteristics such as aerodynamic lift, drag, fineness ratio, volume per surface area, fin size, etc is encompassed. In addition, wind tunnel test data is available for all of the balloons except the natural shape, and full-scale vehicles of each except the modified Mark II have been flown. Realistic size and weight scale factors can therefore be obtained for analyzing balloons designed for many wind velocities and altitudes.

B. BALLOON DESCRIPTION

1. General

A ballonet system for accommodating volume change and maintaining pressure for all aerodynamically shaped balloons was assumed. A blower and battery type were assumed for all ballonet systems except ram air C. For this type, it was assumed that dynamic pressure alone, such as in the barrage balloons, was sufficient to retain pressurization. Additional work is required to ascertain the performance capabilities of dilatable-type balloons. In this type, elastic fabric or cords are used to retain balloon pressure.

In order to give relative size of each balloon with respect to a different shape of comparable volume, Table III lists the basic dimensions and areas for the various shapes, each with a hull volume of 1,000,000 ft^3.

Table III. Physical Dimensions of Various Balloon Configurations for a Hull Volume of 1,000,000 Ft^3

Balloon Type	Hull Volume (ft^3)	Length (ft)	Max Dia (ft)	Wetted Area (ft^2)	Fineness Ratio	No. of Horiz Fins	Each Horiz Fin			No. of Vert. Fins	Each Vert. Fin			Total Wetted Area (ft^2)	Total Volume (ft^3)
							Projected Area (ft^2)	Wetted Area (ft^2)	Volume (ft^3)		Projected Area (ft^2)	Wetted Area (ft^2)	Volume (ft^3)		
Navy Class C	1,000,000	262	99.2	55,500	2.64	2	3000	7,000	17,250	1	3000	7,000	17,250	76,600	1,052,000
Vee-Balloon	1,000,000	256	64	69,700	4.0	1	7070	15,600	62,400	2	785	1,800	2,300	88,900	1,067,000
Modified Mark II	1,000,000	352	75.1	67,000	4.7	2	7250	16,000	64,800	2	3150	12,500	36,800	108,000	1,207,000
Ram Air C	1,000,000	262	99.2	55,500	2.64	2	3000	7,000	17,250	1	3000	7,000	17,250	76,600	1,052,000
Superpressure, Natural Shape	1,000,000	96*	104	50,500	--	0	0	0	0	0	0	0	0	50,500	1,000,000

*Maximum height

[1]Trade-mark, Goodyear Aerospace Corporation, Akron, Ohio

2. Navy Class C Configuration

The Navy Class C configuration (Figure 20) was chosen because it represents the typical single-hull, streamlined shape, tethered balloon. The basic shape consists of a streamlined hull with a Y-type tail. The balloon exhibits the lowest aerodynamic lift coefficient and drag coefficient of any of the aerodynamically shaped balloons selected for evaluation.

3. Vee-Balloon Configuration

The Vee-Balloon (Figure 21) was chosen because it represents the high aerodynamic lifting type tethered balloon. The configuration consists of two streamline hulls joined at the nose to form a V. A horizontal tail is connected between the hulls with the two vertical fins mounted on the aft end of each hull. The balloon exhibits one of the highest aerodynamic lift coefficients and the highest drag coefficient of any of the aerodynamically shaped balloons selected for the evaluation.

4. Modified Mark II Configuration

The modified Mark II configuration (Figure 22) was selected because the aerodynamic characteristics fall between that of the Navy Class C and the Vee-Balloon. The configuration consists of a single hull balloon with large end plate type vertical fins mounted on the horizontal fins. The balloon exhibits one of the highest aerodynamic lift coefficients of any of the aerodynamically shaped balloons selected for evaluation, and the drag coefficient is between that of the Navy Class C and the Vee-Balloon.

5. Ram Air C Configuration

The ram air C configuration (Figure 20) is identical with the Navy Class C configuration except for the pressurization system. It was assumed that a ballonet was kept full by the stagnation pressure of the wind, similar to barrage-type balloons.

6. Superpressure, Natural Shape Balloons

A natural shape balloon (Figure 23) was selected for evaluation because it offers possibilities for reefing. These balloons are usually used in non-tethered applications. The basic shape is that of an inverted teardrop, and the balloons are usually designed to have zero stress in the circumferential direction. The aerodynamic drag coefficient of the natural shape balloon was the highest of all the configurations evaluated.

A specific pressurization system was not selected; however, several candidate designs, as shown in Figure 24, could possibly satisfy the design requirements.

C. AERODYNAMIC CHARACTERISTICS

Aerodynamic lift coefficients, drag coefficients, and lift-to-drag ratio versus angle of attack for the aerodynamically shaped balloons are given in Figures 25, 26, and 27. The hull volume to the two-thirds power was used as a reference area.

The angle of attack for zero lift was modified slightly for the Vee-Balloon in order to be consistent with other wind-tunnel test data for this shape.

Since no wind tunnel information is available for the natural shape balloon, the aerodynamic characteristics of a sphere of equal volume were assumed. The lift coefficient is zero, and the drag coefficient versus Reynolds Number is given in Figure 28. The projected area of the sphere was used as a reference area, and data was taken from References 5 through 8. The drag coefficient for the sphere based on hull volume to the two-thirds power for Reynolds Numbers of 300,000 and 500,000 is plotted in Figure 26 to give a comparison of relative magnitudes.

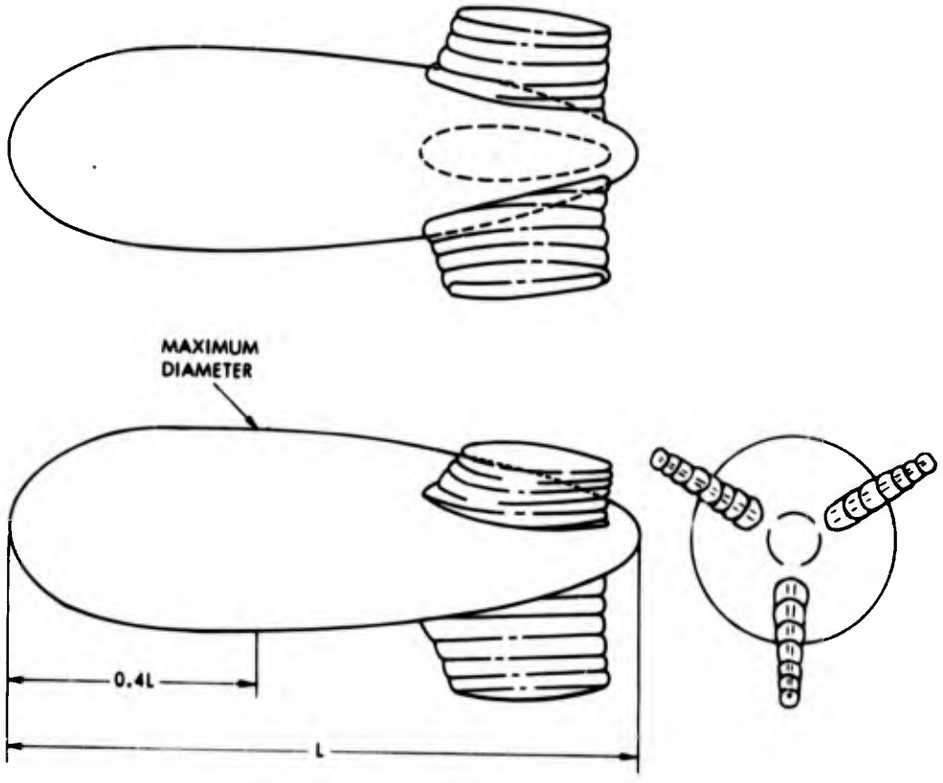

Figure 20. Class C and Ram Air C Balloon Configuration

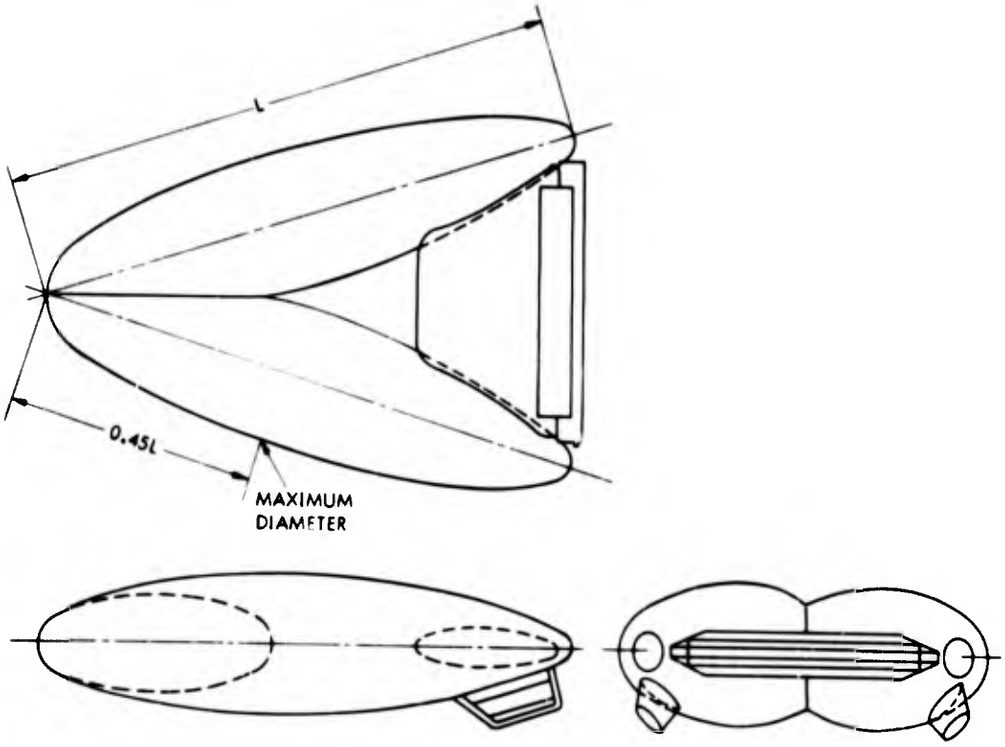

Figure 21. Vee-Balloon Configuration

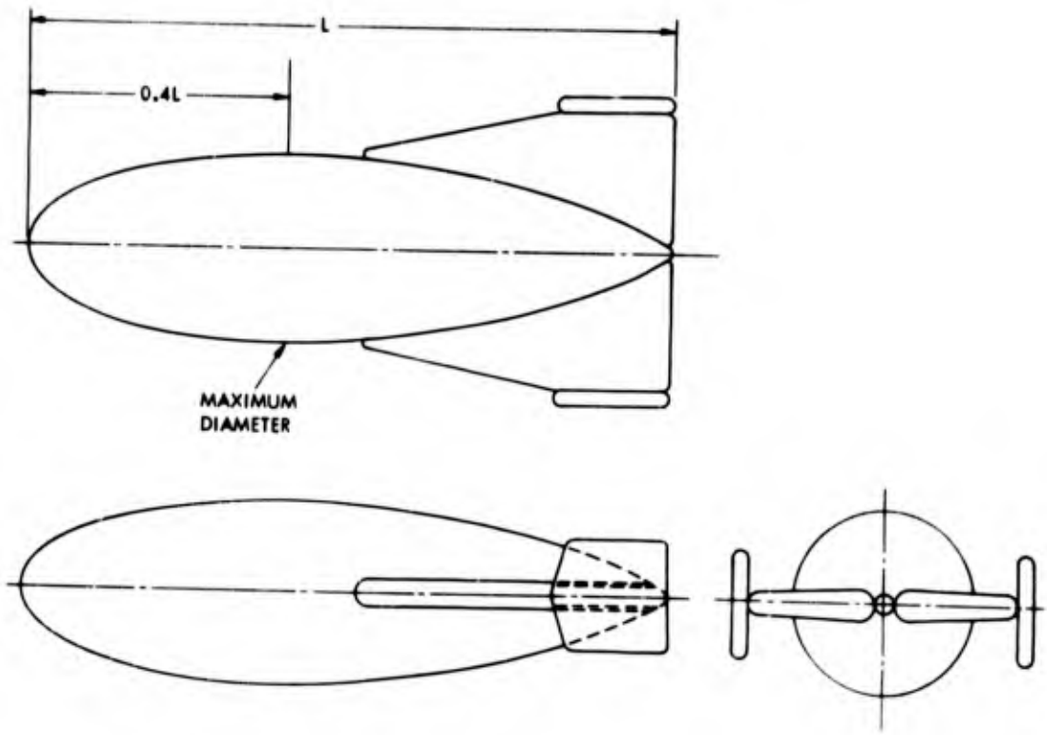

Figure 22. Modified Mark II Balloon Configuration

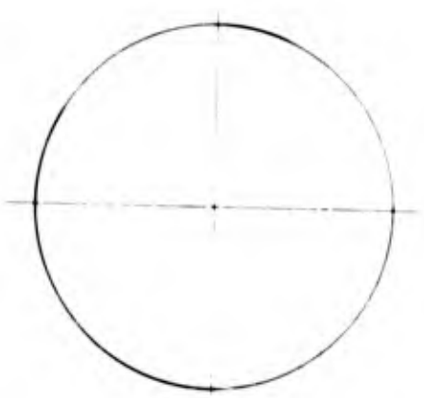

Figure 23. Superpressure, Natural Shape Balloon Configuration

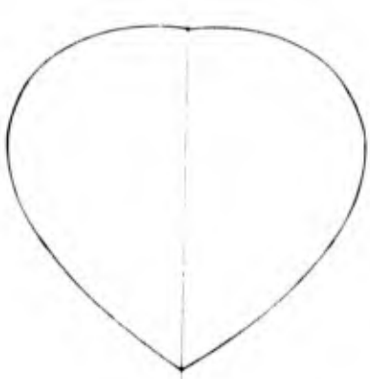

BALLONET-TANGENT HARNESS TYPE

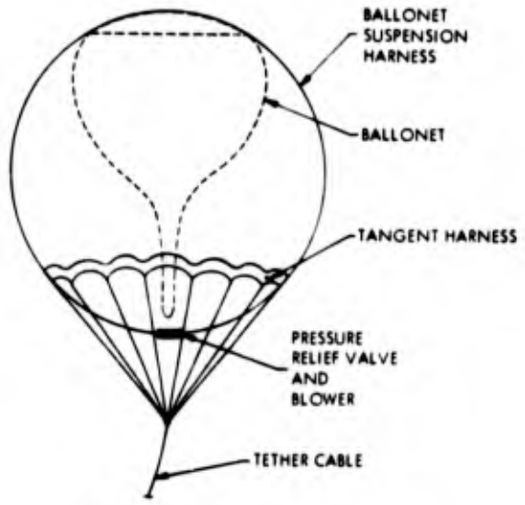

ADVANTAGE	DISADVANTAGES
1. Lightweight	1. Flight duration limited by energy storage capacity for blower. 2. Large drag at intermediate altitudes due to full inflation volume.

INVERTED TYPE

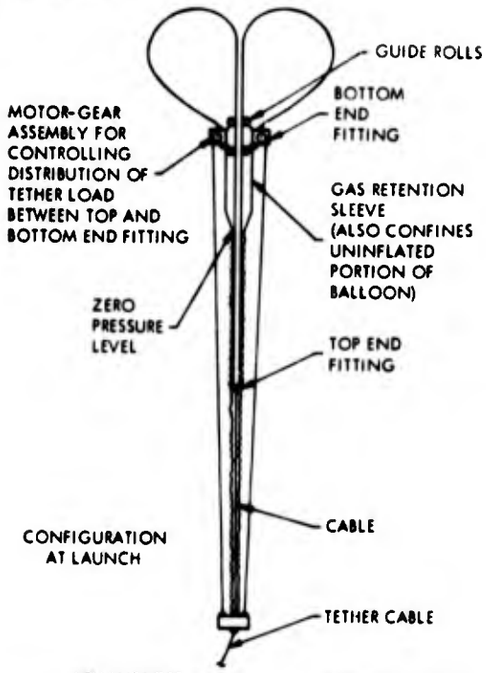

ADVANTAGES	DISADVANTAGE
1. Low stress concentration in balloon. 2. Lightweight balloon material due to top loading. 3. Reefed ascent and descent possible.	1. High design cost.

TRACTION STORAGE DRUM TYPE

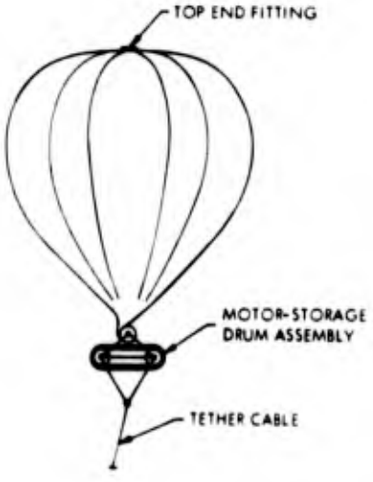

ADVANTAGE	DISADVANTAGES
1. Pressurized ascent and descent possible.	1. Possibly high stress concentration in balloon. 2. Heavy.

REEFED TYPE

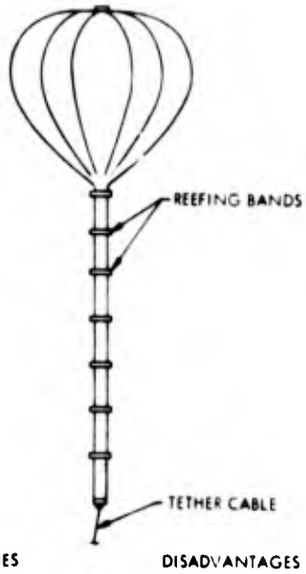

ADVANTAGES	DISADVANTAGES
1. Simple design. 2. Low stress concentration. 3. Low cost. 4. Lightweight.	1. Re-reefing for descent not possible. 2. System reliability poor. (Failure to release any one band causes system failure.)

Figure 24. Potential Pressurization Systems for Superpressure, Natural Shape Balloons

SOURCE OF DATA	SYMBOL	CONFIGURATION	TYPE
GAC, MEMO T-5618, TMI-4, SEPT 1, 1964	◇	SINGLE HULL, f = 4.7, END PLATES ON HORIZ FINS	MODIFIED MARK II
GAC, MEMO T-6372, TMI-4, DEC 13, 1965	△	2 HULLS, f = 4 (EACH), HORIZ FIN BETWEEN HULLS	35-DEG VEE
GMI (UNIV OF DETROIT, PROJ 314)	○	SINGLE HULL, f = 2.64, Y FINS, RUN 86	NAVY CLASS C

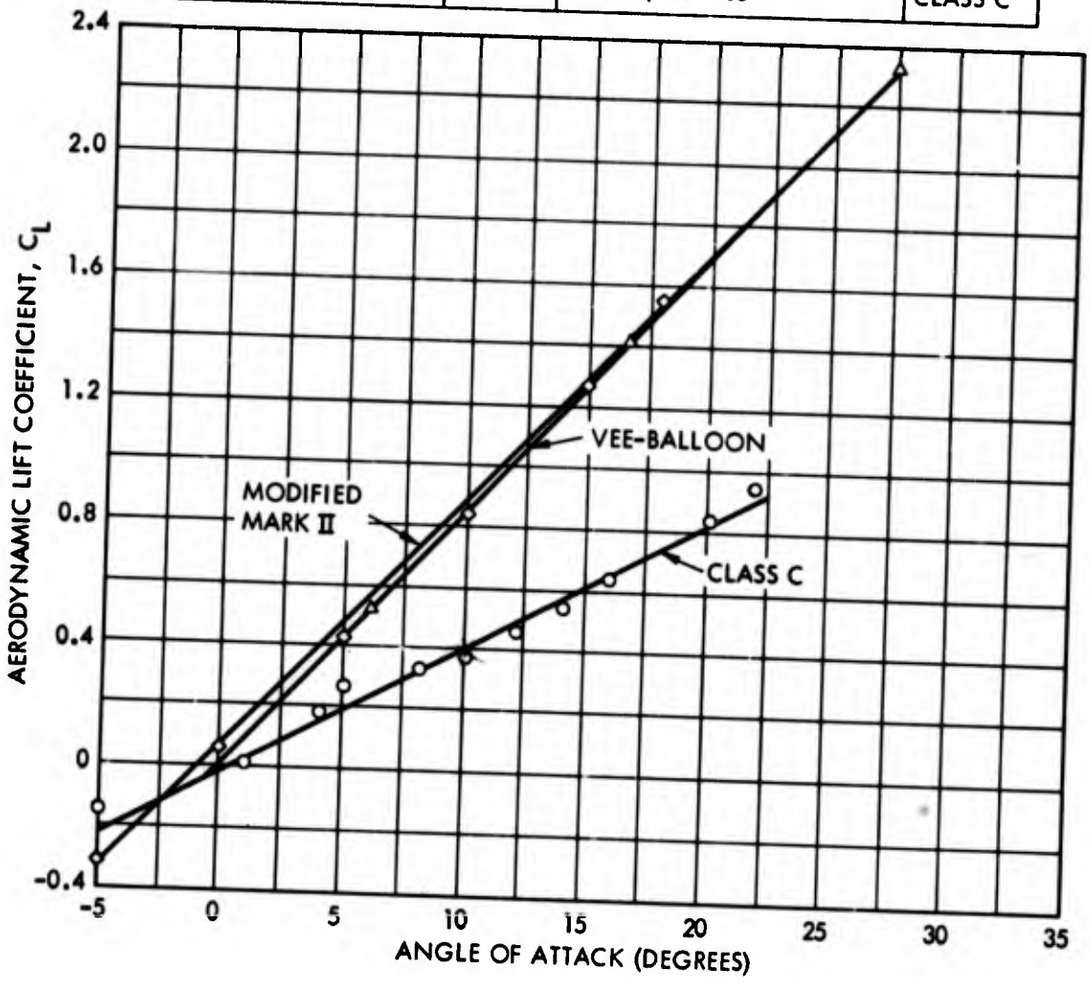

Figure 25. Aerodynamic Lift Coefficient versus Angle of Attack for Various Balloon Configurations

SOURCE OF DATA	SYMBOL	CONFIGURATION	TYPE
GAC, MEMO T-5618, TMI-4, SEPT 1, 1964	◇	SINGLE HULL, f = 4.7, END PLATES ON HORIZ FINS	MODIFIED MARK II
GAC, MEMO T-6372, TMI-4, DEC 13, 1965	△	2 HULLS, f = 4 (EACH), HORIZ FIN BETWEEN HULLS	35-DEG VEE
GMI (UNIV OF DETROIT, PROJ 314)	○	SINGLE HULL, f = 2.64, Y FINS, RUN 86	NAVY CLASS C
	□	SPHERE	

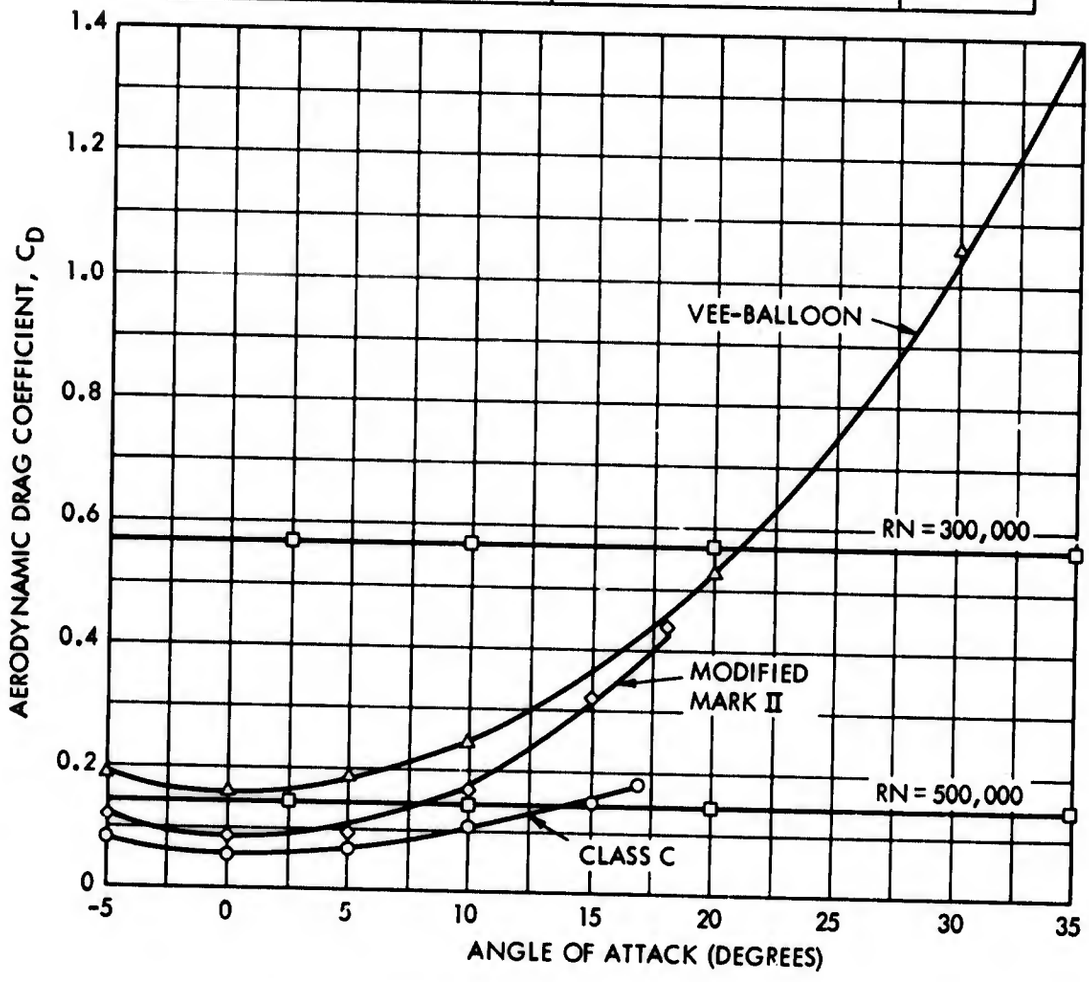

Figure 26. Aerodynamic Drag Coefficient versus Angle of Attack for Various Balloon Configurations

SOURCE OF DATA	SYMBOL	CONFIGURATION	TYPE
GAC, MEMO T-5618, TMI-4, SEPT 1, 1964	◇	SINGLE HULL, f = 4.7, END PLATES ON HORIZ FINS	MODIFIED MARK II
GAC, MEMO T-6372, TMI-4, DEC 13, 1965	△	2 HULLS, f = 4 (EACH), HORIZ FIN BETWEEN HULLS	35-DEG VEE
GMI (UNIV OF DETROIT, PROJ 314)	○	SINGLE HULL, f = 2.64, Y FINS, RUN 86	NAVY CLASS C

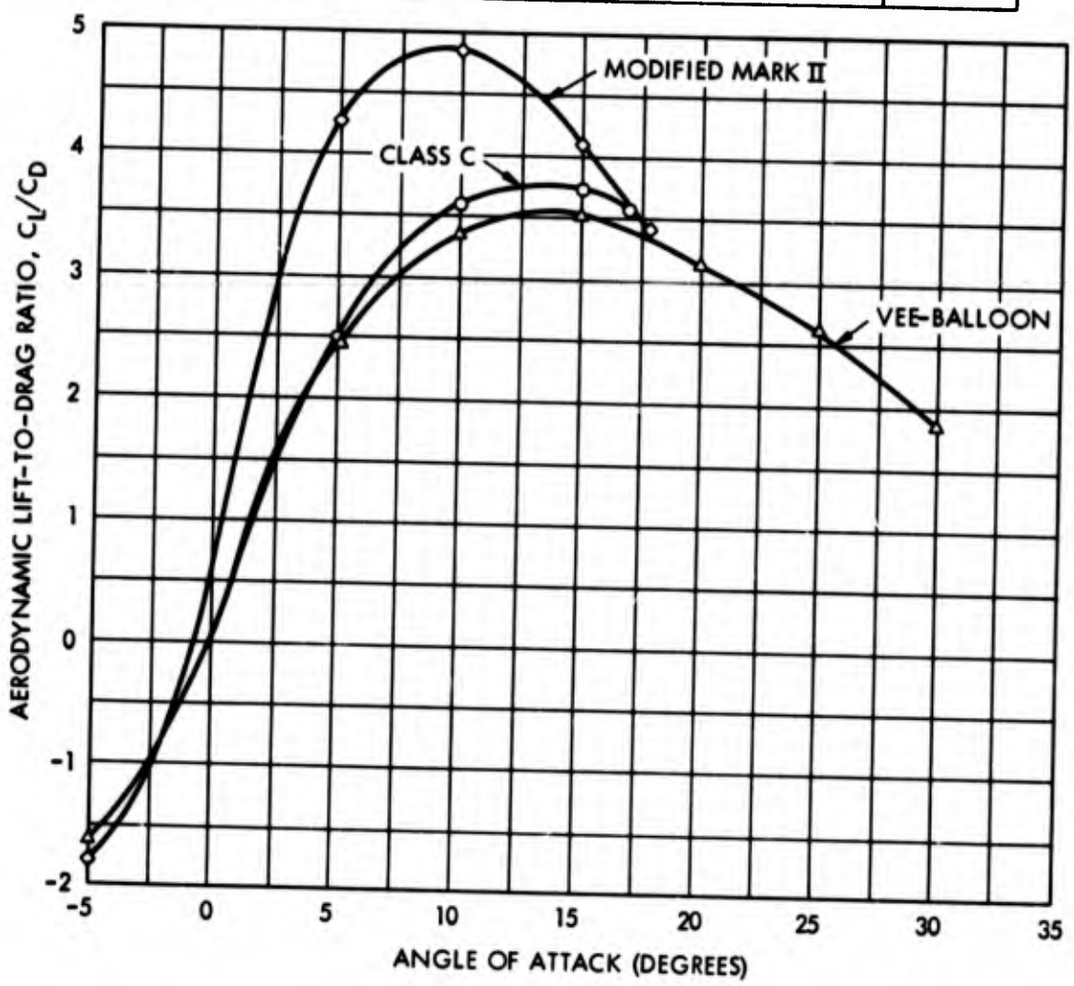

Figure 27. Aerodynamic Lift-to-Drag Ratio versus Angle of Attack for Various Balloon Configurations

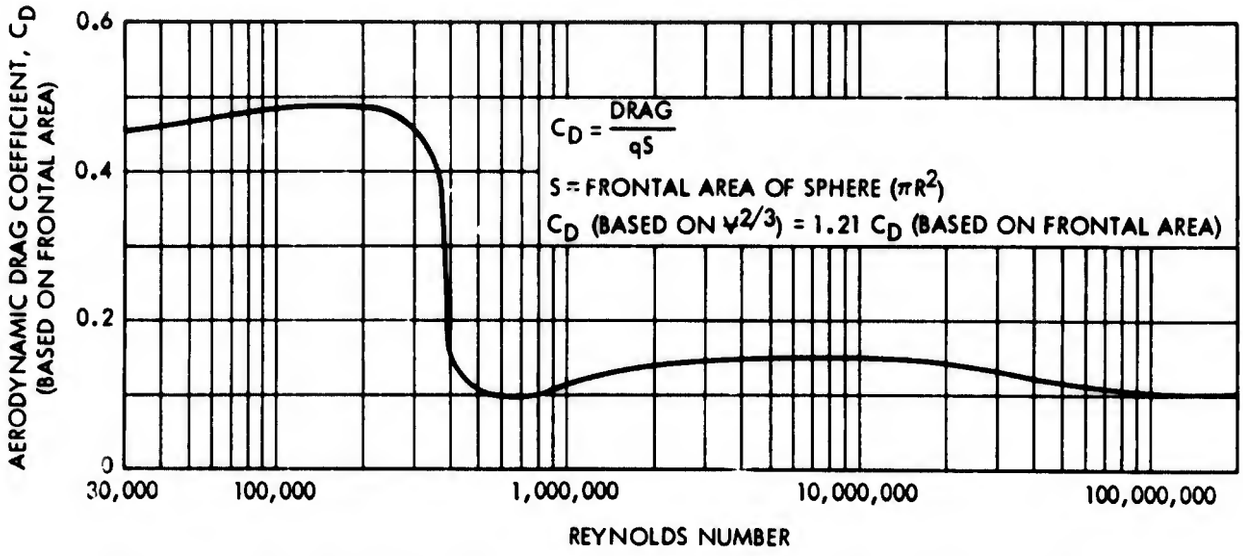

Figure 28. Aerodynamic Drag Coefficient versus Reynolds Number for a Sphere

D. WEIGHT ANALYSIS OF AERODYNAMICALLY SHAPED BALLOONS

1. Stress Considerations

Internal pressure in the balloon at float altitude was based on the following requirements:

(1) The nose of the balloon should not cup or dimple in the wind at that altitude, which would create a large increase in drag, causing the balloon to loose its aerodynamic characteristics.

(2) The minimum operating pressure for a reliable pressure relief valve should have a minimum opening pressure of approximately 1/4 in. H_2O.

Therefore, the required balloon internal pressure was selected to be 1.15 times the stagnation pressure at altitude or 1/4 in. H_2O, whichever is greater. The critical pressure required to prevent buckling of the hull was assumed to be less than that required to prevent dimpling of the nose of the balloon. This was based on the assumption that the suspension or bridle system can be designed to reduce the bending moment to a negligible level. In most cases, the critical pressure to prevent buckling will be less than that required to prevent dimpling. However, in any further detailed design study or prototype development, the validity of this assumption must be verified. The actual stress used in the weight analysis was the sum of the stresses caused by the internal pressure, buoyant lift, and aerodynamic load.

2. Balloon Material

At the present time, material for fabrication of the balloon was investigated only on a strength-to-unit-weight basis. Figure 29 is a plot of breaking strength versus unit weight for various existing materials that are used for fabrication of balloons. The curve of Figure 29 was used in the weight analysis to determine the hull material weight after the stress (allowing a factor of safety of 3) had been determined.

3. Balloon Weight

Once the stress is determined for a particular balloon shape, the weight can be estimated. The product of wetted area and unit weight where wetted area depends on shape and unit weight depends on stress determines the major part of balloon weight. An allowance of 10 percent

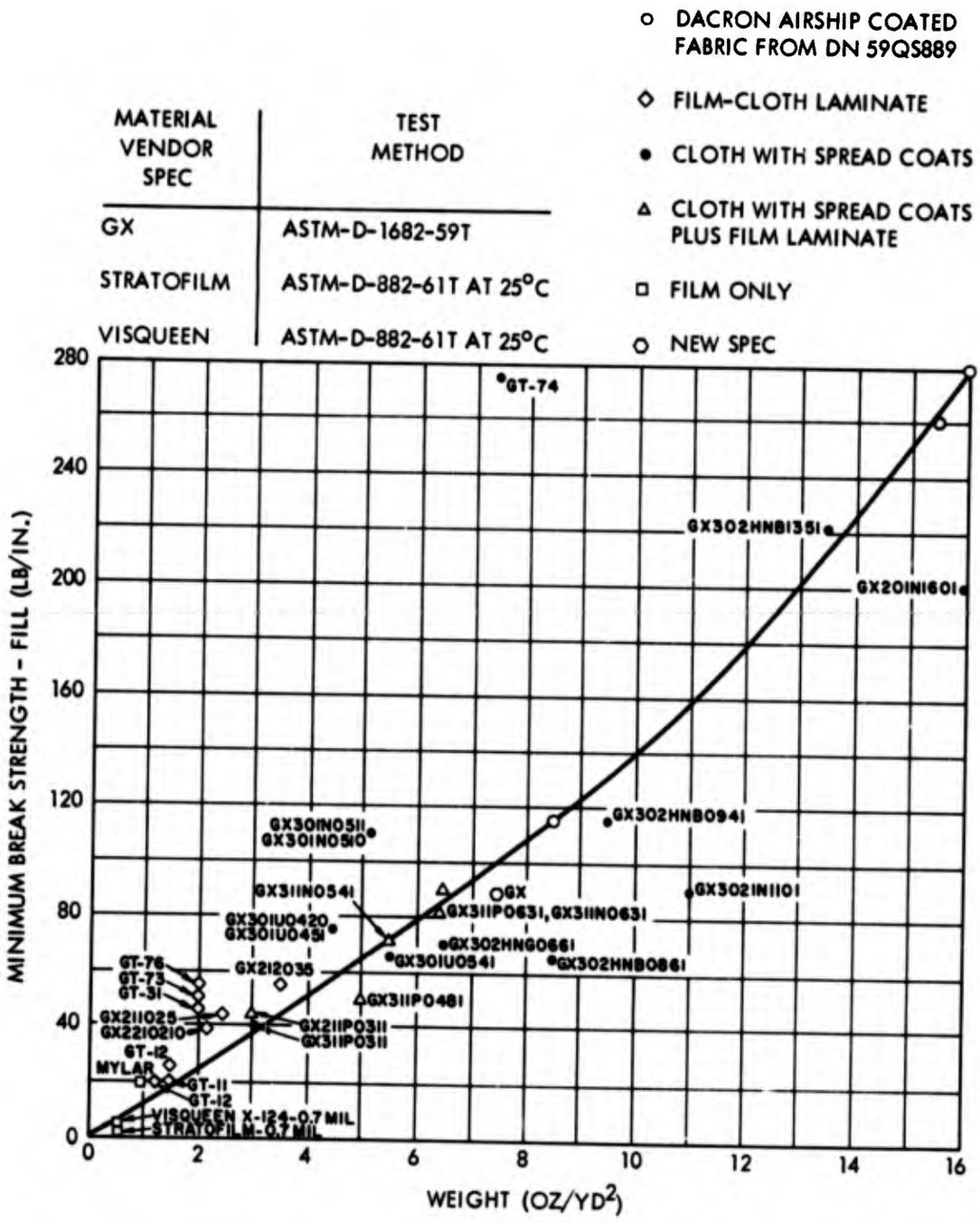

Figure 29. Breaking Strength versus Unit Weight for Various Balloon Materials

was made for seam weight; i.e., hull weight, fin weight, etc were increased by 10 percent. Wetted areas were scaled up from existing sizes, or in the case of the modified Mark II, from model dimensions. Where a blower is provided for pressurization, blower and battery weight depend on design altitude, balloon volume, differential pressure, and power density of the battery. Other weight contributions and the detailed method of calculating stress and weight of aerodynamically shaped balloons are given in Appendix II. Computer printout data for a 1,000,000 ft^3 configuration is given in Table IV.

Table IV. Computer Printout Data for a Class C Balloon Configuration

COMPUTER INPUT DATA:

Payload = 500 lb	Altitude = 50,000 ft
Velocity = 85 ft/sec	Angle of Attack = 5°
Volume = 1,000,000 ft^3	Operating Time = 48 hr

Lift and Drag Coefficients = f (angle of attack)

Hull unit fabric weight (lb/ft^2)	0.022
Stagnation pressure (lb/ft^2)	1.3184
Design stress, includes safety factor of 3 (lb/ft)	466
Hull length (ft)	262
Projection area of 1 horiz tail (ft^2)	3000
Wetted area of 1 horiz tail (ft^2)	7031
Thickness of vert. tail, avg (ft)	5.75
Total volume of balloon (ft^3)	1,051,800
Wetted area of spherical ballonet (ft^2)	44,806
Volume lost by leakage (ft^3/day)	489
Volume flow thru blower (ft^3)	1,973,800
Aerodynamic stress by tether tension (lb/ft)	16.36
Weight of hull fabric (lb)	1199
Weight of intersect attachments (lb)	0
Weight of internal partitions of horiz tail (lb)	129.6
Weight of internal partitions of vert. tail (lb)	129.6
Weight of exit valve (lb)	72.3
Weight of ballonet seams and attachments (lb)	31.1
Weight of suspension system (lb)	574
Buoyant lift (lb)	10,610
Balloon weight (lb)	3292
Unit lift (lb/ft^3)	0.01009
Internal design pressure (lb/ft^2)	1.516
Max hull diameter (ft)	99.2
Projected vert. tail (ft^2)	3,000
Wetted area of 1 vert. tail (ft^2)	7,031
Volume of 1 horiz tail (ft^3)	17,253
Ballonet volume (ft^3)	890,730
Intersect area (ft^2)	0
Volume req'd for temp change (ft^3/day)	105,180
Blower operating time at altitude (min/day)	13.4
Buoyant stress by tether tension (lb/ft)	39
Weight of hull seams (lb)	120
Weight of 1 horiz tail (lb)	152
Weight of 1 vert. tail (lb)	152
Weight of blower (lb)	127
Weight of check valve (lb)	63
Weight of misc equip, battery and blower (lb)	22
Weight of handling lines and catenary (lb)	134
Net lift (lb)	9507
Drag (lb)	928
Wetted hull(s) area (ft)	55,500
Location of max diameter (ft)	104.8
Thickness of horiz tail, avg (ft)	5.75
Volume of 1 vert. tail (ft^3)	17,253
Diameter of spherical ballonet (ft^3)	119
Volume flow rate of blower (ft^3/min)	15,790
Volume to replace each day (ft^3/day)	211,330
Max stress due to inflation (lb/ft)	100
Intersect weight (lb)	0
Weight of attachments of 1 horiz tail (lb)	15.2
Weight of attachments of 1 vert. tail (lb)	15.2
Weight of batteries (lb)	44.6
Weight of ballonet (lb)	311
Aerodynamic lift (lb)	2689
Lift coefficient	0.204
Drag coefficient	0.0704

E. WEIGHT ANALYSIS OF SUPERPRESSURE, NATURAL SHAPE BALLOONS

1. Stress Considerations

In order to retain the shape of the balloon at float altitude, the minimum internal pressure was assumed to be equal to the stagnation pressure at that altitude. This minimum value occurs at the bottom of the balloon.

Stress levels were obtained by computer solutions for equations listed in Reference 9 for a superpressure, natural shape balloon with 25 percent top loading. A top-loaded design was selected because stresses are lower than in a balloon with no top load.

2. Balloon Material

Figure 29 was again used to determine material strength versus unit weight for the basic balloon material.

3. Balloon Weight

Once the stress levels are determined for the superpressure, natural shape balloon flying at a particular altitude and wind condition, the hull material can be selected. The selection of this material is based on a factor of safety of 3 or greater throughout the major portion of the balloon.

The variables that influence the weight of the hull of the balloon are altitude, dynamic pressure, cable tension at the bottom and top of the balloon, volume, and unit weight of material. To obtain the total weight of the balloon the following weights were assumed:

Item	% of Hull Weight
Reinforcement weight	5%
Additional material for end attachment	3%
Inflation ducts	1%
End fittings	6%
Reefing system	35%
Seams	10%

Table V contains typical total data obtained for a superpressure, natural shape balloon.

Table V. Superpressure, Natural Shape Balloon Parameters
(Summer I Wind - 100,000-Ft Altitude)

Balloon Volume (ft^3)	Shell Weight (lb)	Material Unit Weight (lb ft^2)	Total Balloon Weight (lb)	Load at Bottom of Balloon (lb)	Drag, D_A (lb)	Net Lift, L_N (lb)	$\frac{L_N}{D_A}$
961,000	352	0.0056	563	500	116	-211	--
1,681,000	490	0.0056	784	1,000	177	206	1.16
3,038,000	693	0.0056	1,109	2,000	284	1,084	3.82
4,363,000	868	0.0056	1,389	3,000	378	1,979	5.24
5,659,000	1017	0.0056	1,627	4,000	454	2,890	6.38
6,942,000	1154	0.0056	1,846	5,000	529	3,808	7.20
13,220,000	1724	0.0056	2,758	10,000	820	8,466	10.32
25,730,000	2810	0.0060	4,496	20,000	1278	17,810	13.97
38,930,000	456	0.0075	7,226	30,000	1688	26,790	15.87
52,270,000	6335	0.0080	10,140	40,000	2050	35,700	17.41
65,770,000	8304	0.0101	13,280	50,000	2390	44,520	18.62

F. EFFECTS OF VARIOUS DESIGN PARAMETERS ON BALLOON WEIGHT

1. General

To determine the effect of varying the angle of attack, altitude, and wind velocity on the relative magnitude of the weight for the various balloon configurations, one parameter was varied while the others were held constant. Plots of the data available at this time are shown in Figures 30 through 33.

2. Total Balloon Weight versus Hull Volume (See Figure 30.)

As would be expected, if the hull volume is increased, the weight of the balloon increases. Of the aerodynamically shaped balloons, the modified Mark II is the heaviest, the ram air C and Vee-Balloon are lightest at the smaller volume range plotted, and the Vee-Balloon is the lightest at the higher volume range plotted. One reason the modified Mark II is heavy is because of the large fin area on the balloon. The Vee-Balloon is light because the stress (and therefore material weight) is low due to the radius of the balloon being smaller than a single hull balloon of equal volume. Stress is not linearly proportional to radius, but depends on buoyant lift and helium pressure head. Equations 18 through 21 of Appendix II show the method and assumptions used in deriving design stress. The superpressure, natural shape balloon is lighter than any aerodynamically shaped balloon. Note that this is for a 50,000-foot altitude and Summer I winds only.

3. Total Balloon Weight versus Altitude (See Figure 31.)

In a constant volume balloon, the weight of each configuration decreases with increasing altitude due to decreasing aerodynamic and aerostatic forces.

4. Total Balloon Weight versus Relative Wind Velocity (See Figure 32.)

As the wind velocity increases, the weight of each configuration increases due to the rise in stagnation pressure. However, since the internal pressure for the aerodynamically shaped balloon has a minimum value equal to 1/4 in. H_2O, the weight of the balloon remains practically constant for a stagnation pressure times 1.15 lower than 1/4 in. H_2O.

5. Total Balloon Weight versus Angle of Attack (See Figure 33.)

The weight of each aerodynamic balloon configuration increases as the angle of attack increases due to the suspension weight becoming heavier with an increase in aerodynamic loads and higher stresses in the hull due to higher suspension loads.

G. NET LIFT FOR BALLOONS OPERATING IN ZERO WIND BUT DESIGNED FOR HIGH WIND

Net lift for aerodynamically shaped balloons operating in a calm wind condition will be reduced from that occurring in the design wind velocity. The net lift remaining is that amount remaining after aerodynamic lift is deducted. Furthermore, net lift will vary with the angle of attack for which the balloon is designed. For high design angles of attack, the aerodynamic loads will be high, and hence a heavier balloon will be required. Although it would be desirable to design the balloons for operation at a small angle of attack, gust loads and other transient conditions must be accounted for in the structural design. At this time, it is not possible to select an angle of attack for which the structure should be designed.

Figures 34 through 37 show the variation of net lift versus volume, assuming that the balloon is operating in a zero wind, but is designed to operate in the Summer I or Winter I winds at 50,000 feet. A 500-pound payload at balloon is also assumed. These curves are also useful in checking that sufficient net lift is available to lift the cable that is required for the times that the balloon is to operate in the maximum design wind. From the curves it can be seen that only the ram air C shape has a positive net lift when the design is based on Winter I winds, 50,000-foot, altitude and 15-degree angle of attack.

NOTES:

1. EACH POINT ON THE CURVES REPRESENTS A UNIQUE BALLOON DESIGN FOR THAT CONDITION.
2. ALTITUDE = 50,000 FT.
3. ANGLE OF ATTACK = 5°.
4. SUMMER I WIND CONDITION (50.4 KNOTS).

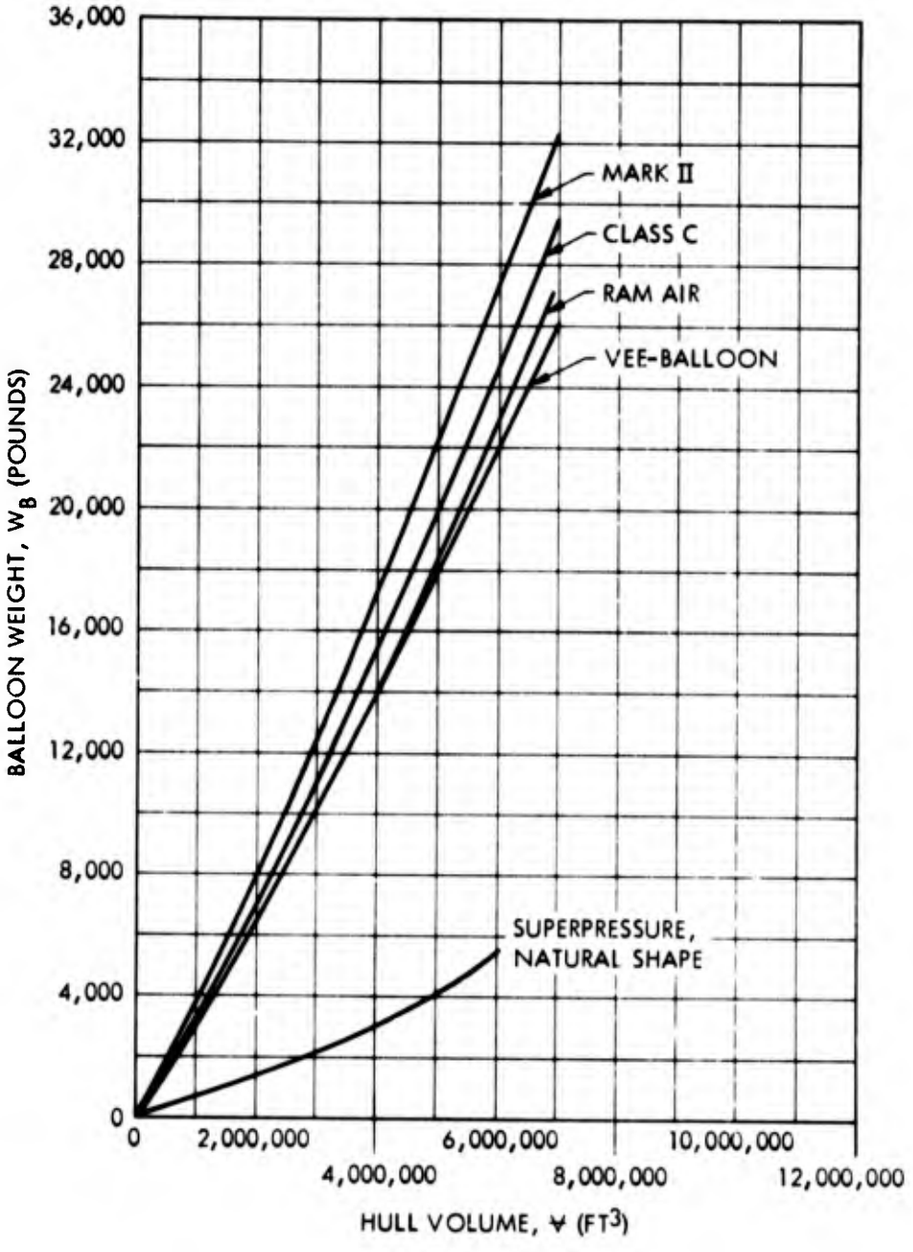

Figure 30. Balloon Weight versus Hull Volume for Various Balloon Configurations

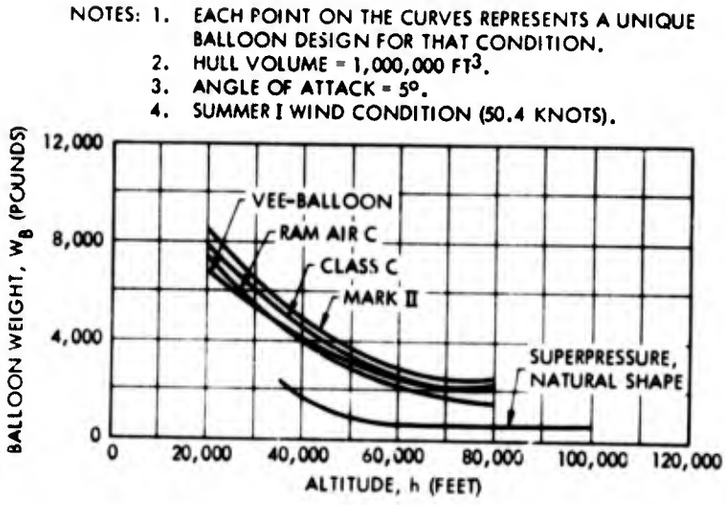

Figure 31. Balloon Weight versus Altitude for Various Balloon Configurations

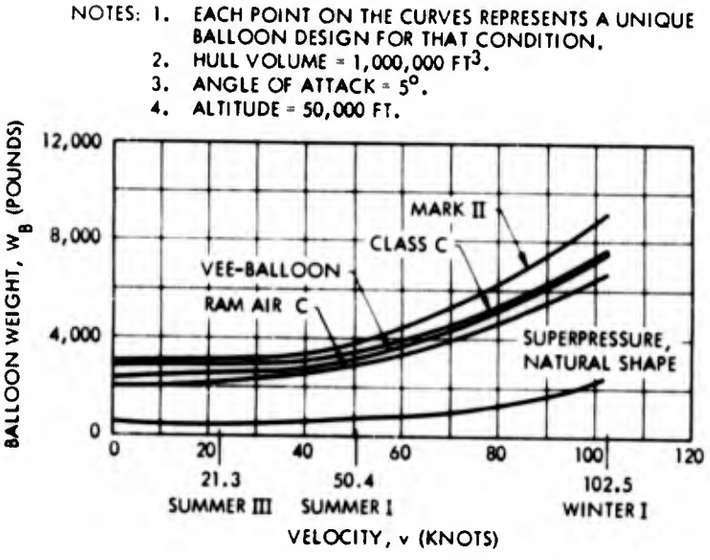

Figure 32. Balloon Weight versus Wind Velocity for Various Balloon Configurations

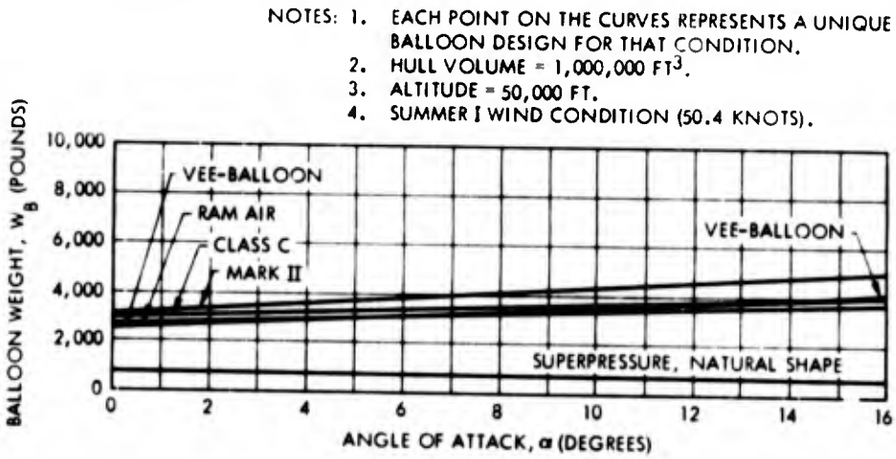

Figure 33. Balloon Weight versus Angle of Attack for Various Balloon Configurations

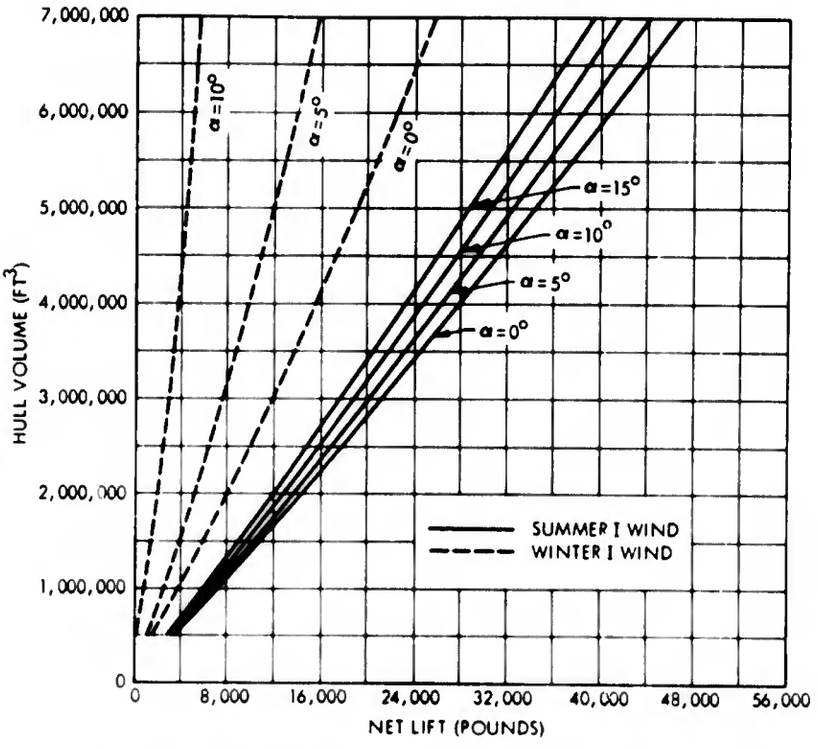

Figure 34. Net Lift of Class C Balloon Configuration Operating in a Zero Wind Condition

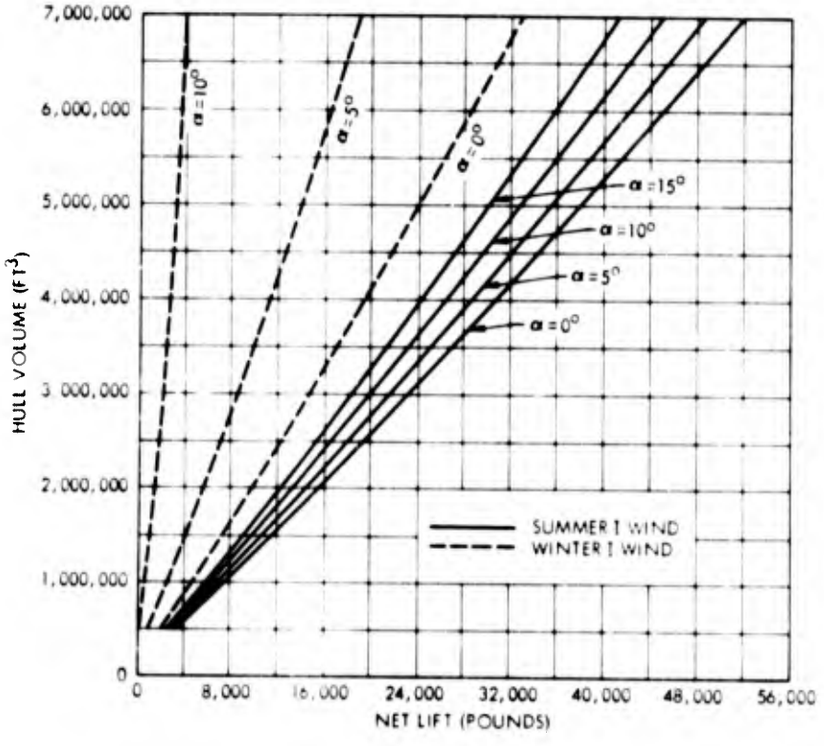

Figure 35. Net Lift of Vee-Balloon Configuration Operating in a Zero Wind Condition

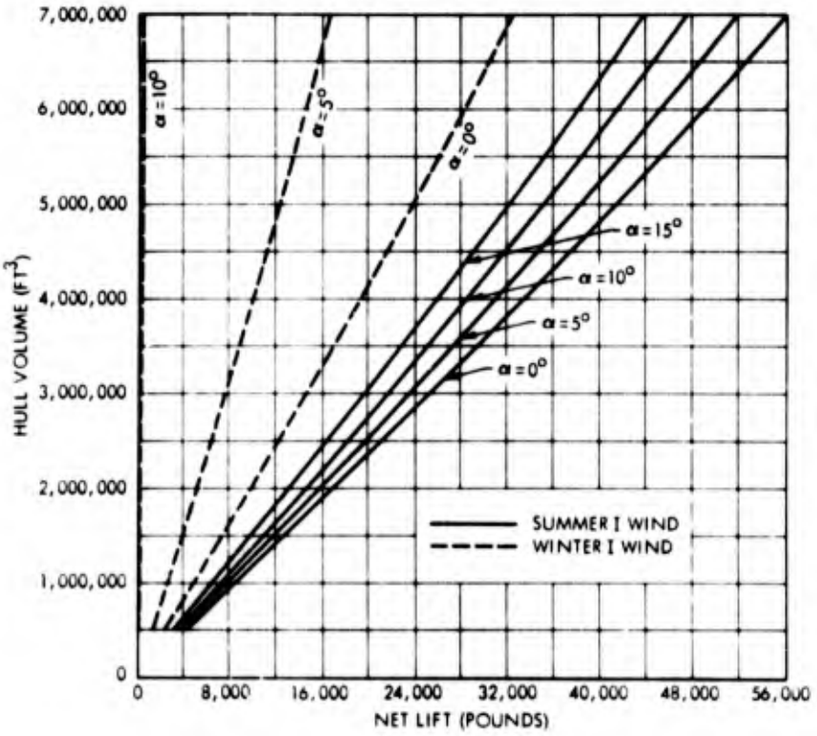

Figure 36. Net Lift of Modified Mark II Configuration Operating in a Zero Wind Condition

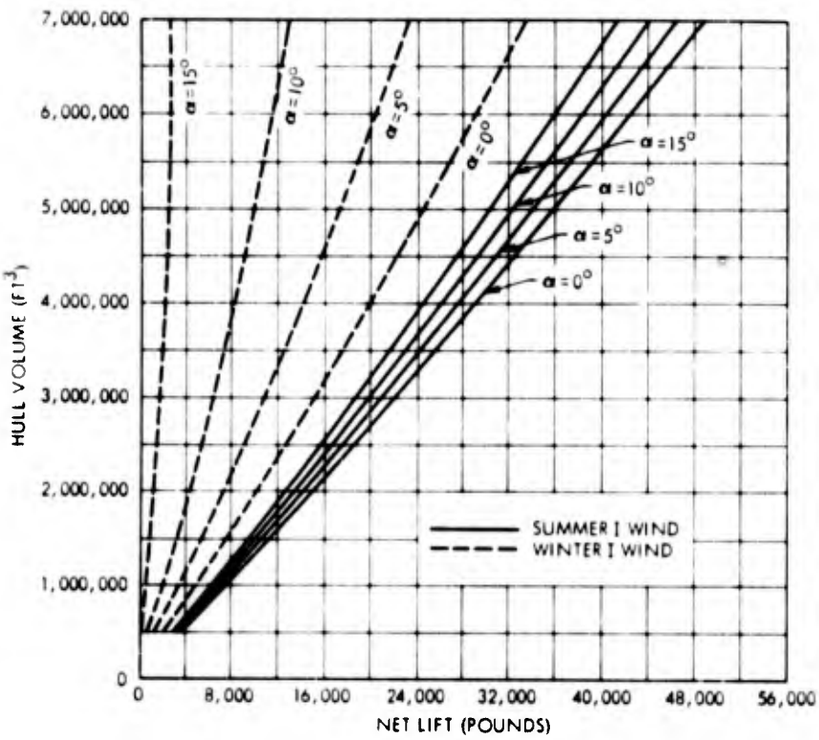

Figure 37. Net Lift of Ram Air C Configuration Operating in a Zero Wind Condition

SECTION VI

BALLOON PERFORMANCE PARAMETERS

Curves relating balloon parameters to net lift and drag are presented in Figures 38 through 43. The abscissas and ordinates chosen for these curves are the same as those used in the cable profile curves (Figures 6 through 19); i.e., the abscissa is net lift (L_N) or resultant of buoyancy, aerodynamic lift, payload, and balloon weight, and the ordinate is net lift-to-drag ratio (L_N/D_A) or tangent of the angle of application of the resultant forces acting on the balloon. Balloon parameters represented are shape, volume ($\forall$), and angle of attack (α). Variables including float altitude and wind profiles are also indicated in the figures.

Weight estimates as described in Section V were made, and values of net lift and drag for each balloon were determined. Note that each balloon design is made on the basis of carrying a 500-pound payload. Thus, the net lift of every balloon has been reduced by this amount. Each balloon design is unique in that a separate design is made each time any parameter is changed. Observe, for example in Figure 38, for a Class C balloon in a Summer I wind, several values of net lift and drag are represented for a volume of 1,000,000 cubic feet. That is, a separate design is shown for each angle of attack as a result of differing stresses, which cause a different strength and weight fabric. Thus, the hull weight will vary with angle of attack as well as with volume.

A summary of the graphs plotted is given in Table VI. Note that no curves are presented for streamlined shaped balloons at an altitude of 100,000 feet. All aerodynamically shaped

Table VI. Summary of Balloon Performance Parameters Plotted

Float Altitude (ft)	Wind Profile	Balloon Type	Parameters Plotted in Fig:
50,000	Summer I	Class C	38
		Vee-Balloon	39
		Modified Mark II	40
		Ram Air Class C	41
		Superpressure, Natural Shape	42
	Winter I	Class C	38
		Vee-Balloon	39
		Modified Mark II	40
		Ram Air Class C	41
		Superpressure, Natural Shape	42
100,000	Summer I	Superpressure, Natural Shape	43
	Winter I	Superpressure, Natural Shape	43

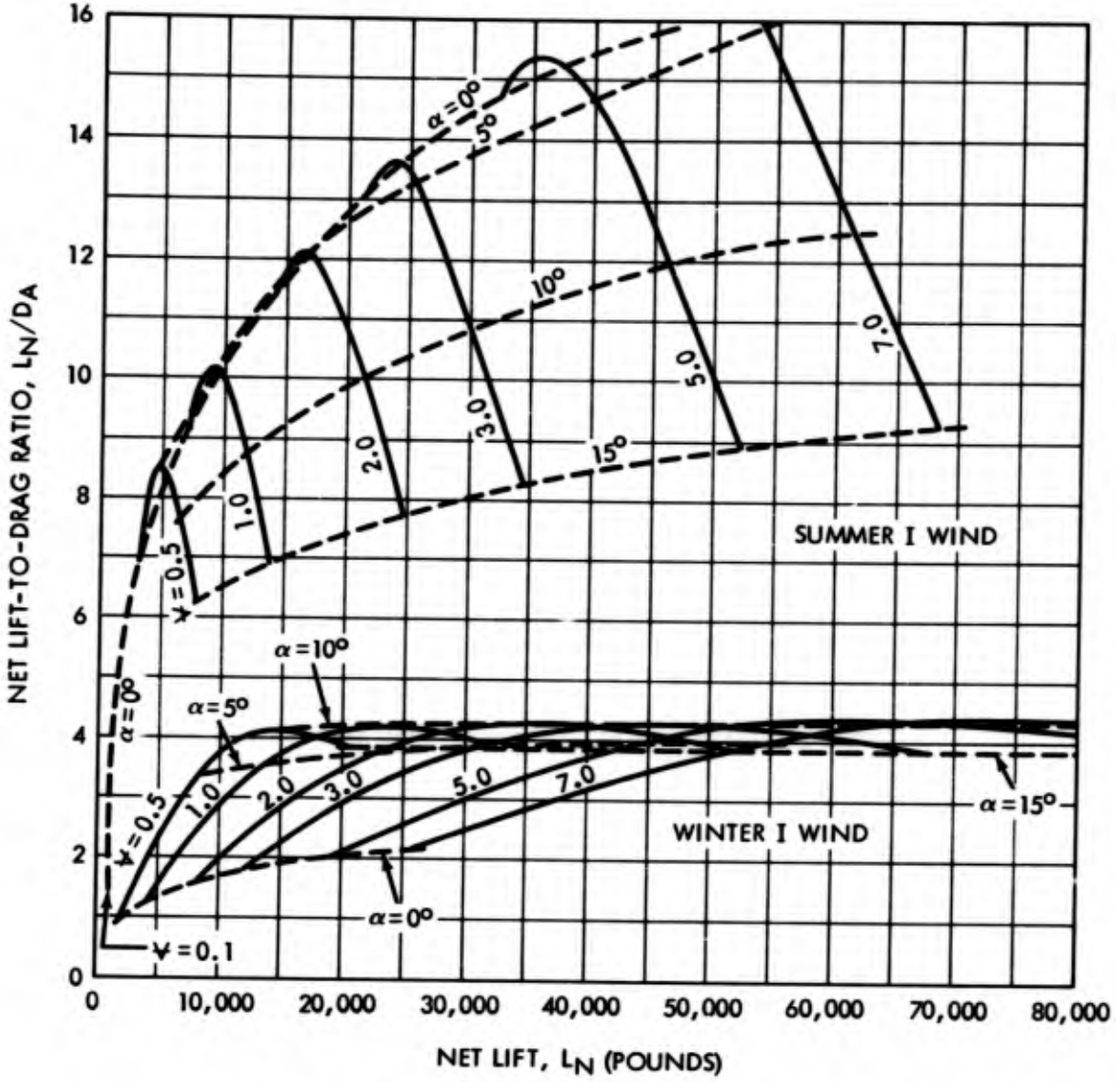

NOTES:

1. EACH POINT ON THE CURVES REPRESENTS A UNIQUE BALLOON DESIGN FOR THAT CONDITION.
2. PAYLOAD = 500 POUNDS.
3. ∀ = HULL VOLUME x 10^{-6} FT^3.

Figure 38. Net Lift and Drag Characteristics of Class C Balloon for Altitude of 50,000 Feet

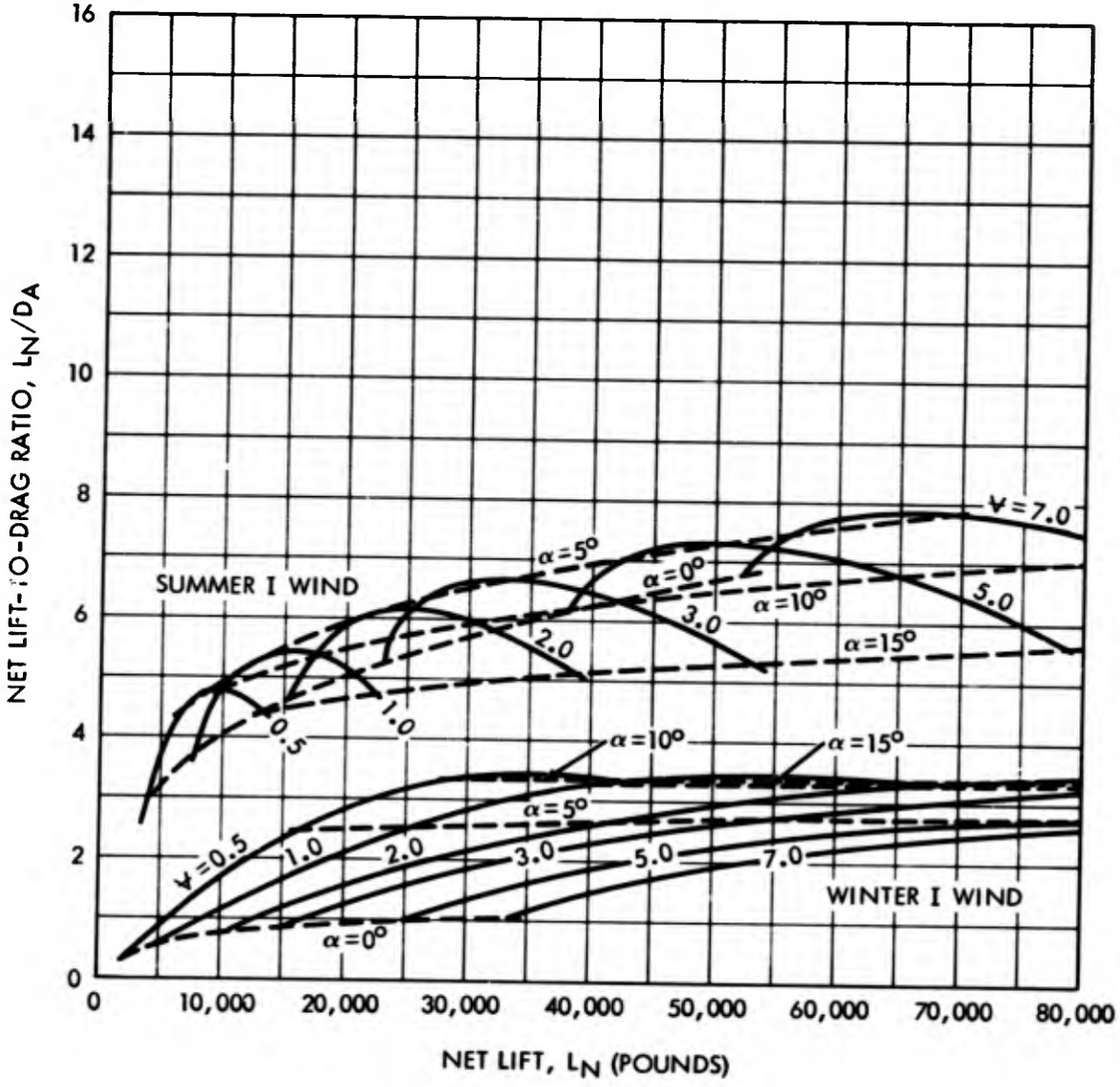

NOTES:

1. EACH POINT ON THE CURVES REPRESENTS A UNIQUE BALLOON DESIGN FOR THAT CONDITION.
2. PAYLOAD = 500 POUNDS.
3. $\forall$ = HULL VOLUME x 10^{-6} FT^3.

Figure 39. Net Lift and Drag Characteristics of Vee-Balloon for Altitude of 50,000 Feet

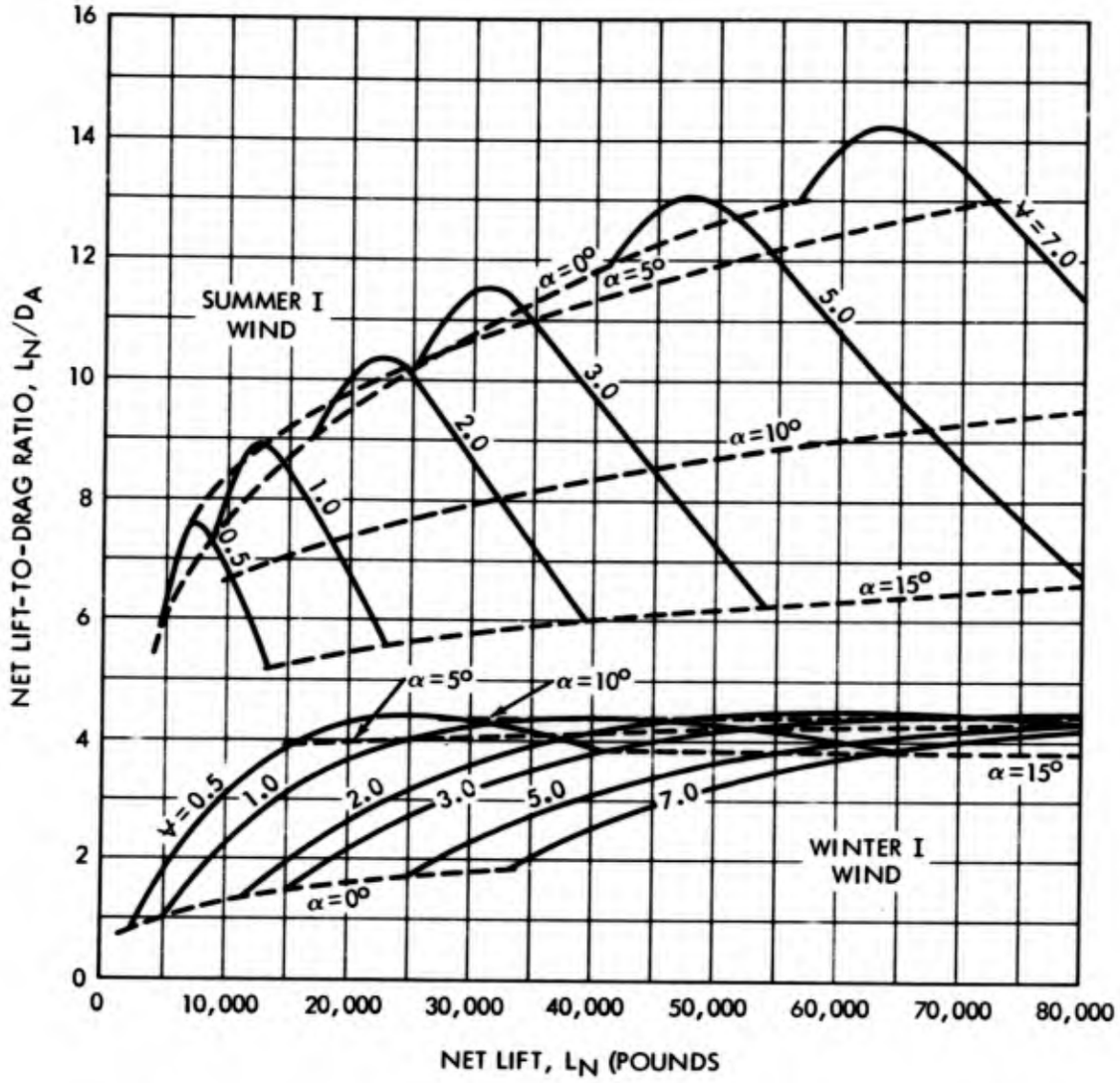

NOTES:

1. EACH POINT ON THE CURVES REPRESENTS A UNIQUE BALLOON DESIGN FOR THAT CONDITION.
2. PAYLOAD = 500 POUNDS.
3. $\forall$ = HULL VOLUME x 10^{-6} FT^3.

Figure 40. Net Lift and Drag Characteristics of Modified Mark II Balloon for Altitude of 50,000 Feet

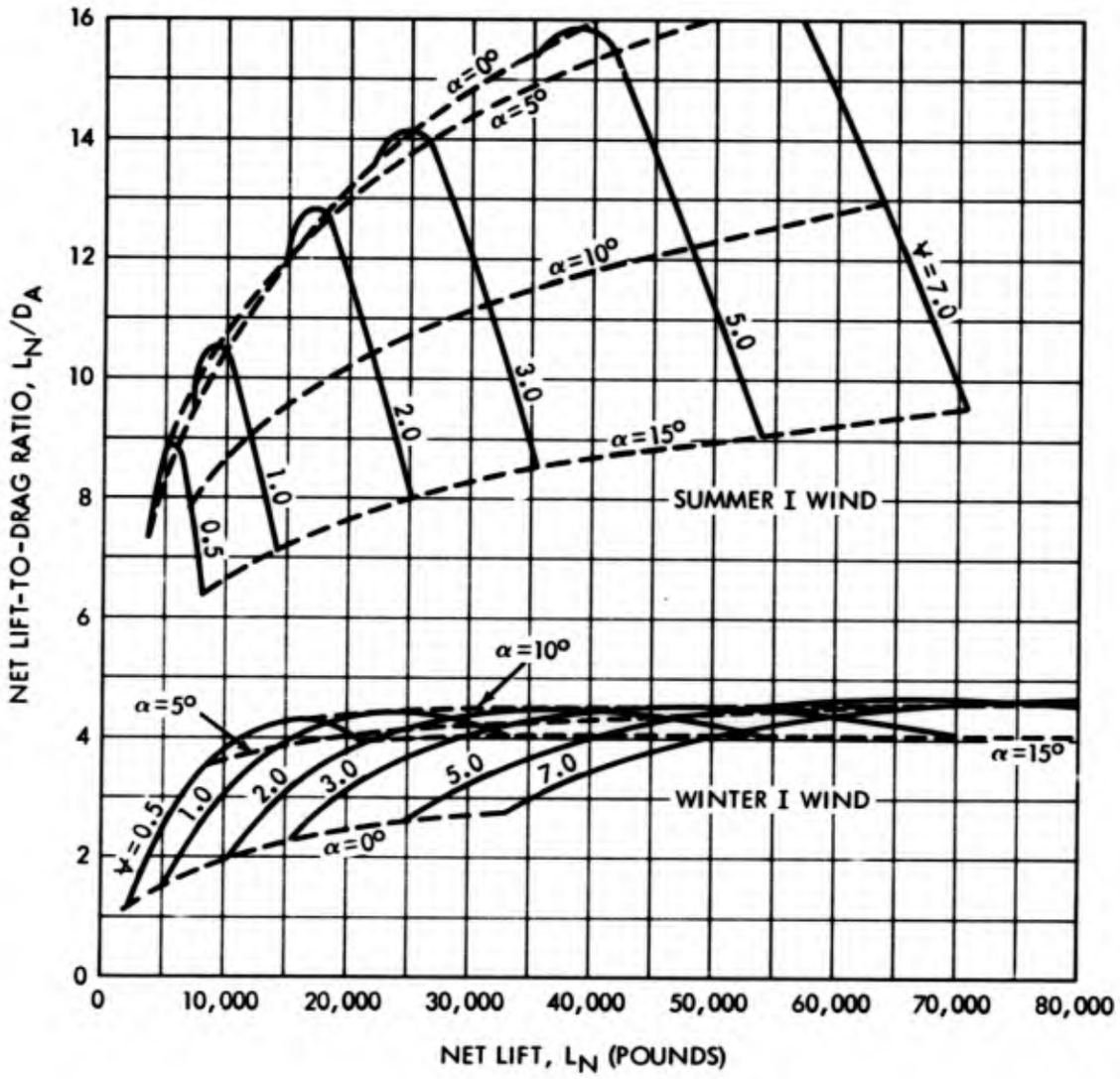

NOTES:

1. EACH POINT ON THE CURVES REPRESENTS A UNIQUE BALLOON DESIGN FOR THAT CONDITION.
2. PAYLOAD = 500 POUNDS.
3. ∀ = HULL VOLUME x 10^{-6} FT^3.

Figure 41. Net Lift and Drag Characteristics of Ram Air C Balloon for Altitude of 50,000 Feet

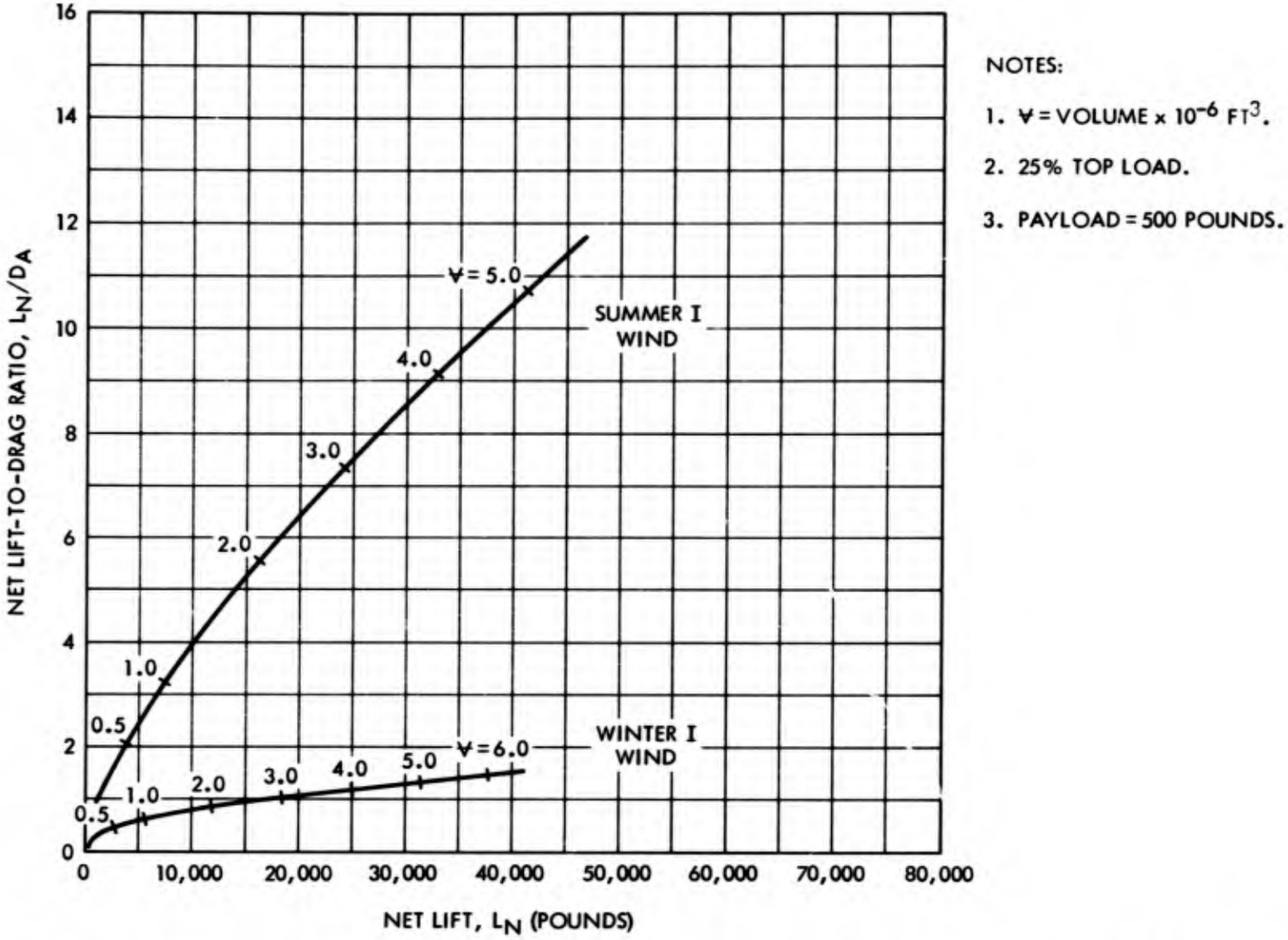

Figure 42. Net Lift and Drag Characteristics of Superpressure, Natural Shape Balloon for Altitude of 50,000 Feet

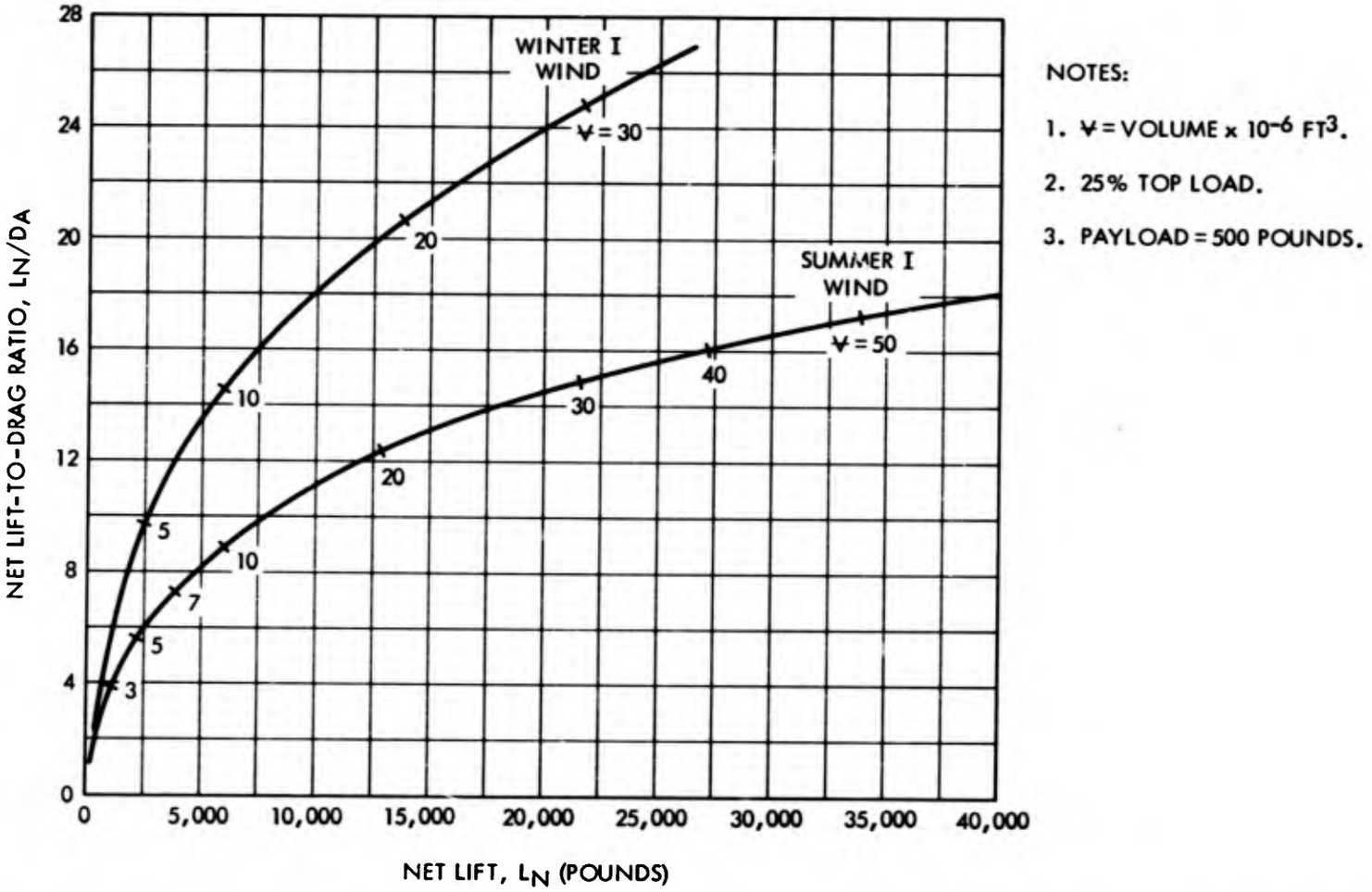

Figure 43. Net Lift and Drag Characteristics of Superpressure, Natural Shape Balloon for Altitude of 100,000 Feet

Table VII. Superpressure, Natural Shape Balloon Characteristics (Winter I Wind, 50,000-Ft Altitude)

Balloon Volume (ft^3)	Shell Weight (lb)	Material Unit Weight (lb/ft^2)	Total Balloon Weight (lb)	Load at Bottom of Balloon (lb)	Drag, D_A (lb)	Net Lift, L_N (lb)	L_N/D_A
148,000	438	0.0240	701	1,000	2,874	237	0.0825
284,000	757	0.0290	1,211	2,000	4,072	1,046	0.257
414,000	1,026	0.0322	1,642	3,000	5,213	1,884	0.361
545,000	1,300	0.0350	2,080	4,000	6,147	2,720	0.442
680,000	1,615	0.0378	2,584	5,000	7,002	3,531	0.504
1,340,000	3,024	0.0481	4,838	10,000	10,690	7,686	0.719
2,644,000	5,702	0.0594	9,123	20,000	16,250	16,080	0.990
3,950,000	8,406	0.0684	13,450	30,000	20,000	24,500	1.220
5,270,000	11,230	0.0760	17,970	40,000	23,960	32,800	1.367
6,561,000	13,790	0.0821	22,070	50,000	27,100	41,200	1.521

balloons investigated are too heavy for operation above approximately 80,000 feet in the wind conditions assumed.

Lift-to-drag ratios for the natural shape balloons are small for Winter I when compared to Summer I wind at a 50,000-foot altitude, due to increased helium pressure head (which results in a heavier balloon) required to retain shape and the increase in aerodynamic drag. Typical values are given in Table VII.

Maximum L_N/D_A ratio for aerodynamically shaped balloons occurs at angles of attack less than the angles for maximum aerodynamic lift-to-drag ratio. That is, maximum L_N/D_A occurs between 0 and 5 degrees for Summer I wind condition and near 10 degrees for Winter I winds for all aerodynamically shaped balloons.

In all cases except for the natural shape balloons at 100,000 feet, the L_N/D_A ratio is greater in Summer I wind than in Winter I wind. Wind velocity is higher in summer at 100,000 feet in area I.

For the aerodynamically shaped balloons, L_N varies nearly directly with volume for all cases of wind loading and angle of attack. The L_N/D_A ratio, however, exhibits considerable varieties. For large volumes, the L_N/D_A ratio tends to be constant. For small volumes and low winds, the L_N/D_A ratio increases greatly with small changes in volume.

For the wind conditions assumed, only natural shape balloons provide a possible solution for tethering at a 100,000-foot altitude.

From Figure 42, it appears that aerodynamic drag for the Winter I wind is very high, thereby reducing L_N/D_A. Winter I wind is characterized by a velocity of 102.5 knots at an altitude of 50,000 feet.

SECTION VII

CABLE-BALLOON SYSTEM OPTIMIZATION

Curves of cable tension components (Figures 6 through 19) and net lift and drag characteristics of balloon shapes (Figures 38 through 43) have been presented. Each group of curves relates cable or balloon parameters and presents them as functions of L_N and L_N/D_N. That is, after float altitude and wind profile are chosen, given values of L_N and L_N/D_N completely define a particular Glastran or missile wire tether line. Additionally, these values of L_N and L_N/D_N completely define a Class C, Vee-Balloon, modified Mark II, ram air class C, or natural shape balloon, provided that the angle of attack is specified.

The total balloon-cable system requirements may be defined by noting values of L_N and L_N/D_N that are common to both balloon and cable. After a particular balloon-cable system is defined by this method, it must be checked to determine if the system will be adequate if the wind velocity reduces to zero. To make this check, compare the cable weight as determined in Figures 8, 11, 14, and 17 to the net lift for the balloon under a zero wind condition as shown in Figures 34 through 37. If the cable weight is less than this new net lift, the system will be capable of performance in a zero wind condition as well as in its design wind condition. An allowance should be made for the reduction in cable length to be lifted in a zero wind, but provisions for making this check are not presented in this report.

The curves showing net lift in zero wind are obtained from computer runs of a balloon type in which the balloon weight is that weight required for design at a particular wind velocity. The net lift in zero wind is the remaining lift available after aerodynamic lift has been deducted.

The optimum system would be determined by comparing solutions for other balloon-cable system combinations. Performance factors including base cable angle and blowdown distance must be considered in addition to cost and reliability.

The design as described above is adequate for system operation at a prescribed altitude for the prescribed wind conditions, and the system can operate at any altitude between float altitude and the ground provided that the design dynamic pressure at intermediate altitude is not greater than at the design float altitude.

The procedure for combined use of the curves is given below.

1. Determine the following basic system requirements and design conditions:
   a. Float altitude of payload
   b. Wind profile

2. Select required balloon parameters such as the following:
   a. Balloon type
   b. Design criteria for balloon solution, i.e., angle of attack to be used in design

3. Select required cable parameters such as the following:
   a. Cable type
   b. Design criteria for cable solution, i.e., minimum angle permitted at base of each segment, blowdown distance, or total cable weight

4. Using graphs representing the above requirements, i.e., one graph giving cable parameters and another giving balloon parameters, check various balloon-cable systems that satisfy the conditions. Solutions are possible at points on the two graphs where L_N and L_N/D_N are equal. For a tandem balloon system, calculations are required to find L_N and D_N at the top end of intermediate cable lengths,

i.e., cable tension components immediately below the lower balloons. Methods of comparing performance of tandem balloon systems will be presented in Task Report No. 2.

5. Check design for flight capability in a zero wind condition.

6. Compare workable systems and choose the most desirable.

SECTION VIII

REVIEW AND COMPARISON OF CONCEPTS PROPOSED IN ARPA CONTRACT STUDIES

A. GENERAL

Various concepts to place a 500-pound payload at a 100,000-foot altitude using a tethered balloon system were originated from studies conducted under ARPA Contracts SD-198, SD-199, SD-200 and SD-201. These studies are reported in References 1 through 4. Each system proposed varied in the number of balloons used, volume of each balloon, the shape of the balloons, tether cable strength, altitude at which each balloon was to be flown (except the topmost balloon, which was at 100,000 feet), and in one case, the tether line material. Figure 44 depicts the balloon and tether systems proposed.

An extensive description of handling equipment and facilities is given in two of the reports. A discussion of these requirements is not included in this report, since it is of secondary importance to system feasibility. Later in the program, when performance capabilities of the various systems are more completely defined, equipment and facilities requirements will be considered as well as costs. Brief descriptions of the various concepts are given in this section.

B. CONCEPT PROPOSED UNDER ARPA CONTRACT SD-198

General Mills Inc proposed the use of a single-balloon system. The balloon portion of the system consists of a 215,000 cubic foot natural shape launch balloon to be jettisoned during ascent and a 12,360,000 cubic foot natural shape main balloon. The tether line proposed was a spliced cable made from missile wire of 11 different diameters, varying from 0.106 to 0.230 inch in diameter.

In moderate winds the balloon and airborne winch are released from an exploding shelter and allowed to rise. At an altitude of 5000 feet, the winch unreels cable at a rate equal to that of the ascent rate of the balloon. When the balloon reaches 80,000 feet, the winch, which is still at 5000 feet, is retrieved by a helicopter, and the entire system is towed to the tethering site where the remainder of the cable is winched out. In winds below 15 knots, the airborne winch is attached to the ground, and the balloon ascends in the conventional manner. During retrieval, the payload is released and steered to the launching area by a parasail. The balloon is winched down to 50,000 feet, where it is ruptured. A parasail opens, and the cable is winched in faster than the parasail descends. If the balloon is ruptured above 50,000 feet, the parasail opens and deposits the cable in a predetermined location. A helium detection device such as a thermal conductivity cell was proposed for mounting in an open duct so that when the pressure increases, the sensor in the duct will cause a switch to close, thereby opening a pressure relief valve.

C. CONCEPT PROPOSED UNDER ARPA CONTRACT SD-199

Goodyear Aerospace Corporation proposed the use of a multiballoon system. The balloon portion of the system consists of five balloons stationed at various altitudes; the top two balloons are of the single-hull design, and the other three are Vee-Balloons. Spliced missile wire was proposed for the tether cable.

To protect the topmost balloon from the high dynamic pressures at the lower altitudes, it is imbedded in the top of the No. 2 balloon, which is substantially more rugged.

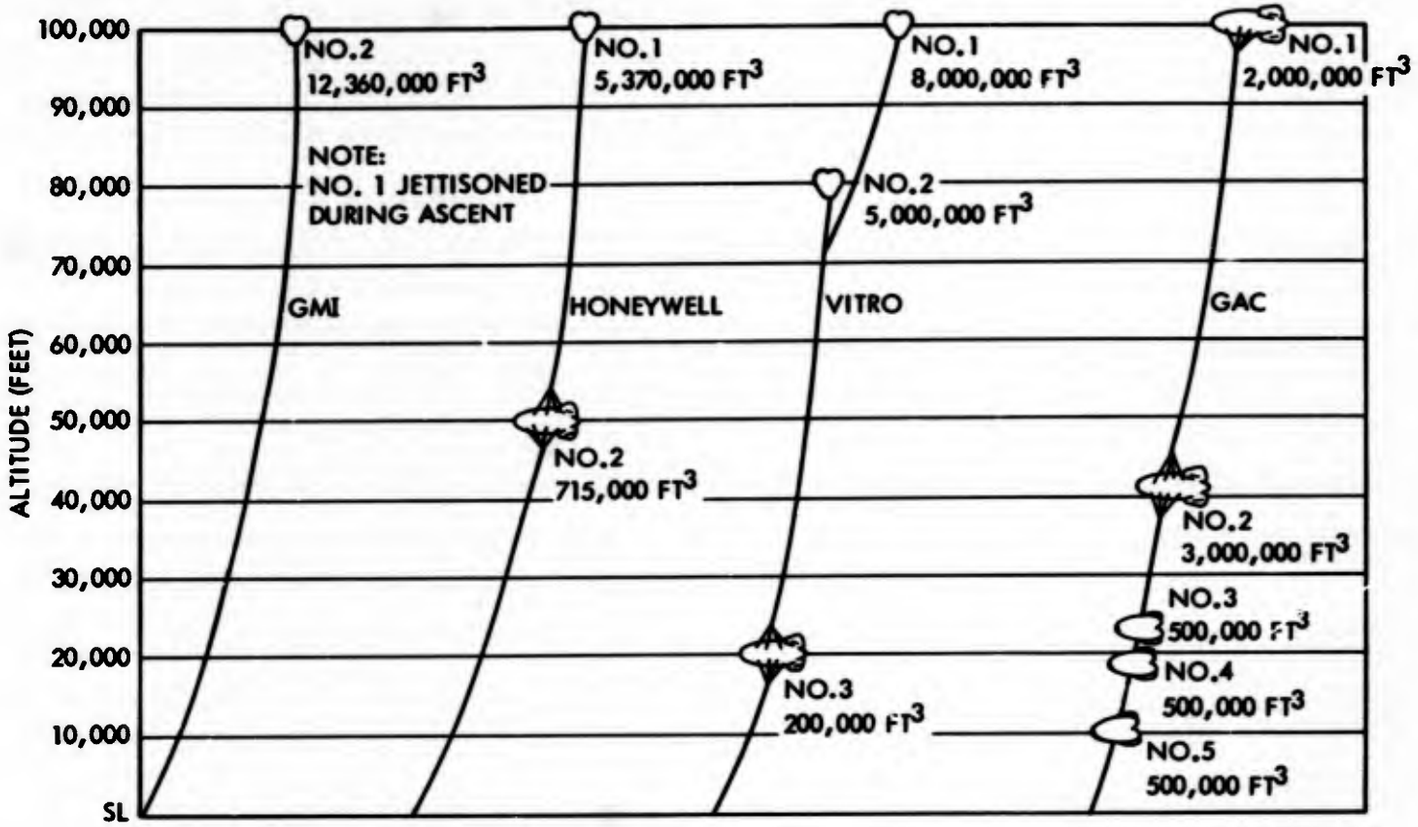

Figure 44. Configurations Proposed by the ARPA Contractors

The first balloon launched is the No. 2 balloon. Each successive balloon is then attached at the appropriate location to the tether line until the No. 2 balloon reaches an altitude of approximately 40,000 feet. At this time, the top balloon with the payload attached is released and ascends to the required 100,000-foot altitude.

The payload is recovered by letting it free fall in a projectile shaped body until it reaches an altitude of 15,000 feet, where a parachute is deployed.

While the payload is being retrieved, the balloons are reeled in and removed from the system as they reach the ground. The top balloon is possibly destroyed as it descends into regions of high dynamic pressure.

All the balloons except the top balloon are equipped with ballonets, pressurized by ram air inflation. The top balloon is fabricated in such a way that the outer skin is in radial folds that "peel" away as the balloon ascends to altitude, thus keeping the balloon pressurized.

D. CONCEPT PROPOSED UNDER ARPA CONTRACT SD-200

Minneapolis-Honeywell proposed a two-balloon system. A 5,370,000 cubic foot natural shape balloon was proposed for the top balloon, and a 715,000 cubic foot single-hull aerodynamically shaped balloon for tethering at an altitude of 50,000 feet. A tapered nylon rope was proposed for the tether cable between the balloons and a tapered missile wire between the lower balloon and the ground. The balloons were to be constructed of a plastic film/fiber composite scrim material.

The payload is retrieved by letting it slide down the cable and then retrieving it with the lower balloon. The upper balloon is cut free in high winds.

Launch and ascent techniques were not described.

A roll diaphragm pump was suggested as a possible means of pressurizing the aerodynamically shaped balloon and the natural shaped balloon was to be reefed.

E. CONCEPT PROPOSED UNDER ARPA CONTRACT SD-201

Vitro Corporation also proposed the use of a multiballoon system. The balloon portion of the system consists of three balloons stationed at various altitudes; the top two balloons are of the natural shape design, and the bottom balloon is a single-hull design. Fourteen segments of missile wire spliced together were suggested for the tether cable. Wire diameter varied from 0.121 to 0.251 inch in diameter.

The top balloon is launched first with the payload attached, and each successive balloon is then attached at the appropriate location to the tether line until the payload reaches an altitude of 100,000 feet.

For retrieval, the balloons are reeled in and removed from the system as they reach the ground. In an emergency, the payload would be ejected and recovered by parachute, while the cable above the bottom balloon would be severed. The lower balloon would then be reeled in and recovered.

Pressurization for the natural shape balloons is achieved by reefing bands that are cut as the balloon ascends to altitude. No pressurization system was proposed for use during descent.

F. COMPARISON OF CONCEPTS

In order to make an equitable comparison of system proposals, modifications were made to the systems proposed by the various contractors. Each contractor had assumed a different design wind profile; therefore, comparisons cannot be made without changing the balloon and

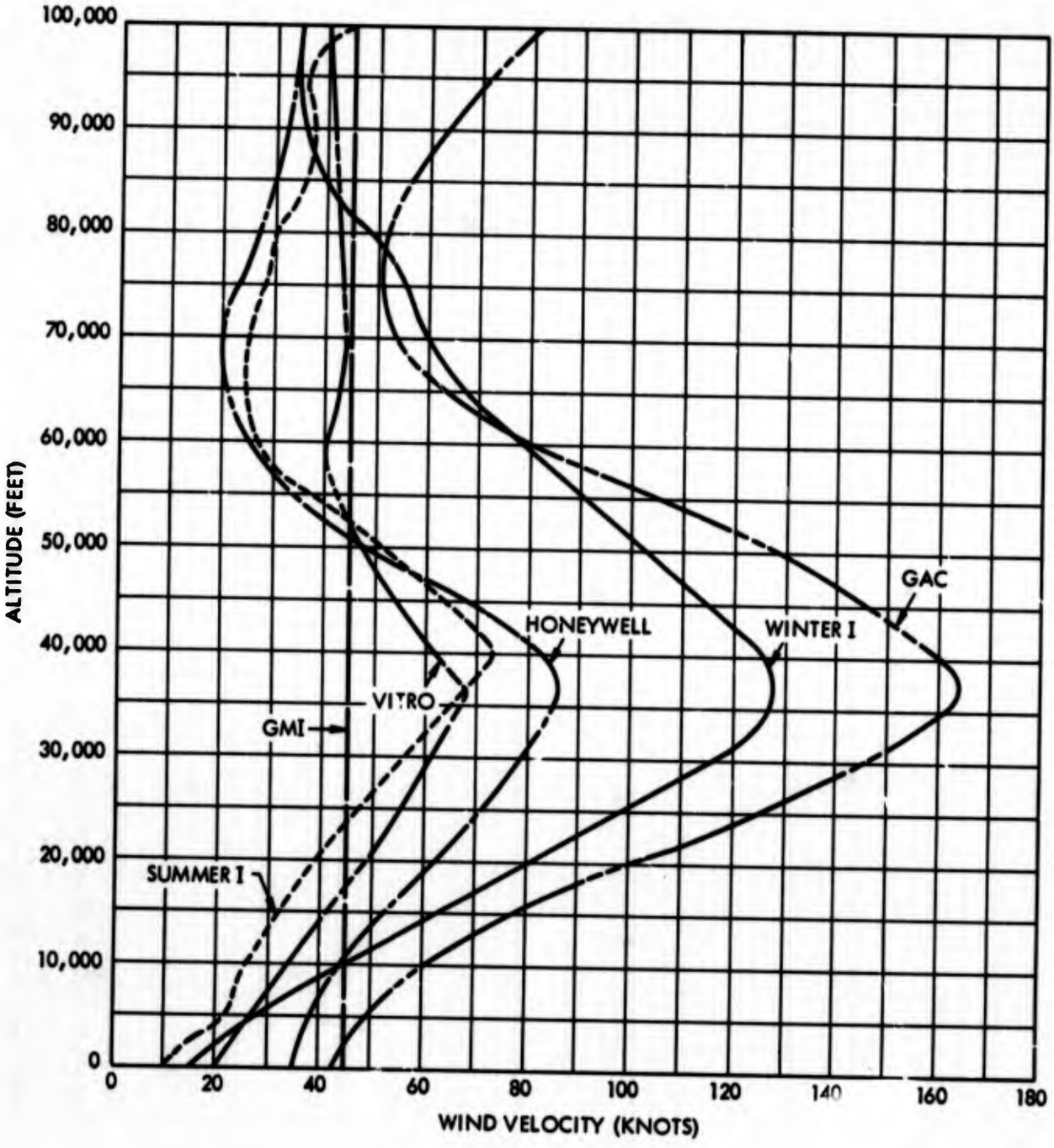

Figure 45. Altitude versus Wind Velocity Assumed by the ARPA Contractors

cable proposed designs in some way. For this reason, all systems are compared on the basis of the same wind profile rather than the various profiles proposed. Figure 45 shows the wind profiles assumed by the contractors. Other changes in proposed quantities concern the weight of balloon and cable components. Balloon weight of streamlined balloons is obtained as described earlier in this report. Weight of natural shape balloons is obtained by assuming that the balloons have zero circumferential stress, zero superpressure, a flat top, and are designed in accordance with the design sigma tables given in Reference 9. Balloon surface area was assumed to be the theoretical value from the sigma tables, and end reinforcements were assumed where load in the material exceeded the design strength.

Cable weight is also computed as proposed previously: a tapered constant stress cable is generated as part of the computer solutions for cable profile. With these changes, care should be exercised in the conclusions drawn, since the balloon systems proposed by the contractors may be subjected to a loading condition entirely different from that assumed by the contractor.

Table VIII is a summary of the ARPA contractor proposed concepts. It is seen from Table VIII that a Class C balloon was assumed where a single-hull streamlined balloon was specified. The Vee-Balloon was used for specific cases of the GAC concept. Design angles of attack of 6 degrees for the Class C and 4 degrees for the Vee-Balloon were selected so that L_N/D_N is maximum for each type.

For the sake of comparing the effects of certain changes in cable type and number of balloons in the systems proposed, modifications are included in Table VIII.

G. CABLE-BALLOON SYSTEM SOLUTIONS

From the data in Table VIII, cable-balloon system solutions were performed for each system. Observations and comparisons of the system solutions are described in the following paragraphs.

1. Balloon Weight

Weights of natural shape balloons were calculated to be greater than those proposed by GMI and Honeywell by approximately 58 percent and 17 percent, respectively. The two natural shape balloons of the Vitro study were, however, too heavy by 15 and 36 percent. For the study presented here, the weight of natural shape balloons is the same for Winter I or Summer I winds. In reality, the weight should be slightly different due to the different winds and therefore the superpressure requirement.

In all cases, the weights proposed for the streamlined balloons were heavier than those proposed by the contractor. Here, allowance for heavier balloons was made as the wind conditions became more severe. Note that at 100,000 feet, a more severe design condition occurs for Summer I wind than for Winter I wind.

2. Net Lift

Values of net lift given in Table VIII are the summation of lift at the top end of each cable segment. This lift not only includes forces acting on the balloon but also the cable load from segments above the cable section of interest. Note that in the case of GAC balloon No. 1, the weight proposed resulted in a negative net lift. Using the contractor's proposed weight, however, a positive net lift was obtained. To obtain a solution, this contractor's proposed net lift was utilized. It is reasoned that by choosing a slightly larger natural shape balloon, this net lift could be realized. A natural shape balloon would have resulted in a larger drag. This fact was not accounted for here. As will be shown later, the result of this solution will be useful for the sake of comparison; however, the reservation of this assumption must be kept in mind.

Table VIII. Summary of ARPA Contract Studies (Sheet 1 of 2)

	Contractor	Balloon No.	Balloon Type	Alt (ft)	Vol (ft^3)	Angle of Attack (deg)	Weight (lb) Proposed	Weight (lb) Re-Estimated Summer I	Weight (lb) Re-Estimated Winter I	Net Lift (lb) Proposed Summer I	Net Lift (lb) Proposed Winter I	Net Lift (lb) Re-Estimated Summer I	Net Lift (lb) Re-Estimated Winter I	Total He Vol at Alt = 0', All Balloons (ft^3)	Total wt, All Balloons (lb) Summer I	Total wt, All Balloons (lb) Winter I
BALLOON DATA	GMI	1	Natural	--	215,000	--	400	--	--	--	--	--	--	--	--	--
		2	Natural	100,000	12,360,000	--	3000*	4,747	4,747	7870	--	6,123	6,123	172,100	3,000	3,000
	Honeywell	1	Natural	100,000	5,370,000	--	1440	2,018*	2,018*	--	--	2,412	2,412	184,200	4,353	4,627
		2	Class C	50,000	715,000	6	2000	2,335*	5,609*	--	--	8,552	12,809			
	Vitro	1	Natural	100,000	8,000,000	--	4040	2,980*	2,879*	--	--	3,880	3,880	398,000	24,814	28,503
		2	Natural	80,000	5,000,000	--	2920	2,543*	2,543*	--	--	11,576	13,047			
		3	Class C	20,000	200,000	6	1180	1,259*	3,208*	--	--	9,358	--			
	GAC	1	Class C (mod)	100,000	2,000,000	6	1220*	1,842	1,787	561	440	-53	-128	1,650,000	33,556	70,304
		2	Class C	41,000	3,000,000	6	8620	22,947*	48,405*	--	--	45,506	--			
		3	Vee	24,000	500,000	4	2210	3,150*	8,544*	--	--	48,170	--			
		4	Vee	19,000	500,000	4	2170	3,053*	7,152*	--	--	66,080	--			
		5	Vee	11,000	500,000	4	2170	3,186*	4,983*	--	--	78,172	--			
	MODIFIED ARPA SYSTEM COMPARISONS (To Compare Cable Parameters Only)															
	GAC	1	Class C (mod)	100,000	2,000,000	6	1220	--	--	561	--	--	--	--	24,167	--
		2	Class C (mod)	41,000	3,000,000	6	--	22,947	--	--	--	45,506	--			
	Vitro	1	Natural	100,000	8,000,000	--	--	2,980	--	--	--	3,880	--	--	--	--
	Honeywell	1	Natural	100,000	5,370,000	--	--	2,018	--	--	--	2,412	--	--	--	--

*Balloon weights used to obtain cable profile solutions.

3. Cable Data

A discussion of the cable profile solutions is presented so that those systems that provide solutions may be determined before examining total weight of all balloons. In Table VIII note that certain weight values represent the balloon weights chosen for use in the profile study. In all cases, the weights as proposed in this report were used except for the case as noted above and for the GMI single balloon. This GMI exception is made to show that no profile solution exists, even though a balloon of underestimated weight was utilized.

4. Summer I Wind Solutions

Elements of the cable profile solution are self-explanatory. It can be observed that the only systems that provide solutions in a Summer I wind are the Vitro and the modified GAC systems. The system proposed by Honeywell would require only a slight modification to provide a solution. Presently, the lower end of the bottom segment becomes horizontal approximately 4000 feet above the ground. For purposes of making comparisons, it was assumed that the cable reached MSL. The GMI system would result in the cable becoming horizontal approximately 18,000 feet above MSL.

Table VIII. Summary of ARPA Contract Studies (Sheet 2 of 2)

	Cable Type	Vert. Height of Segment (ft)	Angle at Base of Segment (deg) Summer I	Angle at Base of Segment (deg) Winter I	Alt where Cable becomes Horiz (ft) Summer I	Alt where Cable becomes Horiz (ft) Winter I	Blowdown Distance of Segment (ft) Summer I	Blowdown Distance of Segment (ft) Winter I	Weight of Cable Segments (lb) Summer I	Weight of Cable Segments (lb) Winter I	Total Blowdown, all Segments (ft) Summer I	Total Blowdown, all Segments (ft) Winter I	Zero Wind Check[b] Summer I	Total wt, All Segments (lb) Summer I	Total wt, All Segments (lb) Winter I	Total wt Proposed by Contractor (lb)
CABLE DATA (Parameters Based on Tapered Design)	Missile wire	100,000	Horiz	Horiz	18,336	33,319	55,287	39,518	7,218	6,594	55,287[d]	39,518[d]	6,123	7,218[d]	6,594[d]	5,300
	Nylon rope	50,000	43.3	80.8	[c]	[c]	20,110	29,449	1,572	1,717						
	Missile wire	50,000	Horiz	Horiz	4,208	5,832	53,472	65,292	7,451	10,381	73,582	94,741[d]	2,412 -1,479[e]	9,023	12,098[d]	5,665
	Missile wire	20,000	13.1	8.4	[c]	[c]	3,803	2,335	1,226	1,202						
	Missile wire	60,000	54.3	Horiz	[c]	32,085	23,703	41,711	8,683	10,786	39,455	--	3,880 11,576	13,955	--	10,586
	Missile wire	20,000	41.0	--	[c]	--	11,949	--	4,046	--			4,752			
	Missile wire	59,000	57.1	Horiz	[c]	48,716	31,706	41,354	419	347			207			
	Missile wire	17,000	20.7	--	[c]	--	4,208	--	16,540	--			24,806			
	Missile wire	5,000	19.2	--	[c]	--	1,619	--	3,369	--	43,870	--	21,448	54,806	--	Not given
	Missile wire	8,000	20.5	--	[c]	--	2,605	--	13,369	--			39,764			
	Missile wire	11,000	21.9	--	[c]	--	3,732	--	21,109	--			48,367			
	MODIFIED ARPA SYSTEM COMPARISONS (Different Cable Types or Lengths)															
	Missile wire	59,000	57.1	--	[c]	--	31,706	--	419	--			--		--	--
	Missile wire	41,000	47.9	--	[c]	--	20,239	--	32,289	--	51,947	--	--	32,708	--	--
	Glastran	20,000	11.7	--	[c]	--	3,595	--	789	--	--	--	--	--	--	--
	Glastran	50,000	21.4	--	[c]	--	12,983	--	852	--	--	--	--	--	--	--

[b] Excess lift at top end of cable segment if wind velocity reduces to zero. [c] A cable solution exists.
[d] Incomplete solution. [e] Negative value indicates that the system will not fly in a zero wind condition.

5. Winter I Wind Solution

None of the proposed systems was capable of providing a solution in a Winter I wind condition, although only minor modifications to the Honeywell and GAC systems would be required to provide a workable system.

6. Total System Blowdown

Total blowdown of all cable segments in the Summer I wind indicates that the three-balloon Vitro system results in the least amount of blowdown with 39,400 feet, the GAC system is second with 43,900 feet, and Honeywell is third with approximately 73,600 feet.

7. Total Weight of All Cable Segments

For the Summer I wind solution, the two-cable system of Honeywell is lightest at approximately 9000 pounds, Vitro second at approximately 14,000 pounds, and GAC third with approximately 54,800 pounds. The nylon rope proposed by Honeywell is not the best choice. As shown in Table VIII, Glastran cable provides a lesser blowdown distance and a lighter cable, in addition.

8. Total Weight of All Balloons

For the Summer I wind condition, the Honeywell system is lightest at approximately 4,400 pounds, Vitro is second at approximately 24,800 pounds, and GAC third at approximately 33,600 pounds.

H. COMMENTS AND CONCLUSIONS

Choice of balloon volume, altitude, and number of balloons in the system is very critical. A suitable method of making these selections has not as yet been determined.

A modified solution of the GAC proposal is provided in Table VIII. The lower three balloons were removed without changing the volume of the upper two balloons or the cable type. The new solution indicates that total balloon and cable weights reduce significantly, while blowdown increases, as would be expected. This modified GAC concept is still many times heavier than the Honeywell system. The significant differences in the systems are the balloon volumes. That is, the top balloon of the GAC system is 2,000,000 cubic feet, whereas the Honeywell balloon is 5,370,000 cubic feet. The intermediate balloons are 3,000,000 and 715,000 cubic feet, respectively.

The comments presented herein do not compare any design condition except those at float altitude. Launch and retrieval problems must be considered before a final comparison can be made.

Although the balloon volume proposed for a single-balloon system did not provide a solution, selection of a larger balloon, 25,000,000 to 30,000,000 cubic feet, will provide a solution, as can be seen from Figures 18 and 43. This system appears to be least complex. Of the systems that provided solutions, the two-balloon system proposed by Honeywell appears better than any other system proposed from the standpoint of system complexity, balloon weight, cable weight, and system loads. This judgment is made even though net lift available is insufficient to lift the cable when aerodynamic lift is reduced to zero.

Performance characteristics are better for the Vitro and GAC systems when total blowdown is considered.

Best performance, as measured by small blowdown distances, is obtained from a system of many balloons and favorable base cable angles for each segment. Compare the blowdown of the lower four segments of the GAC system ($d = \approx 12,200$ feet, $h = 41,000$ feet) with that for the lower segment of the Honeywell system ($d = \approx 53,500$ feet, $h = 50,000$ feet).

To obtain a minimum weight solution, proportioning of balloon volumes appears to be such that the lower end of each cable segment becomes nearly horizontal.

Tapered missile wire appears to be a good choice of cable, whereas nylon provides no apparent advantage for the conditions assumed in this study. Tapered Glastran cable provides a slightly better solution for the single comparison made, that of the Vitro concept.

SECTION IX

CONCLUSIONS AND RECOMMENDATIONS

Investigation of methods for determining optimum single and multiple balloon systems will be continued. A method for determining a workable balloon system has been established with a multiple balloon system the only solution in many of the wind and altitude conditions considered. However, a method for optimizing the number of balloons, float altitude, and balloon size has not yet been developed at this time.

Equations of motion of the balloon and cable system during ascent and descent should be derived and computer solutions obtained.

Methods of penetrating the region of high dynamic pressure without structurally over-designing the balloon for operation at float altitude should be investigated. Launch as a free balloon and means of containment in a second balloon are methods that merit further study.

A review of all potential balloon pressurization systems is needed, particularly methods of reefing a natural shape balloon.

BLANK PAGE

APPENDIX I

CABLE PROFILE ANALYSIS[2]

A. MATHEMATICAL ANALYSIS

The mathematical analysis of a cable-balloon system subjected to a wind-vector profile involves techniques similar to those used in the solution of related cable studies arising in a variety of engineering disciplines. These studies include problems on towing cables, mooring lines, supporting cables in bridges, cable-car lines, electric power lines, submarine cables, etc. Problems of this type in their greatest generality involve determination of cable tension as well as three-dimensional cable shape for a transient condition, i.e., time-dependent cable configuration; while reduced problems involve determination of above parameters in two dimensions for transient as well as steady-state condition and also three-dimensional steady-state configuration.

Many problems have been worked out in two dimensions for a flexible cable for a steady as well as transient motion of a cable. The shape and tension of a cable subjected to a fluid flow have been studied by H. Glauert (Reference 10) for a steady condition on the assumption that the cable is uniform and the speed of the fluid is the same at every point of the cable. In this study, only the normal component of cable drag was considered, neglecting tangential or a frictional component; while a study which incorporates both the normal and the tangential components was performed by L. Landweber and M. H. Protter (Reference 11). A transient cable motion has been studied by F.O. Ringleb (Reference 12) and by T.S. Walton with H. Polacheck (Reference 13). In the former work, the change in cable tension was investigated due to a sudden impulse, while in the latter, an extensive analysis has been performed on cable tension due to a periodic motion of one end of the cable with the other end fixed.

The techniques developed for the above two-dimensional problems are useful for the three-dimensional problem at hand. The prime objective of these studies is to select appropriate balloon-cable designs such that they will be operable at a desired altitude under a variety of wind vector profiles, as well as to determine the "operative envelope", i.e., to indicate the optimum configuration of different parameters for various operative conditions.

B. STEADY CONDITION

The problem for a steady-state condition is to determine the tension in a cable as well as the shape, with one end of the cable attached to a free balloon at a given altitude and the other end fixed at the ground. From this then, it is possible to determine the elevation required at tether site. In the solution of the problem, the variation of the following parameters is considered:

(1) Wind-vector profile in the operating range
(2) Wind-vector at float altitude
(3) Float altitude
(4) Terrain height at tether side (determined parameter)
(5) Cable geometry - diameter as function of cable length
(6) Cable weight/length as function of cable length
(7) Cable weight
(8) Balloon buoyancy and drag at float altitude.

To evaluate the effect of these parameters on cable form and tension, a mathematical model is developed incorporating these quantities.

[2]Subsections A through D of this appendix are excerpts from Reference 1.

C. MATHEMATICAL MODEL

In developing a mathematical model for the steady-state condition, a set of assumptions are imposed so as to make the problem tractable. It is assumed that the only forces acting on a cable element are the gravity force, pressure drag force, and tension. The gravity is assumed to be uniform in the operating range in the light of the fact that the change is approximately 1.0 percent. The skin-fraction drag is neglected due to the fact that the skin-fraction drag coefficient is smaller by two orders of magnitude as compared to basic drag coefficient (see Reference 14) and the fact that the cable is nearly vertical. The buoyancy on the cable is negligible compared to other forces and also is not taken into account. It is assumed that the moments are not transmitted in the cable, thus implying that the cable is perfectly flexible. A physical assumption made is that the drag force on the cable element normal to the element can be determined using the wind vector component normal to the element. This is so-called cosine or sine principle, depending on the definition of angle of attack.

Selecting the origin of the coordinate system at the balloon (see Figure 46) and equating the sum of the forces on an infinitesimal cable element to zero, three equations are obtained.

$$\left.\begin{aligned} &(ds)\ F'_{unx} - (T \sin\phi \cos\theta)_s + (T \sin\phi \cos\theta)_{s+ds} = 0 \\ &(ds)\ F'_{uny} - (T \sin\phi \sin\theta)_s + (T \sin\phi \sin\theta)_{s+ds} = 0 \\ &(ds)\ F'_{unz} - (T \cos\phi)_s + (T \cos\phi)_{s+ds} - \omega(ds) = 0 \end{aligned}\right\} \quad (1)$$

where

T is cable tension

s is length of cable from the origin to the element

ds is infinitesimal cable length

ϕ and θ are spherical coordinates that determine the direction of tangent vector to the cable at position s

ω is weight of cable/length as function of s

u is magnitude of wind-vector as function of z

α is direction of wind-vector horizontally as function of z (the vertical is neglected)

F'_{unx} is drag force on cable element/length in x direction

F'_{uny} is drag force in y direction

F'_{unz} is drag force in z direction.

To evaluate the drag forces, a normal component of the wind-vector has to be computed (as mentioned above) from which the drag force normal to the element can be evaluated, leading thus to the desired results, which become:

$$\left.\begin{aligned} F'_{unx} &= D\ [\cos\alpha - \sin^2\phi \cos\theta \cos(\theta - \alpha)] \\ F'_{uny} &= D\ [\sin\alpha - \sin^2\phi \sin\theta \cos(\theta - \alpha)] \\ F'_{unz} &= -D\ [\sin\phi \cos\phi \cos(\theta - \alpha)] \end{aligned}\right\} \quad (2)$$

with

$$D = 1/2\,\rho C_D d \left| [1 - \sin^2\phi \cos^2(\theta - \alpha)]^{1/2} \right| u^2,$$

where

u is wind speed

ρ is air density as function of z

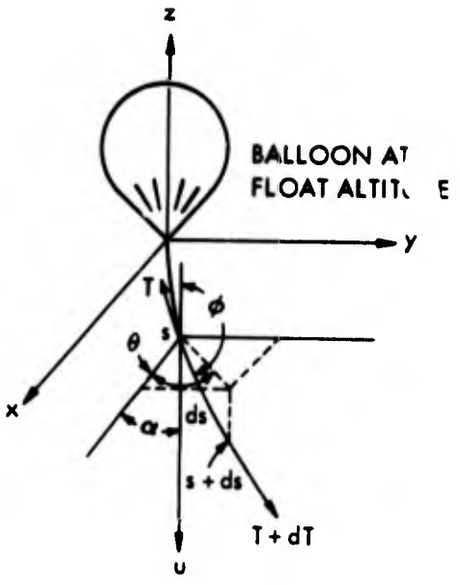

Figure 46. Coordinate System

C_D is cable drag coefficient

d is diameter of cable as function of s.

Dividing each of the equations in set 1 by (ds) and in the limit as ds$\rightarrow$0, the following differential equations are obtained:

$$\left.\begin{aligned} \frac{d}{ds}\ (T \sin\phi \cos\theta) + F'_{unx} &= 0 \\ \frac{d}{ds}\ (T \sin\phi \sin\theta) + F'_{uny} &= 0 \\ \frac{d}{ds}\ (T \cos\phi) + F'_{unz} - \omega &= 0 \end{aligned}\right\} \qquad (3)$$

with the boundary conditions $T = T_o$, $\theta = \theta_o$, and $\phi = \phi_o$ at $s = s_o$. It is of interest to note at this point that for u = o everywhere (except at float altitude) and ω independent of s, the above three differential equations simplify to a simple equation, which is the equation of a catenary:

$$A\ \frac{d^2y}{dx^2} = \omega\sqrt{1 + \left(\frac{dy}{dx}\right)^2}$$

where A is arbitrary.

To find an analytical solution to the three differential equations is an extremely difficult, if not impossible, task since the diameter of a cable and the linear density are arbitrary functions of s as well as wind-vector profile and air density are both functions of z. In the light of these facts, an approximate technique has to be developed. This is accomplished by representing the differential equations by a set of difference equations which can easily be evaluated by means of a digital computer. Denoting the position s on a cable by i and the position s + ds by i + 1, the following set of equations result from set 3:

$$\theta_{i+1} = \theta_i + \arctan\left[\frac{(ds)\,F'_{unxi} \sin\theta_i - (ds)\,F'_{unyi} \cos\theta_i}{T_i \sin\phi_i - (ds)\,F'_{unxi} \cos\theta_i - (ds)F_{unyi} \sin\theta_i}\right]$$

$$\phi_{i+1} = \phi_i + \arctan$$

$$\left\{ \frac{\left[T_i \sin\phi_i \sin\theta_i - (ds)F'_{unyi}\right] - \sin\theta_{i+1} \tan\phi_i \left[T_i \cos\phi_i + \omega_i(ds) - (ds)\,F_{unzi}\right]}{\sin\theta_{i+1}\left[T_i \cos\phi_i + \omega_i\,(ds) - (ds)F'_{unzi}\right] + \tan\phi_i\left[T_i \sin\phi_i \sin\theta_i - (ds)\,F_{unyi}\right]} \right\}$$

$$T_{i+1} = \frac{\omega_i\,(ds) + T_i \cos\phi_i - (ds)\,F'_{unzi}}{\cos\phi_{i+1}}$$

$$z_{i+1} = (ds) \sum_{k=0}^{i} \cos\phi_k$$

$$x_{i+1} = (ds) \sum_{k=0}^{i} \sin\phi_k \cos\theta_k$$

$$y_{i+1} = (ds) \sum_{k=0}^{i} \sin\phi_k \sin\theta_k$$

This set of six equations together with boundary conditions are used to compute cable form as well as the tension for a given wind-vector profile and a given cable hence known $d = d(s)$ and $\omega = \omega(s)$. It is of importance to get an approximate error resulting from the difference equations. An estimate of this is presented below.

D. ERROR ANALYSIS

The errors in the cable form and tension resulting from approximate computing technique depends, of course, on the magnitude of cable increment chosen for the computation - the smaller the increment the greater the accuracy in the two quantities. However, with decreasing increment the computation time increases, thus leading to a trade-off between accuracy and cost. Preliminary analysis indicates that the ratio (ds)/(cable length) in the range 1/200 to 1/240 is quite satisfactory to satisfy the two requirements.

The comparison of the approximate solutions is possible with an exact one in special cases, i.e., when the differential equations can be solved analytically. Such a comparison has been made with the result that the errors in cable position and tension increase with cable length, as would be expected, with maximum errors of 0.75 and 0.45 percent, respectively, at approximately half of the required length. The maximum error for the entire cable would be nearly double these numbers.

E. SOLUTIONS OF DIFFERENCE EQUATIONS

The differential equations in subsection C lead to difference equations in unknowns θ, ϕ, and T. The difference equations were derived as follows:

$$T_{i+1} \sin\phi_{i+1} \cos\theta_{i+1} - T_i \sin\phi_i \cos\theta_i + F'_{unx}\,\Delta S = 0$$

$$T_{i+1} \sin\phi_{i+1} \sin\theta_{i+1} - T_i \sin\phi_i \sin\theta_i + F'_{uny}\,\Delta S = 0$$

$$T_{i+1} \cos\phi_{i+1} - T_i \cos\phi_i + F'_{unz}\,\Delta S - \omega\,\Delta S = 0.$$

Solutions for unknowns θ, ϕ, and T are found sequentially.

$$\tan \theta_{i+1} = \frac{T_i \sin \phi_i \sin \theta_i - F'_{uny} \Delta S}{T_i \sin \phi_i \cos \theta_i - F'_{unx} \Delta S}$$

$$\tan \phi_{i+1} = \frac{T_i \sin \phi_i \sin \theta_i - F'_{uny} \Delta S}{(T_i \cos \phi_i - F'_{unz} \Delta S + \omega \Delta S) \sin \theta_{i+1}}$$

For small values of θ_{i+1} where $\sin \theta_{i+1} \rightarrow 0$, an alternate equation is used.

$$\tan \phi_{i+1} = \frac{T_i \sin \phi_i \cos \theta_i - F'_{unx} \Delta S}{(T_i \cos \phi_i - F'_{unz} \Delta S + \omega \Delta S) \cos \theta_{i+1}}$$

Then to avoid angle adjustment due to quadrant variations, the solutions for θ and ϕ are changed to difference equations by the identity

$$\tan (a - b) = \frac{\tan a - \tan b}{1 + \tan a \tan b}.$$

Tan $(\theta_{i+1} - \theta_i)$ and tan $(\phi_{i+1} - \phi_i)$ are therefore computed before solving for θ_{i+1} and ϕ_{i+1}. Then

$$T_{i+1} = \frac{T_i \cos \phi_i - F'_{unz} \Delta S + \omega \Delta S}{\cos \phi_{i+1}}$$

unless $\phi_{i+1} \rightarrow$ 90 degrees where $\cos \phi_{i+1} \rightarrow 0$. But if $\phi_{i+1} \rightarrow 90$ degrees, the computation is terminated, since at ϕ_{i+1} = 90 degrees, the cable is parallel to the ground plane.

F. DESIGN OF CONSTANT STRESS CABLE

1. General

An optimum cable design would, of course, be one where stress was constant over its entire length. For instance, sections at the higher end must have adequate strength to lift the lower end and therefore must be of larger size provided that the cable has homogeneous properties. In a like manner, cable size should be tailored in accordance with distribution of aerodynamic load. Therefore, in solving the difference equations, the cable properties as shown in Figures 3 and 4 were assumed to be representative of the types of cables available in order to calculate parameters such as blowdown distance, cable angle, and total cable weight for a tapered constant stress cable. The equations defining physical properties were derived by fitting the curves of Figures 3 and 4 to the data provided by manufacturers of the three cable types. These equations are given in the following paragraphs.

2. Glastran

a. Cable Weight/Foot (lb/ft)

$\omega = (0.001)(5.6 + 0.662\, S^2)$ for $0 < S < 9$

where $S = \frac{B.S.}{1000} = \frac{F.S. \times \text{tension}}{1000}$.

$\omega = \frac{S}{153}$ for $S \geq 9$.

b. Diameter (feet)

$$d = \frac{1}{12}\left(\frac{\omega}{0.596}\right)^{1/2} \text{ for } 0 < \omega < 0.150.$$

$$d = \frac{1}{12}\left(\frac{\omega - 0.009}{0.573}\right)^{1/2} \text{ for } 0.15 < \omega \geq 0.582.$$

3. Missile Wire (Acco, 1 x 37 x 7)

a. Cable Weight/Foot (lb/ft)

$$\omega = \frac{S}{112.5} \text{ for } 0 < S < 9.$$

$$\omega = 0.001\left(80 + \frac{S - 9}{0.0772}\right) \text{ for } S \geq 9.$$

b. Diameter (feet)

$$d = \frac{1}{12}\left(\frac{\omega}{1.888}\right)^{1/2} \text{ for all values of } \omega.$$

4. Sampson Braided Rope (Nylon)

a. Cable Weight/Foot (lb/ft)

$$\omega = 0.001\left(\frac{S}{0.1105}\right) \text{ for all values.}$$

b. Diameter (feet)

$$d = \frac{1}{12}\left(\frac{\omega}{0.256}\right)^{1/2} \text{ for all values.}$$

APPENDIX II

DETAILED ANALYSIS OF TETHERED AERODYNAMICALLY SHAPED BALLOONS

A. GENERAL

This appendix contains additional information on the physical dimensions, stress analysis, and weight analysis of the aerodynamically shaped balloons.

B. PHYSICAL SHAPE

For geometrically similar balloons, the linear dimensions are proportional to the one-third power of balloon volume, and the surface area is proportional to the two-thirds power of balloon volume. Therefore, the various lengths and surface areas for various balloon shapes can be obtained by determining the appropriate proportionality constants. These scaling factors (proportionality constants) for the Class C, ram air C, and modified Mark II balloons were based on wind tunnel models, and the scaling factors for the Vee-Balloon were based on actual balloon designs.

Table IX, which contains scaling factors, and the relationships listed below were used in the computer program to determine the physical size for each balloon shape.

Hull Length (ft)

$$L = K_1 \forall^{1/3} \tag{4}$$

Maximum Hull Diameter (ft)

$$D = \frac{1}{f} L \tag{5}$$

Wetted Hull(s) Area (ft^2)

$$A_h = K_3 \forall^{2/3} \tag{6}$$

Projected Area of One Horizontal Tail (ft^2)

$$A_{pht} = K_4 \forall^{2/3} \tag{7}$$

Projected Area of One Vertical Tail (ft^2)

$$A_{pvt} = K_5 \forall^{2/3} \tag{8}$$

Location of Maximum Diameter (ft)

$$L_{max\ d} = K_L L \tag{9}$$

Wetted Area of One Horizontal Tail (ft^2)

$$A_{wht} = K_h A_{pht} \tag{10}$$

Wetted Area of One Vertical Tail (ft^2)

$$A_{wvt} = K_v A_{pvt} \tag{11}$$

Table IX. Proportionality Constants for the Physical Dimensions of Various Aerodynamically Shaped Balloons

Proportionality Constant	Symbol	Used in Eq	Balloon Type			
			Vee-Balloon	Mod Mark II	Navy Class C	Ram Air C
Hull Length	K_1	4	2.56	3.53	2.62	2.62
Fineness Ratio	f	5	4.00	4.70	2.64	2.64
Wetted Hull(s) Area	K_3	6	6.97	6.70	5.55	5.55
Projected Area of One Horizontal Tail	K_4	7	0.707	0.725	0.30	0.30
Projected Area of One Vertical Tail	K_5	8	0.0785	0.515	0.30	0.30
Location of Maximum Diameter	K_L	9	0.45	0.400	0.40	0.40
Wetted Area of One Horizontal Tail	K_h	10	2.21	2.21	2.3439	2.3439
Wetted Area of One Vertical Tail	K_v	11	2.32	2.41	2.3439	2.3439
Tail Thickness	K_t	12	0.105	0.105	0.105	0.105
Number of Horizontal Tails	n_{ht}	16	1	2	2	2
Number of Vertical Tails	n_{vt}	16	2	2	1	1
Hull Intersect Area	K_{int}	20	0.336	0	0	0
Gas Leakage Rate Constant	K_{le}	21	← 0.00639 $ft^3/ft^2/day$ →			
Ratio of Temp Difference over Avg Temp at Altitude	K_{temp}	22	0.1	0.1	0.1	0.1

Average Thickness of Horizontal Tail (ft)

$$h_{hta} = K_t \sqrt{A_{pht}} \tag{12}$$

Average Thickness of Vertical Tail (ft)

$$h_{vta} = K_t \sqrt{A_{pvt}} \tag{13}$$

Volume of One Horizontal Tail (ft^3)

$$\forall_{ht} = h_{hta} A_{pht} \tag{14}$$

Volume of One Vertical Tail (ft^3)

$$\forall_{vt} = h_{vta} A_{pvt} \tag{15}$$

Volume of Total Balloon (ft^3)

$$\forall_{tot} = \forall + n_{ht} \forall_{ht} + n_{vt} \forall_{vt} \tag{16}$$

Ballonet Volume (ft^3)

$$\forall_{bnt} = \left(1 - \frac{\rho_{alt}}{\rho_0}\right)\forall_{tot} \tag{17}$$

Diameter of Spherical Ballonet (ft)

$$D_{bnt} = 1.24\left(\forall_{bnt}\right)^{1/3} \tag{18}$$

Wetted Area of Spherical Ballonet (ft^2)

$$A_{bnt} = 4.84\left(\forall_{bnt}\right)^{2/3} \tag{19}$$

Hull Intersect Area (ft^2)

$$A_{int} = K_{int}\,\forall^{2/3} \tag{20}$$

Volume of Gas Lost by Leakage (ft^3/day)

$$\forall_{leak} = K_{le}\left(A_h + n_{ht}A_{wht} + n_{vt}A_{wvt}\right) \tag{21}$$

Volume due to Temperature Change at Float Altitude per Day (ft^3/day)

$$\forall_{temp} = K_{temp}\,\forall_{tot} \tag{22}$$

C. STRESS ANALYSIS

1. General

As noted in the text of the report, the design stress used in the balloon analysis was the sum of the stresses caused by the internal pressure, buoyant lift, and aerodynamic load with the appropriate factor of safety. Bending moment was neglected. Therefore,

$$N_{des} = F.S.\left(N_i + N_b + N_a\right) \tag{23}$$

where

N_{des} is design stress for selection of balloon material (lb/ft)

F.S. is factor of safety

N_i is stress due to internal pressure (lb/ft)

N_b is stress due to buoyant lift (lb/ft)

N_a is stress due to aerodynamic loads (lb/ft).

Maximum stresses on the balloon due to internal pressure and buoyant lift occur at the maximum diameter of the balloon. Maximum stresses due to aerodynamic loads occur somewhat forward of the maximum diameter, but for this analysis, were conservatively assumed to act at the maximum diameter. Therefore, the location of maximum stress occurs at the maximum diameter just above the attachment points of the balloon suspension (bridle) system, which were assumed to be attached near the equator of the balloon. The calculations given in the following paragraphs determine the stresses in the balloon skin at the equator.

2. Stress due to Internal Pressure

The required balloon internal pressure at altitude, as explained in Section V, was selected to be 15 percent greater than the dynamic pressure at altitude, or 1/4 in. H_2O = 1.3 lb/ft^2, whichever is greater. Therefore, P_i = 1.15q or 1.30 lb/ft^2, whichever is greater. This pressure was assumed to be at the bottom of the balloon.

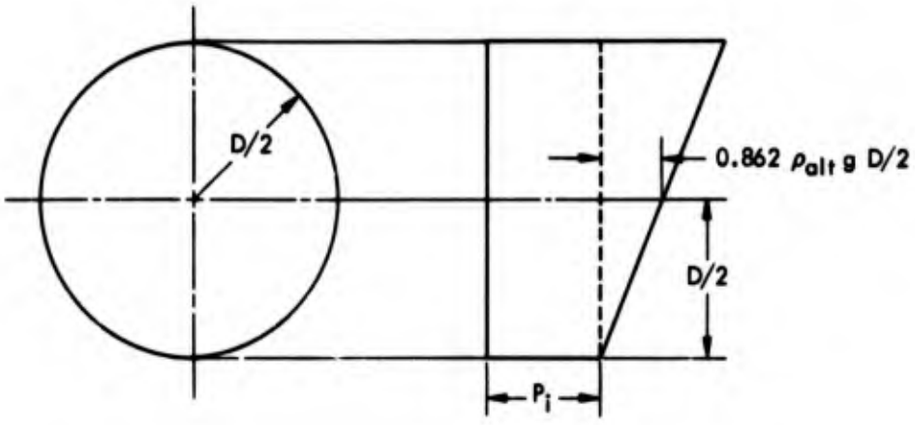

Figure 47. Internal Pressure Occurring in the Balloon at the Maximum Diameter

Referring to Figure 47, the pressure at the balloon equator is

$$P_{eq} = P_i + 0.862\,\rho_{alt}\,g\,\frac{D}{2}\,.$$

The second term represents the helium pressure head at altitude between the bottom of the balloon and the equator.

The maximum internal pressure stress is

$$N_i = P_{eq}\,\frac{D}{2}$$

$$= \left(P_i + 0.862\,\rho_{alt}\,g\,\frac{D}{2}\right)\frac{D}{2}\ \text{lb/ft.} \qquad (24)$$

3. Stress due to Buoyant Lift

From Figure 48, the maximum stress due to buoyant load at altitude acting on a one-foot section of the hull is

$$N_b = \frac{1}{2}\left[L_b(\text{one-foot section})\right]$$

where

L_b = buoyant lift of helium at altitude

= b x volume of the section.

Therefore,

$$N_b = \frac{1}{2}\left[(0.862\,\rho_{alt}\,g)\left(\pi\,\frac{D^2}{4}\right)\right]\text{lb/ft.} \qquad (25)$$

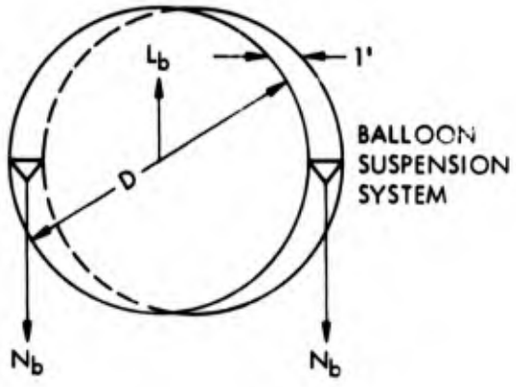

Figure 48. Buoyant Force on Balloon at the Maximum Diameter

4. Stress due to Aerodynamic Loads

From wind tunnel tests on the General Mills Aerocap Model Balloon (Reference 15), the maximum local pressure was determined to be approximately

$$x = 0.1q\alpha$$

where

x is maximum local pressure (lb/ft^2)

q is dynamic pressure (lb/ft^2)

α is angle of attack (degrees).

This occurs at approximately 30 percent aft of the balloon nose. However, for this analysis, it was assumed to act at the maximum diameter (see Figure 49).

Therefore, the total aerodynamic force acting on the one-foot section (assuming a linear load distribution) is

$$F = (x)\left(\frac{D}{2}\right) = 0.1q\,\alpha\,\frac{D}{2} \text{ lb.}$$

This load is reacted by the suspension lines of the balloon. Therefore, the stress in the fabric directly above the suspension lines is

$$N_a = \frac{1}{2} F = 0.05q\,\alpha\left(\frac{D}{2}\right) lb/ft. \quad (26)$$

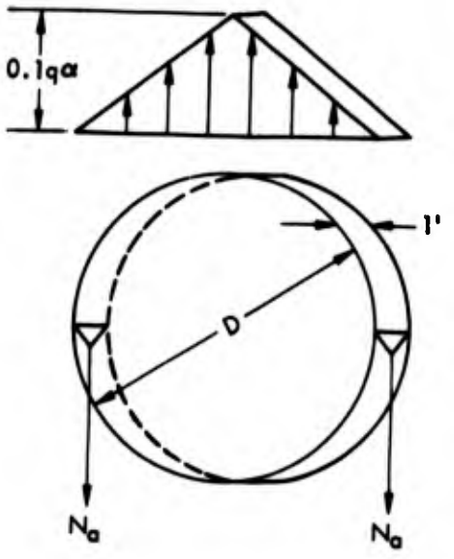

Figure 49. Assumed Aerodynamic Loading on the Maximum Diameter of the Balloon

D. BALLOON WEIGHT

1. Balloon Material

Once the design stress has been determined, the unit fabric weight can be determined to be

$$w = 0.463 \times 10^{-4} N_{des} \; lb/ft^2 \quad (27)$$

or

0.01041,

whichever is greater.

This is the equation of the line in Figure 29 for values of material weight up to approximately 8 oz/yd^2. Due to ground-handling problems, a minimum weight material of 1.5 oz/yd^2 (0.01041 lb/ft^2) was assumed to be the lightest material from which an aerodynamically shaped balloon would be fabricated.

2. Hull, Tail, and Ballonet Weights

Based on the determined unit material weight and the various physical dimensions that were determined in the previous sections of this appendix, the hull and tail weights can be determined. However, since little differential pressure acts across the ballonet, a one oz/yd^2 (0.00695 lb/ft^2) ballonet material was assumed for all sizes of all balloon types.

Proportionality constants for the weights of components of various aerodynamically shaped balloons are given in Table X. The equations used in the computer solution are as follows.

Weight of Hull Fabric (lb)

$$W_{hf} = wA_h \quad (28)$$

Table X. Proportionality Constants for the Weights of the Components of Various Aerodynamically Shaped Balloons

Proportionality Constant	Symbol	Used in Eq	Balloon Type			
			Vee-Balloon	Mod Mark II	Navy Class C	Ram Air C
Factor of Safety on Fabric Stress	F.S.	21	3	3	3	3
Seam Weight	K_s	27	0.10	0.10	0.10	0.10
Unit Weight of Tail Fabric	w_t	30	w	w	w	w
Unit Weight of Partition Material	w_p	32	$2w_t$	$2w_t$	$2w_t$	$2w_t$
Unit Weight of Ballonet Material	w_b	36	0.00695 lb/ft^2	0.00695 lb/ft^2	0.00695 lb/ft^2	0.00695 lb/ft^2
Power Density of Battery	K_{bat}	45 - 47	3600 watt minutes /lb ⟶			Not applicable
Miscellaneous Equipment Weight	K_{me}	48	0.5	0.5	0.5	0
Total Balloon Weight	K_{tb}	54	1.791	1.791	1.791	1.791
Suspension Line Weight	K_{sus}	55	0.000591	0.000591	0.000591	0.000591
Handling Line and Catenary	K_{hl}	56	0.234	0.234	0.234	0.234

Weight of Hull Seams (lb)

$$W_{hs} = K_s W_{hf} \tag{29}$$

Intersect Weight (lb)

$$W_{int} = w\, A_{int} \tag{30}$$

Weight of Intersect Attachments (lb)

$$W_{int\ a} = \frac{1}{2} W_{int} \tag{31}$$

Weight of One Horizontal Tail (lb)

$$W_{ht} = w_t\, A_{wht} \tag{32}$$

Weight of Attachments of One Horizontal Tail (lb)

$$W_{hta} = K_s\, W_{ht} \tag{33}$$

Weight of Interior Partitions of One Horizontal Tail (lb)

$$W_{iha} = w_p\, A_{pht} \tag{34}$$

Weight of One Vertical Tail (lb)

$$W_{vt} = w_t\, A_{wvt} \tag{35}$$

Weight of Attachments of One Vertical Tail (lb)

$$W_{vta} = K_s W_{vt} \tag{36}$$

Weight of Interior Partitions of One Vertical Tail (lb)

$$W_{iva} = w_p A_{pvt} \tag{37}$$

Weight of Ballonet (lb)

$$W_{bnt} = w_b A_{bnt} \tag{38}$$

Weight of Ballonet Seams and Attachment (lb)

$$W_{bnt,s} = K_s W_{bnt} \tag{39}$$

3. Blower, Battery, and Exit Valve Analysis

a. Volume and Volume Flow Rate of Air through an Exit Valve or Blower. The volume of air to be expelled through an exit valve of a balloon during ascent or to be filled by a blower during descent may be determined by the expressions given below. It is assumed that the total volume of the balloon remains constant and that the weight of a given mass of air is constant throughout the elevations considered.

The weight of a certain volume (V) of air at an altitude (h) is given by

$$W_h = \gamma_h V_h \text{ lb}$$

where γ_h is the weight density (lb/ft^3) of air at float altitude h. Also, at altitude h - dh,

$$W_{h-dh} = (\gamma_h + d\gamma) V_{h-dh},$$

but

$$W_h = W_{h-dh}.$$

Therefore,

$$\gamma_h V_h = (\gamma_h + d\gamma) V_{h-dh}$$

or

$$V_{h-dh} = \left(\frac{\gamma_h}{\gamma_h + d\gamma} \right) V_h .$$

Let Qt be the volume filled during the change in altitude from h to h-dh. Therefore,

$$d(Qt) = V_h - V_{h-dh}$$

$$= V_h \left(1 - \frac{\gamma_h}{\gamma_h + d\gamma} \right)$$

$$= V_h \frac{d\gamma}{\gamma_h + d\gamma}.$$

Neglecting second-order effects,

$$d(Qt) = V_h \frac{d\gamma}{\gamma_h} .$$

However, V_h = constant = $\forall_{tot}$.

Therefore,

$$Qt = \forall_{tot} \int_{h}^{0} \frac{d\gamma}{\gamma_h}$$

$$Qt = \forall_{tot} \ln \frac{\gamma_0}{\gamma_h} ft^3 \tag{40}$$

where

Qt is volume filled by blower (ft^3)

$\forall_{tot}$ is total volume of balloon (ft^3)

γ_0 is weight density of air at sea level launch altitude (lb/ft^3)

γ_h is weight density of air at float altitude (lb/ft^3).

To determine the volume flow rate (Q) through the exit valve or blower, an ascent and descent rate of 400 ft/min was assumed.

$$Q = Qt \left(\frac{400}{h}\right) ft^3/min \tag{41}$$

or

2000 ft^3/min, whichever is greater. (h is again the float altitude of the balloon.)

b. Blower and Check Valve Weight. An empirical relation based on information listed in a blower catalog (Reference 16) is given in Figure 50. The plot contains blower weight versus differential pressure for blowers rated at 4000 ft^3/min. Blowers used in this plot include rated flow rates from 500 to 4000 ft^3/min, which were modified to an equivalent rate of 4000 ft^3/min by use of the following relation:

$$W_{blo} = W_{actual} \left(\frac{4000}{Q_{rated}}\right)$$

where

W_{blo} is blower weight equivalent (lb)

W_{actual} is blower weight listed in catalog (lb)

Q_{rated} is flow rate of blower, as listed in catalog (ft^3/min).

Ratings for these blowers are for standard atmospheric conditions. The resulting expression based on Figure 50 is

$$W_{blo} = \frac{Q}{4000} (7.5\ P_{io} + 17.8)\ lb$$

where

P_{i0} is the differential pressure at sea level in in. H_2O.

Use of this blower at higher altitudes will result in differential pressures that vary with the density of the air being blown. That is,

$$P_i = \frac{\rho_{alt}}{\rho_0} P_{io} \frac{1}{0.1922} lb/ft^2 \tag{42}$$

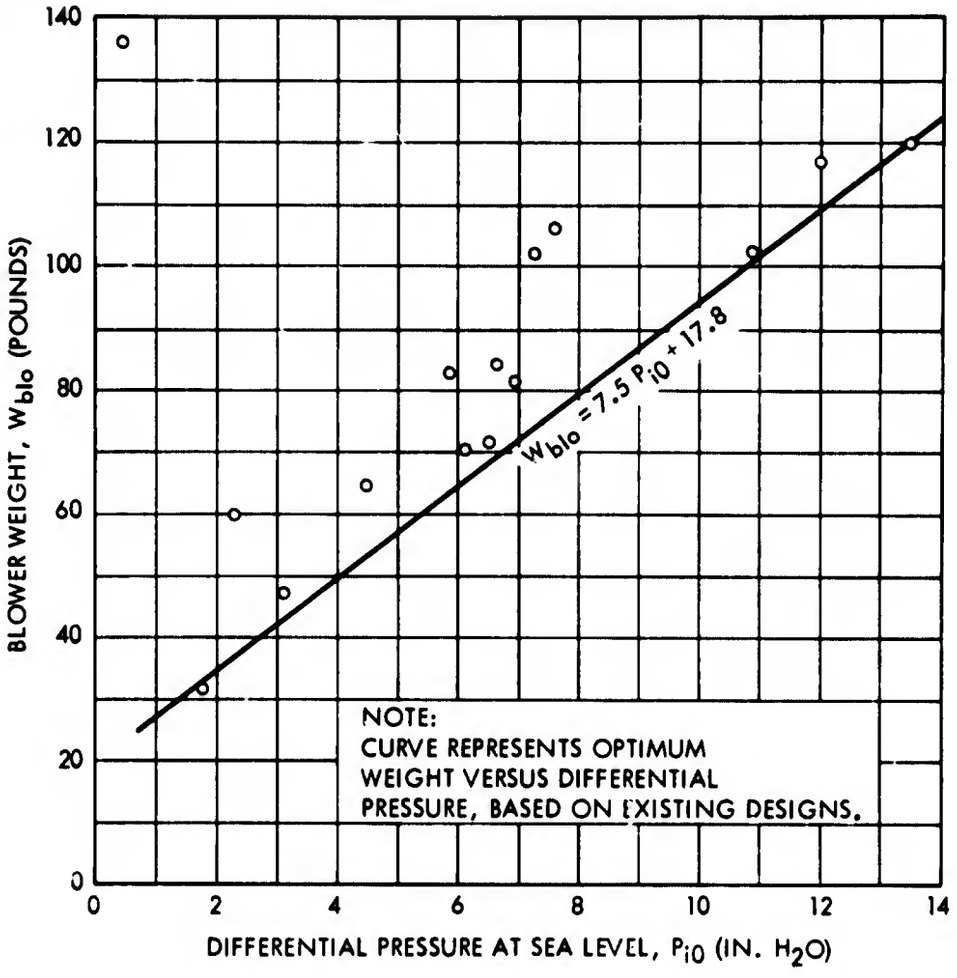

Figure 50. Blower Weight versus Differential Pressure for Volume Flow Rate of 4000 Ft^3/Min

where

P_i is differential pressure at altitude

$\frac{\rho_{alt}}{\rho_0}$ is ratio of air density at altitude to sea level.

Thus,

$$W_{blo} = \frac{Q}{4000}\left(1.442\ \frac{\rho_0}{\rho_{alt}}\ P_i + 17.8\right) lb \tag{43}$$

where Q is the desired flow rate of the blower (ft^3/min).

The check valve is mounted on the blower, and therefore its weight was assumed to be proportional to the blower weight. Previous experience has shown that this constant of proportionality is approximately 1/2. Therefore, the weight of the check valve is

$$W_{chk} = \frac{1}{2}\ W_{blo}\ lb. \tag{44}$$

c. Battery Weight. Battery power is required to operate the blower at altitude to account for daily temperature changes and leakage losses and to operate the blower during descent to maintain a full ballonet. The typical equation for battery weight is

$$W_{bat} = \frac{Pt_{oper}}{K_{bat}}$$

where

W_{bat} is the battery weight (lb)

P is the power required (watts)

t_{oper} is the operating time of the blower (minutes)

K_{bat} is the power density of the battery (watt min/lb).

By plotting battery power versus sea level differential pressure for equivalent 4000 ft^3/min blower capacity, an empirical relation for power required to operate the blowers can be determined to be

$$P = 1000\ P_{io} \text{ watts}$$

where P_{io}, as previously defined, is the differential pressure at sea level in in. H_2O (see Figure 51).

Battery weight required at altitude is that required to operate the blower at an equivalent sea level pressure of

$$P_i = \frac{\rho_{alt}}{\rho_0} P_{io} \quad \frac{1}{0.1922} ,$$

as defined in Equation 42. Thus, the power required is

$$P' = 1000\ (0.1922)\ \frac{\rho_0}{\rho_{alt}}\ P_i \text{ lb/ft}^2.$$

However, this power would operate the blower at sea level, whereas the power required at altitude varies directly with the density of the air being blown. Thus, the actual power required for the battery is

$$P = \frac{\rho_{alt}}{\rho_0}\ P'$$

$$P = \frac{\rho_{alt}}{\rho_0}\ (1000)\ (0.1922)\ \frac{\rho_0}{\rho_{alt}}\ P_i$$

$$= 192.2\ P_i \text{ watts.}$$

The battery weight was analyzed as that required while at float altitude and that required during descent. Therefore,

$$W_{bat} = W_{bat,a} + W_{bat,d} \text{ (lb)}$$

where

$W_{bat,a}$ is amount of batteries required at altitude (lb)

$W_{bat,d}$ is amount of batteries required during descent (lb).

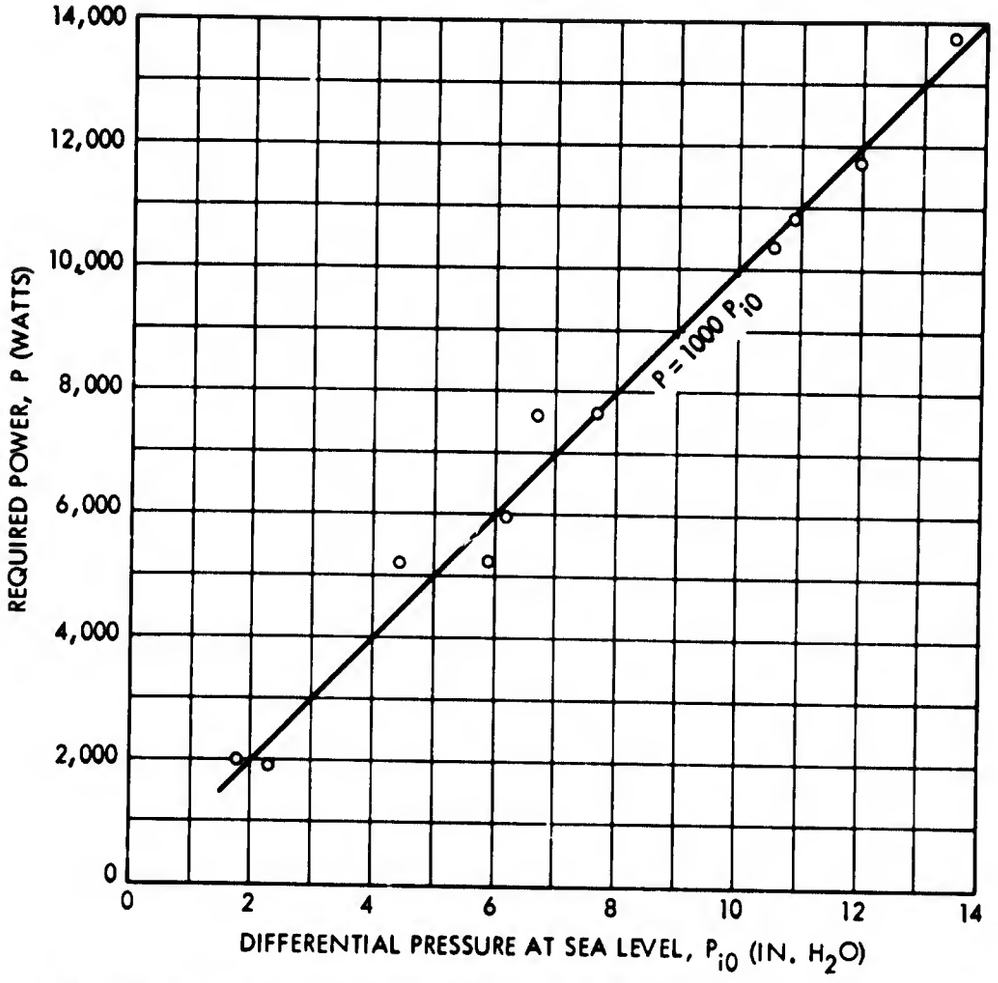

Figure 51. Required Blower Power versus Differential Pressure for Volume Flow Rate of 4000 Ft^3/Min

The equivalent time of operation of the blower at altitude is equal to the volume of air to be replaced each day ($\forall_{repl}$) divided by the 4000 ft^3/min blower rate and multiplied by the number of days at float altitude (t/24). Thus, the battery weight required at altitude is

$$W_{bat,a} = \frac{192.2 P_i \ (\forall_{repl}) \ (t/24)}{K_{bat} \ (4000)} \text{ pounds.} \tag{45}$$

Note that V_{repl} is modified in the computor program to provide a factor of safety of 2.

The work done on the gas during descent is equivalent to the work done on the gas if entirely filled at sea level. It will be assumed that the differential pressure to be maintained in the balloon at all times is P_i, the pressure that was required at altitude. This assumption neglects the fact that dynamic pressure at lower altitudes will probably be greater than that designed at altitude.

However, the fabric in the balloon is also designed for conditions at altitude while neglecting conditions below so that the assumptions are consistent. Thus,

$$P_{i0} = P_i \ (0.1922) \ lb/ft^2,$$

which is identical with Equation 40 when

$$\rho_{alt} = \rho_0 .$$

The operating time of the blower during descent is that time required for a 4000 ft^3/min blower to fill the ballonet, or ($\forall_{bnt}/4000$).

Therefore, with a safety factor of 2,

$$W_{bat,d} = (2)\frac{192.2P_i\,\frac{\forall_{bnt}}{4000}}{K_{bat}}$$

$$= (2)\frac{192.2P_i\,\forall_{bnt}}{K_{bat}\,(4000)}\ \text{lb.} \tag{46}$$

The total battery weight is

$$W_{bat} = W_{bat,a} + W_{bat,d}$$

$$W_{bat} = \frac{192.2P_i}{K_{bat}\,(4000)}\left[\forall_{repl}\left(\frac{t}{24}\right) + 2\,\forall_{bnt}\right]\text{lb} \tag{47}$$

where

P_i is differential pressure at altitude (lb/ft^2)

$\forall_{repl}$ is volume of air that blower has to replace at altitude (ft^3/day)

t is float time at altitude (hr)

$\forall_{bnt}$ is balloon ballonet volume (ft^3).

The weight of the miscellaneous equipment for the blower and battery is

$$W_{me} = K_{me}\,W_{bat}, \tag{48}$$

which was included to cover the weight of the battery heater, wiring, etc. See Table X for the values of K_{bat} and K_{me}.

d. Weight of Exit Valve. The volume rate of flow through an orifice is given in any fluid mechanics book (e.g., Reference 17) as

$$Q = CA\sqrt{2gZ}$$

where

Q is volume rate of flow through orifice (ft^3/min)

C is discharge coefficient

A is exit area of orifice (ft^2)

Z is pressure head on the fluid at the orifice (ft).

The pressure head (Z) may be written as

$$Z = \frac{p}{\gamma}$$

where

p is pressure head (lb/ft^2)

γ is weight density of the fluid (lb/ft^3).

Therefore,

$$Q = CA\sqrt{2g\frac{p}{\gamma}}$$

$$Q = CA\sqrt{2\frac{p}{\rho}}\,. \tag{49}$$

For purposes of scaling the weight of the valve, assume that the weight is proportional to its exit area. That is,

$$\frac{W_1}{W_2} = \frac{A_1}{A_2}\,. \tag{50}$$

Solving Equation 49 for A_1, and adding the subscripts 1, we have

$$A_1 = \frac{1}{C}\frac{Q_1}{\sqrt{2\frac{p_1}{\rho_1}}} \tag{51}$$

However, the value of the discharge coefficient may be obtained using data from an existing valve, since C is a constant for a particular orifice type. Thus,

$$C = \frac{Q_2}{A_2\sqrt{\frac{2p_2}{\rho_2}}} \tag{52}$$

Substituting Equations 51 and 52 into Equation 50,

$$\frac{W_1}{W_2} = \frac{A_2\sqrt{\frac{2p_2}{\rho_2}}}{Q_2}\;\frac{Q_1}{A_2\sqrt{\frac{2p_1}{\rho_1}}}$$

or

$$W_1 = W_2\sqrt{\frac{p_2}{\rho_2}}\sqrt{\frac{\rho_1}{p_1}}\;\frac{Q_1}{Q_2}\,.$$

Values for a typical exit valve are as follows:

Size = 28 inch in diameter

A_2 = 4.24 ft^2

Q_2 = 8500 ft^3/min

p_2 = 3 in. H_2O = 15.62 lb/ft^2

W_2 = 31.0 lb (aluminum)

ρ_2 = ρ_0 at sea level

$$W_1 = (31.0)\sqrt{\frac{15.62}{\rho_0}}\sqrt{\frac{\rho_1}{p_1}}\ \frac{Q_1}{8500}$$

$$W_1 = 0.01445\sqrt{\frac{\rho_1}{\rho_0}}\ \frac{Q_1}{\sqrt{p_1}}\ .$$

To compute the weight of a value required at float altitude, note the following changes in notation:

$\rho_1 = \rho_{alt}$

$p_1 = p_i$.

Therefore,

$$W_1 = 0.01445\sqrt{\frac{\rho_{alt}}{\rho_0}}\ \frac{Q_1}{\sqrt{p_i}}\ . \qquad (53)$$

e. Suspension (bridle) System Weight. The weight of the suspension system is proportional to the length of the balloon and the tether tension in the bridle.

$W_{sus} \propto LT$,

or from Equation 4,

$W_{sus} \propto \Psi^{1/3}\, T$.

However, to obtain the tether tension, the weight of the balloon (which we are trying to estimate) has to be known. Therefore, an initial estimate of the total weight is made by summing the already estimated parts of the balloon, which include everything except the suspension system, handling line, and catenary weights, and multiplying by an appropriate factor.

The initial estimate of the tether tension is

$$T_{lb} = \left\{\left[L_a + L_b - P - (K_{tb})\, W_{i(tot)}\right]^2 + D_b{}^2\right\} \qquad (54)$$

where

L_a, aerodynamic lift, = $C_L q \Psi^{2/3}$ (lb)

L_b, buoyant lift, = $0.862 g V_{tot}\ \rho_{alt}$ (lb)

P is payload package weight (lb)

K_{tb} is the factor to obtain total balloon weight

$W_{i(tot)}$ is the initial estimate of weight, which includes all weight except the suspension, handling line, and catenary weight (lb)

D_b, aerodynamic drag on balloon, = $C_D q \Psi^{2/3}$ (lb).

Therefore, the weight of the suspension system is

$$W_{sus} = K_{sus}\, T_{lb}\, (\forall_{tot})^{1/3} \text{ lb.} \tag{55}$$

The weight of the handling line and catenary is

$$W_{hl} = K_{hl} W_{sus} \text{ lb.} \tag{56}$$

See Table X for the values of K_{tb}, K_{sus} and K_{hl}.

f. Total Balloon Weight. The total balloon weight can be obtained for a particular balloon type (Vee-Balloon, Class C, etc) from the previous equations by imputing the following information:

Payload weight, P (lb)

Float altitude, h (ft)

Wind velocity, v (knots)

Angle of attack, α (degrees)

Hull volume, $\forall$ (ft^3)

Operating Time at altitude, t (hr)

The total balloon weight is equal to the following:

$$\begin{aligned} W_{tot} = {} & W_{hf} + W_{hs} + W_{int} + W_{int\,a} \\ & + W_{ht} + W_{hta} + W_{iha} + W_{vt} \\ & + W_{vta} + W_{iva} + W_{blo} + W_{bat} \\ & + W_{val} + W_{chk} + W_{bnt} + W_{bnt,s} \\ & + W_{me} + W_{sus} + W_{hl} \text{ (pounds).} \end{aligned} \tag{57}$$

BLANK PAGE

REFERENCES

1. Feasibility Study for a High-Altitude Tethered Balloon System (Haltoon) (U). Technical Report 2452. ARPA Contract SD-198.Electric Division of General Mills, Inc, St. Paul, Minnesota, 21 October 1963. (Downgraded to Confidential)

2. Feasibility Study, High-Altitude Tethered Balloon System for Advanced Research Projects Agency. Technical Report GER 11287. ARPA Contract SD-199. Goodyear Aerospace Corporation, Akron, Ohio, 23 October 1963.

3. Final Report, Feasibility Study (U). Technical Report 1724-TR1. ARPA Contract SD-200. Minneapolis-Honeywell Regulator Company, Aeronautical Division, Minneapolis, Minnesota, 8 October 1963. (Confidential)

4. One-Hundred-Thousand Foot Tethered Balloon Feasibility Study (U). Technical Report TR 01820.01-1. Prepared for Office of Secretary of Defense, Advanced Research Projects Agency. ARPA Contract SD-201. Vitro Laboratories Division of Vitro Corporation of America, 9 October 1963. (Confidential)

5. Fage, A.: Experiments on a Sphere at Critical Reynolds Number. R & M 1766. September 1936.

6. Sauerwein, R.T.: "Sphere Drag Determined by Coasting through Still Air." Journal of the Aeronautical Sciences, Vol. I, July.

7. Horner, S.: Tests of Spheres with Reference to Reynolds Number, Turbulence and Surface Roughness. NACA TM No. 777. October 1935.

8. Zahn, A.F.: Flow and Drag Formulas for Simple Quadrics. NACA Report No. 253. 1927.

9. Smalley, J.H.: Determination of the Shape of a Free Balloon - Summary. Final Report. AFCRL-65-92, Litton Systems, Inc, Applied Science Division, 5 February 1965.

10. Glauert, H.: The Form of a Heavy Flexible Cable Used for Towing a Heavy Body below an Aeroplane. Reports and Memoranda 1952. British Advisory Committee for Aeronautics, February 1934.

11. Landweber, L., and Protter, M.: "The Shape and Tension of a Light Flexible Cable in a Uniform Current. Journal of Applied Mechanics. June 1947, pp. A-121 to A-126.

12. Ringleb, F.O.: "Motion and Stress of an Elastic Cable due to Impact." Journal of Applied Mechanics. March 1957, pp. 417-425.

13. Walton, T.S., and Polacheck, H.: Calculation of Nonlinear Transient Motion of Cables. David Taylor Model Basin Report 1279, 1959. A condensed paper is given in Mathematics of Computation (The Siam Review) No. 69-72, 1960, pp. 27-46.

14. Hoerner, Sighard F.: Aerodynamic Drag. Published by the author, 1951, page 138.

15. Wind Tunnel Tests of the General Mills Aerocap Model, Part 1. University of Detroit, Project 314, March 1960.

16. Aircraft and Electronic Fan Catalog (Revised). Joy Manufacturing Company.

17. Mark's Mechanical Engineers' Handbook. 6th Edition. 1958, p. 3-62.